Graduate School ETD Form 9
(Revised 12/07)

PURDUE UNIVERSITY
GRADUATE SCHOOL
Thesis/Dissertation Acceptance

This is to certify that the thesis/dissertation prepared

By Sandeep Ayyar

Entitled The Molecular Mechanism of Break Induced Replication

For the degree of Master of Science

Is approved by the final examining committee:

Dr. Anna Malkova
Chair

Dr. Teri Belecky-Adams

Dr. Andrew Kusmierczyk

To the best of my knowledge and as understood by the student in the *Research Integrity and Copyright Disclaimer (Graduate School Form 20)*, this thesis/dissertation adheres to the provisions of Purdue University's "Policy on Integrity in Research" and the use of copyrighted material.

Approved by Major Professor(s): Dr. Anna Malkova

Approved by: Dr. Simon Atkinson 7/13/2012
Head of the Graduate Program Date

Graduate School Form 20
(Revised 9/10)

PURDUE UNIVERSITY
GRADUATE SCHOOL

Research Integrity and Copyright Disclaimer

Title of Thesis/Dissertation:
The Molecular Mechanism of Break Induced Replication

For the degree of Master of Science

I certify that in the preparation of this thesis, I have observed the provisions of *Purdue University Executive Memorandum No. C-22,* September 6, 1991, *Policy on Integrity in Research.**

Further, I certify that this work is free of plagiarism and all materials appearing in this thesis/dissertation have been properly quoted and attributed.

I certify that all copyrighted material incorporated into this thesis/dissertation is in compliance with the United States' copyright law and that I have received written permission from the copyright owners for my use of their work, which is beyond the scope of the law. I agree to indemnify and save harmless Purdue University from any and all claims that may be asserted or that may arise from any copyright violation.

Sandeep Ayyar
Printed Name and Signature of Candidate

7/13/2012
Date (month/day/year)

*Located at http://www.purdue.edu/policies/pages/teach_res_outreach/c_22.html

THE MOLECULAR MECHANISM OF BREAK INDUCED REPLICATION

A Thesis

Submitted to the Faculty

of

Purdue University

by

Sandeep Ayyar

In Partial Fulfillment of the

Requirements for the Degree

of

Master of Science

August 2012

Purdue University

Indianapolis, Indiana

My beloved parents have always strived, for me to be able to pursue and realize my dreams. I dedicate this work to them.

AKNOWLEDGEMENTS

Coming with no prior research experience, my masters' thesis demanded a lot of hard work and perseverance. My mentor, Dr. Anna Malkova provided unwavering support, motivation and enthusiasm to help me adjust to these demands. She has deeply influenced my inclination and dedication towards research, higher education and science. I thank her for all her support and care.

I express gratitude towards my committee members Dr. Teri Belecky-Adams and Dr. Andrew Kusmierczyk. They have provided valuable inputs from time to time and have shown encouraging interest in my work. I thank them for all their consideration and help.

I have been able to achieve successful masters because I always enjoyed working as a researcher. This enjoyment came from working in the Anna Malkova lab, an ambitious, competitive yet friendly lab where Anna, Sreejith, Angie, Cynthia, Ruchi, Soumini, Yu-Hsiang, Rajula, Robert, Kelsey, Megan, Caleb, Andrew, David, Corrine, Jacob and *Saccharomyces Cerevisiae* have provided a wonderful environment. I thank them all for their sheer presence.

The Biology Department including Faculty, Staff and fellow researchers gave me an opportunity to participate in really good science. My family, friends and my extended family here at IUPUI have been my pillars of strength and source of inspiration. It is their support that I can never forget.

TABLE OF CONTENTS

Page

Page

Page

LIST OF TABLES

LIST OF FIGURES

LIST OF ABBREVIATIONS

ALT	Alternative Telomere Lengthening
BIR	Break-Induced Replication
dNTP	deoxyribonucleotide triphosphate
DNA	Deoxyribonucleic Acid
DSB	Double-Strand Break
DSBR	Double-Strand Break Repair
GC	Gene Conversion
GCR	Gross Chromosomal Rearrangement
HR	Homologous Recombination
IR	Ionizing Radiation
MHEJ	Microhomology-Mediated End Joining
NHEJ	Non-Homologous End Joining
PCR	Polymerase Chain Reaction
PFGE	Pulsed-Field Gel Electrophoresis
Pol	Polymerase
SDSA	Synthesis-Dependent Strand Annealing
SSA	Single-Strand Annealing
ssDNA	Single-stranded DNA

ABSTRACT

Ayyar, Sandeep. M.S., Purdue University, August 2012. The Molecular Mechanism of Break Induced Replication. Major Professor: Anna Malkova.

DNA double strand break (DSB) is one of the most threatening of all types of DNA damages as it leads to a complete breakage of the chromosome. The cell has evolved several mechanisms to repair DSBs, one of which is break-induced replication (BIR). BIR repair of DSBs occurs through invasion of one end of the broken chromosome into a homologous template followed by processive replication of DNA from the donor molecule. BIR is a key cellular process and is implicated in the restart of collapsed replication forks and several chromosomal instabilities. Recently, our lab demonstrated that the fidelity of DNA synthesis associated with BIR in yeast *Saccharomyces Cerevisiae* is extremely low. The level of frameshift mutations associated with BIR is 1000-fold higher as compared to normal DNA replication. This work demonstrates that BIR stimulates base substitution mutations, which comprise 90% of all point mutations, making them 400-1400 times more frequent than during S-phase DNA replication. We show that DNA Polymerase δ proofreading corrects many of the base substitutions in BIR. Further, we demonstrate that Pif1, a 5'-3' DNA helicase, is responsible for making BIR efficient and also highly mutagenic. Pif1p is responsible for the majority of BIR mutagenesis not only close to the DSB site, where BIR is less stable but also at chromosomal regions far away from the DSB break site, where BIR is fast, processive and stable.

This work further reveals that, at positions close to the DSB, BIR mutagenesis in the absence of Pif1 depends on Rev3, the catalytic subunit of translesion DNA Polymerase ζ. We observe that mutations promoted by Pol ζ are often complex and propose that they are generated by a Pol ζ- led template switching mechanism. These complex mutations were also found to be frequently associated with gross chromosomal rearrangements. Finally we demonstrate that BIR is carried out by unusual conservative mode of DNA synthesis. Based on this study, we speculate that the unusual mode of DNA synthesis associated with BIR leads to various kinds of genomic instability including mutations and chromosomal rearrangements.

CHAPTER 1. INTRODUCTION

1.1 Objectives

The overall goal of this research was to investigate the molecular mechanisms responsible for Break Induced Replication, a homologous recombination based DNA double strand break repair pathway. This research is described with respect to the following specific aims:

1. To identify the genetic components responsible for BIR associated frameshift mutagenesis.

2.To investigate the phenomenon of base substitutions associated with BIR.

3. To determine the mode of DNA synthesis associated with BIR.

1.2. Organization

Chapter 2 in the thesis provides a literature review to familiarize the reader in the field of DNA repair and genomic instabilities with a special focus on HR repair mechanisms, especially BIR. The Materials and Methods used in this research are described in Chapter 3. Data obtained during this research are presented and discussed in Chapters 4, 5 and 6. Chapter 4 summarizes findings related to the pathways of mutagenesis in BIR, Chapter 5 describes the phenomenon of base substitutions associated with BIR and Chapter 6 describes the mode of synthesis associated with BIR.

CHAPTER 2. LITERATURE REVIEW

2.1 DNA double-strand breaks threaten genomic integrity

DNA breaks can compromise genomic integrity and if not repaired can result in loss of important genetic information. DNA breaks can be divided in two categories: single-strand breaks and double-strand breaks. Single-strand breaks in double-stranded DNA (commonly produced during repair mechanisms such as base excision repair, nucleotide excision repair, oxidative damage etc.) do not pose a critical problem to the cell since the double helix maintains its overall intactness and the break can be repaired easily by template-dependent DNA synthesis. A double stranded break (DSB) poses a more serious problem as the double helix is converted into two separate fragments, which have to be brought back together to repair the break and restore the original double helix. Hence a DSB is the most threatening of all breaks since the linear integrity of the chromosome is lost.

DSBs may arise at stalled replication forks, due to advancement of replication fork over pre-existing nicks/ lesions in the DNA backbone (Aguilera, 2005; Kuzminov, 1997), by excision of DNA transposable elements, due to inability of topoisomerases in completing their strand breakings and re-joining. DSBs may also be the result of mechanical stress such as formation of dicentric chromosomes (chromosomes with two centromeres), exposure to ionizing radiation (or ultraviolet light), other chemical agents or also by site-specific cleavage activities of endonucleases. DSBs are also made in the cell in a controlled fashion during genome rearranging activities of T cells and B cells of immune

system (to generate antibody diversity of immunoglobulin molecules in immune system). DNA double strand breaks pose an important threat to genomic integrity. Failure to repair DSBs can lead to chromosome aberrations (Natarajan et al*.,* 1980), affecting many genes in the process, and lead to genomic instability that causes cell death and malfunctioning (Reviewed in Van Gent et al., 2001). Hence repair of DSBs is crucial towards maintaining genomic integrity.

2.2 Yeast *Saccharomyces Cerevisiae* as our model organism to study repair of DSBs

Saccharomyces Cerevisiae (S. Cerevisiae) serves as a simple experimental system to study DSB break repair mechanisms. The availability of a relatively small and completely sequenced genome makes *S. Cerevisiae* a powerful eukaryotic model system where gene manipulations are easy. Several genes and mechanisms are conserved from yeast to higher eukaryotes and therefore studying of yeast DNA repair pathways provides valuable insight into DSB repair of mammals and humans.

Our experimental system to study repair of DNA DSBs utilizes an HO endonuclease mediated generation of DSBs. The system exploits the natural phenomenon of mating type-switching that exists in yeast. Haploid yeast cells use mating type switching as means of forming diploids. They achieve this through a DSB created at *MAT* locus on CHRIII that is repaired by recombination with one of two silenced donor cassettes, present at either end of the chromosome (Strathern et al., 1982). This DSB is created by a specific HO-endonuclease (makes a 4bp cut at a 24bp recognition site), encoded by an HO gene. The HO gene was cloned under the regulation of a galactose promoter (Jensen and Herkowitz, 1984) and is now frequently used in research aiming to understand mechanisms of DSB repair in yeast. In our system, it serves as a useful tool to monitor the repair of DSBs by various methods.

2.3 DSB repair pathways in *S. Cerevisiae*

DSB repair can occur by two primary mechanisms: 1. Homologous Recombination (HR) mechanisms that utilize extensive homology or nearly perfectly matched DNA sequences as a condition for DSB repair 2. Non-homologous end joining (NHEJ) mechanism or illegitimate repair that can repair DSBs by simple ligation of broken DNA ends (end joining) without any requirement of homology.

2.3.1 Non-Homologous End Joining

A Non Homologous End Joining (NHEJ) pathway, without a homologous donor template, can repair DSBs. NHEJ typically utilizes very short homologous sequences to directly ligate the ends of broken chromosomes. These short homologous sequences are usually present at the ends of the broken DNA as single strand overhangs. When these ends are compatible, NHEJ can repair breaks very accurately. However, NHEJ is often accompanied by insertions and deletions when overhangs are incompatible (Daley et al., 2005).

Alternatively, in the absence of the NHEJ pathway, an end joining mechanism similar to NHEJ can also repair DSBs. This pathway called microhomology- mediated end joining (MMEJ) occurs in the absence of Ku protein, an essential NHEJ repair protein, and when the overhanging ends have limited complementary base pairs (or very short homology- called micro-homology; Ma et al., 2003).

Even though the genetic control of NHEJ and MMEJ are different, both are essential in repairing DNA DSBs in the absence of a homologous donor template (Lee and Lee, 2007; Ma et al., 2003). As opposed to yeast where HR is the dominant mechanism to repair DSBs, NHEJ is reported to occur frequently in mammalian cells. This process is critical in the generation of antibody diversity through a process called VDJ recombination (Stavnezer et al., 2008; Sonoda et al., 2006).

2.3.2 Homologous Recombination

Homologous Recombination (HR) is the DNA repair mechanism that uses genetic information of a homologous DNA sequence as a template to repair DNA breaks. The choice of template molecule utilized determines the fate of or genetic consequences of DNA repair. Sister chromatid recombination utilizes the identical and intact sister chromatid, as its preferred template (Kadyk and Hartwell, 1992). This type of recombination is the most secure form of recombination repair and maintains genome integrity. The fact that a large amount of DSBs occur during S-phase replication make such type of sister chromatid recombination the major recombination event in mitotic cells of yeast to mammals (almost 10% of cells undergoing S-phase replication incur DSBs (Reviewed in Aguilera, 2007). Hence, HR repair is often coupled with replication and is highly active in S and G2 phase of cell cycle (Ayalon et al., 2004; Ira et al., 2004). However, allelic (using a homologous chromosome) or ectopic recombination (other homologous chromosomes located elsewhere in the genome to repair DSBs) can compromise genomic integrity by causing deletions, inversions, translocations or loss of heterozygosity.

Three types of HR mechanisms are known to exist in yeast cells: gene conversion (GC), single strand annealing (SSA) and break-induced replication (BIR).

2.3.2.1 Gene conversion

In *S. Cerevisiae* GC, or non-reciprocal transfer of genetic information from molecule to its homologue, is the preferred or dominant pathway of DSB repair. GC requires both ends of a DSB to share homology with DNA sequences located on a homologous chromosome. Using this homology as a template, GC repairs the DSB with a short patch DNA synthesis. Two forms of GC are known to exist; gene conversion associated with crossing over of flanking DNA sequences (frequently occurs in meiotic cells) and gene conversion without crossing over (frequent in mitosis).

The Szostak et al. Model (1999) best explains GC associated with crossing over. It is based on the DSB repair model suggested by Resnick and Martin (1976) and early conceptions by Holliday (1964) and Messelson (1975). According to Szostak model, (Figure 2.1) DSB formation is followed by a 5’ to 3’ resection of the ends; the resulting 3’ ends can then initiate recombination by invading a homologous template to begin new DNA synthesis. Two Holliday Junctions (a mobile junction between 4 strands of DNA) are formed (Figure 2.1A) and are independently resolved either by cutting the crossed (open arrowhead) strands (Figure 2.1B) or noncrossed (closed arrowhead) strands (Figure 2.1B), resulting in crossover or noncrossver products respectively. Mitotic GC not associated with a crossing over event proceeds through synthesis dependent strand annealing (SDSA) (Ira et al., 2003; Paques and Haber, 1999) which does not involve formation of Holliday Junctions. During SDSA, 5’ to 3’ resection on both sides of the DSB is followed by invasion of at least one of the ssDNA ends into the donor sequence to initiate DNA synthesis (Figure 2.1D-E). This model suggests that the newly synthesized strands are displaced from the template and anneal to each other leading to conservative DNA synthesis (all newly synthesized sequences are on the same molecule). Conversely the Szostak model suggests that such an event could occur by topoisomerases or helicases that continuously disassemble the replication structure, resulting in newly synthesized strand being continuously unwound from its template leading to semiconservative DNA.

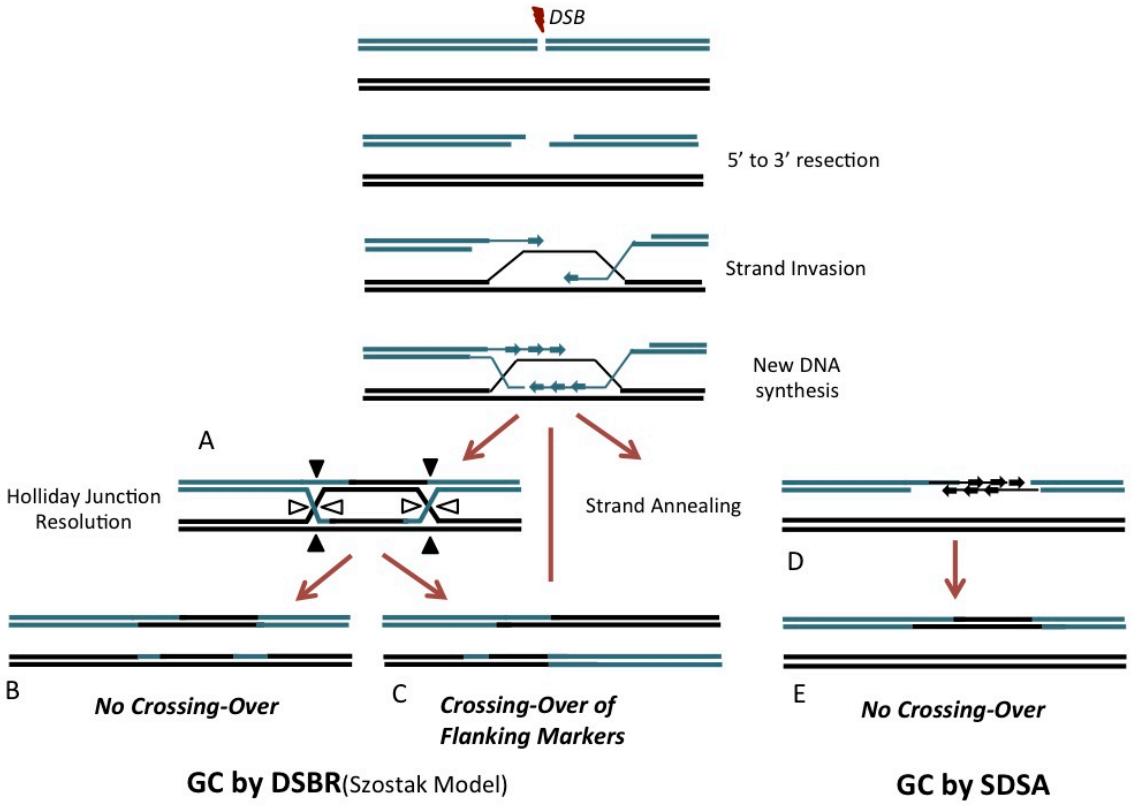

Figure 2.1 DSB repair by BC. Repair of DSBs by GC can occur through two mechanisms. 1. GC by DSBR. During meiosis, invasion of both sides of the DSB into the homologous donor template requires resolution of Holliday Junctions and results in an approximately equal distribution of crossover versus non-crossover events. 2. GC by SDSA. Mitotic GC does not require HJ resolution. After invasion of one side of DSB followed by DNA synthesis, the duplex molecule dissociates and re-anneals to the other side of the lesion, making crossover events less unlikely.

2.3.2.2 Break Induced Replication

BIR, unlike GC, repairs DSBs that have only one end available for homologous recombination. Previous studies demonstrated a BIR-like recombination in phage T4 (Mosig et al., 1982; Alberts, 1986). Later, studies in *E. coli* showed that one end of the chromosome can initiate replication in a recombination dependent manner in bacteria (Asai et al., 1994; Kuzminov et al., 1999). Subsequent investigations in yeast showed that BIR could repair DSBs in eukaryotes. It was shown that initiation of BIR occurs by a one-ended invasion into a homologous template chromosome followed by extensive DNA synthesis till its end (Malkova et al., 1996; Morrow et al., 1997; Bosco and Haber, 1998; Davis and Symington, 2004; Pacques and Haber, 1999). BIR is important in yeast to preserve genomic stability where it is implicated in the telomerase independent-maintenance of telomeres, known as alternative telomere lengthening (Dunn et al., 1984; Volrath, 1988; Lundbald and Blackburn, 1993; Lydeard et al., 2007). Studies in bacterial systems suggested that stalled or collapsed replication forks occurring during normal DNA replication can be converted into functional replication forks by recombination mechanisms such as BIR (Kusminov et al., 1999). The stalled structures are converted to double strand breaks by specific recombination pathways that can further resolve fork structures (Signeur et al., 1998). The resulting broken chromosome can recombine with an intact chromosome to produce a new replication fork. These observations suggested a possible role of BIR in restarting collapsed replication forks.

According to the current models (Figure 2.2), BIR is initiated by a 5’ to 3’ resection of the broken chromosome following DSB (bound by Rad51) and invasion of 3’single strand end into a homologous donor sequence. This invasion results in assembly of a replication fork that carries extensive DNA synthesis proceeding along the entire length of the template chromosome. This repair replication fork mimics S-phase fork in the rate and processivity at which it proceeds (Malkova et al., 2005). Also, the initiation of BIR requires participation of all factors that are required for initiation of S-phase DNA replication (Lydeard et al., 2010). The early steps are slow and it takes approximately 4-6

hours to initiate BIR replication (Malkova et al., 2005). It was suggested that BIR is unstable at the beginning, and this explains the delayed initiation of BIR replication (Smith et al., 2007). In particular, it has been proposed that BIR frequently undergoes multiple rounds of dissociation and re-invasion before processive replication starts. Jain et al. (2009) proposed an existence of a “recombination execution checkpoint”, which delays initiation of BIR (Jain et al., 2009).

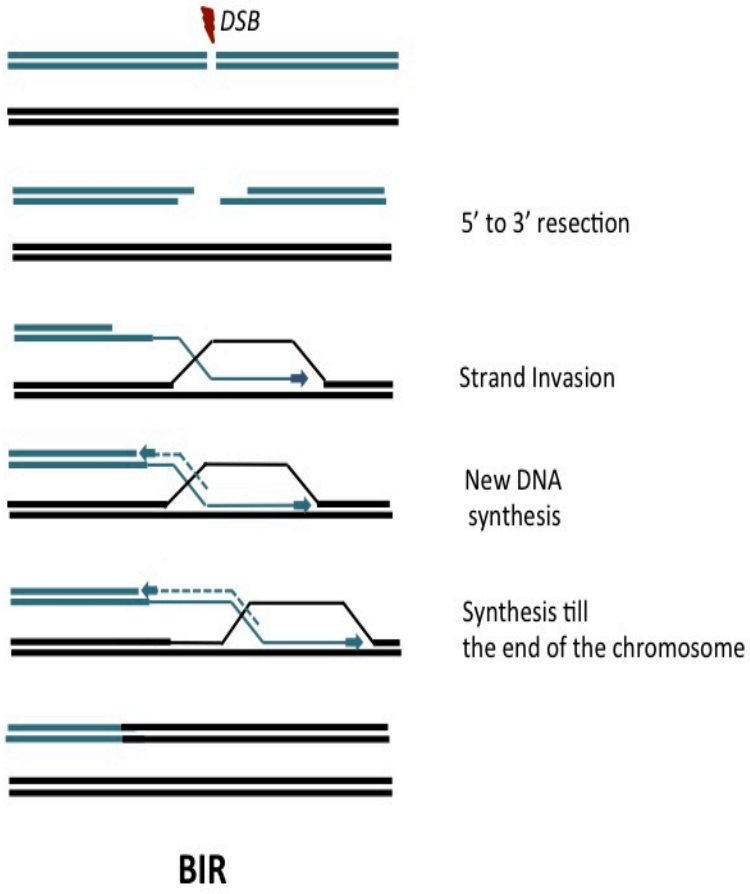

Figure 2.3 DSB repair by BIR. BIR can initiate if a DSB results in a broken chromosome having only one ended homology to a donor template. Following a DSB, 5' to 3' resection exposes 3' end to invade into homologous chromosome (preferably sister chromatid). Strand invasion is followed by continued DNA synthesis from the donor chromosome till the end to fully repair the broken chromosome.

2.3.2.3 Single Strand Annealing

If a DSB occurs between two homologous regions that are forming direct repeats, then the repair of the break is very efficient and occurs by single strand annealing (SSA), a mechanism that was first proposed by Lin et al. (1995) for mammalian DNA repair. As shown in Figure 2.3 SSA proceeds by resection of the ends of DSB resulting in long single stranded tails, exposing the complementary strands in such a way that they can anneal. After annealing of complementary sequences, the extra flaps are clipped off and the resultant gap filed by gap repair. SSA has nearly 100% efficiency in yeast when the homologous regions flanking the DSB are close to 400bp. Repair of DSB is efficient by SSA even if the repeats are as far as 15kb. It is a slow process as compared to GC and takes approximately 6hrs to complete.

Since the repair product involves deletion of intervening sequences, SSA is a dangerous and unfavorable pathway of DSB repair when compared to GC. In spite of this, it has been shown that SSA efficiently competes with GC in repairing 3% of DSBs even when a homologous sequence for GC is available.

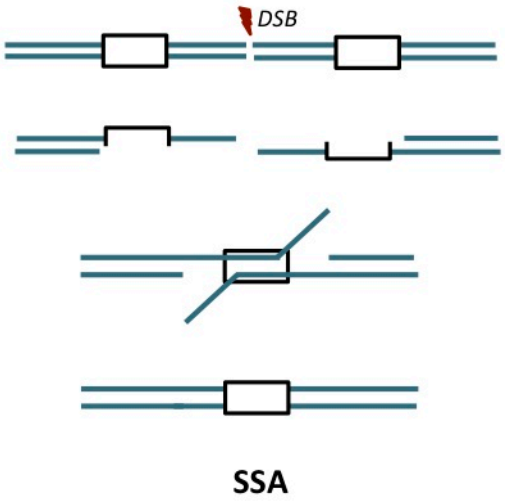

Figure 2.3 DSB repair by SSA. SSA can occur if DSB is flanked by two direct repeats (boxes). 5’ to 3’ resection of DSB ends produces complementary single strands that are annealed to each other. Following excision of non-complementary ends and subsequent DNA synthesis, gaps are filled by ligation.

2.4 The Mechanism of Homologous Recombination

The initial steps in the HR mechanisms described above are essentially the same and can be divided into 3 stages: Pre-synapsis, Synapsis and Post Synapsis. Pre-synapsis is the DNA lesion processing stage to form a Rad51-ATP ssDNA filament (presynaptic /nucleoprotein filament). It is followed by the synapsis stage where the presynaptic filament performs homology search and DNA strand exchange leading to a Displacement loop (D-loop) intermediate by strand invasion. All further steps including release of Rad51 from the heteroduplex DNA, mismatch repair (MMR), DNA synthesis and processing of various junction intermediates constitute post synapsis. Postsynaptic events vary from pathway to pathway.

2.4.1 Pre-synapsis

The repair of DNA DSBs by HR requires that the ends of the broken DNA be available in the form of 3' single stranded DNA (ssDNA) tails or overhangs. These form substrates for the Rad51 strand exchange protein. The switch from DSB to ssDNA is also necessary for activation of ATR-mediated checkpoint response. As the resected DNA ends are inhibitory to NHEJ, DNA resection is the critical step that differentiates HR from NHEJ, thus directing the choice of repair pathway (Lee et al., 1998; Aylon et al., 2004; Ira et al., 2004; Mimitou and Symington, 2008; Bernstein and Rothstein, 2009). This resection is cell cycle regulated in such a way that it occurs during the S and G2 phase of the cell cycle when the sister chromatid is available to provide an accurate template for HR repair.

Shortly after a DSB is formed, the MRX complex comprising of Mre11, Rad 50 and Xrs2 (analogous to mammalian MRN complex where N-Nbs1) is recruited to the DNA ends. MRX co-operates with Sae2 endonuclease to remove short oligonucleotides from the 5' end of the DNA. This forms the early part of DNA end resection or the initial resection (Zhu et al., 2008). MRX and Sae2 proteins are not only responsible for the onset of

resection but also inhibit the NHEJ protein Ku from DSB ends. MRX and Sae2 then perform the essential function of assembling the exonucleases Exo1 or helicases Sgs1 (along with the endonuclease Dna2) to DNA ends, which carry out further extensive or long-range end resection i.e. further degradation of DNA ends (Reviewed in Huertas, 2010). Recent literature demonstrates that these two pathways i.e. Exo1 and Sgs1-Dna2 are somewhat redundant (Zhu et al., 2008).

Extensive resection, occurring in 5' to 3' direction results in exposure of 3' end of ssDNA. A free 3' ssDNA end is quickly bound by RPA (the homolog of *E. coli* SSB), which serves to counteract formation of secondary structures in ssDNA, especially when ssDNA substrates are long. This is particularly important for Rad51-mediated reactions since Rad51 can readily bind to dsDNA that forms as secondary structure in ssDNA. Such an event would interfere formation of a functional presynaptic filament on ssDNA. RPA also functions in DNA strand exchange by binding to the displaced strand and preventing reverse reaction during DNA strand exchange (Sung et al., 1994; Sugiyama et al., 1997; Sigurdson et al., 2001). For SSA repair, RPA coated ssDNA is bound by Rad52p, which enables annealing between the exposed, complementary sequences on ssDNA and repair is completed by repair synthesis and ligation (Sugiyama et al., 1998; Krogh and Symington, 2004).

For GC and BIR, it is essential that Rad51 strand exchange protein displaces RPA and binds ssDNA, thus forming nucleoprotein filament. This reaction is mediated by a group of proteins (in yeast) called recombination mediators (Beernick and Morrical, 1999; Sung et al., 2003). In yeast, mediator proteins include Rad52, Rad55, and Rad57 (Sung, 1997). Rad52 specifically interacts with Rad51 and RPA (Shinohara et al., 1992) and is critical for displacement of RPA from ssDNA by Rad51 (Sugiyama and Kowalczykowski, 2002). It also helps facilitate strand exchange by pairing complementary sequences of the presynaptic nucleoprotein filament and the donor chromosome. Rad55 and Rad57

directly interact with Rad51 and help forming the Rad51 nucleoprotein filament (Johnson and Symington, 1995; Sung, 1997).

2.4.2 Synapsis

The synapsis step occurs after pre-synapsis where Rad54 assists the Rad51 nucleoprotein filament Rad51 in its DNA bound form stimulates the ATPase and motor activity of Rad54 (Heyer et al., 2006). Rad54 then enhances the pairing activities of Rad51. The following possibilities exist to explain how Rad54 helps Rad51, 1) by sliding of target duplex DNA during homology search, or 2) by topological opening of target duplex DNA, or 3) by clearing of Rad51 bound protein to the target DNA, or 4) by Rad54 mediated chromatid remodeling (Alexeev et al., 2003; Jaskelioff et al., 2003).

2.4.3 Post Synapsis

Post synaptic phase of DSB repair involves the following steps: 1) Strand exchange, 2) initiation of DNA synthesis, 3) and branch migration. Strand Exchange involves the following steps. After DNA strand invasion, Rad51 requires ATP hydrolysis to release the resulting heteroduplex DNA. This release allows DNA polymerases to access the invading 3’ end. A Rad54 mediated ATP-dependent turnover of Rad51 is responsible for dissociating Rad51 from the dsDNA. Also during homologous recombination, the invading DNA strand used as a primer for DNA synthesis contains some non-homologous bases at the 3’ end that must be removed (especially during strand interruption occurring in an area of non-homology). In yeast, such heterologies are processed by Rad1-Rad10 family of proteins having 3’ flap endonuclease activity, together with mismatch proteins Msh2, Msh3 and the Srs2 helicase (Ivanov and Haber, 1995; Paques and Haber, 1997). Smaller heterologies may also be processed by the 3’ to 5’ exonuclease activity of Pol δ. The exact biochemical mechanisms of these pathways remain to be determined.

DNA synthesis follows strand invasion and is critical for restoring the genetic information lost due to the DSB. Both GC and SSA are known to proceed through repair synthesis which involves essential polymerases δ (Pol 3) and ε (Pol 2) without formation of a replication fork (Hicks et al., 2010; Wang et al., 2004). Some non-processive translesion polymerases Pol ζ (Rev3, Rev7) and Pol η (Rad30) are also involved in repair synthesis (Rattray and Strathern, 2003; Hirano and Sugimoto, 2006).

DNA synthesis from the homologous template is associated with simultaneous branch migration i.e. progressive movement of the D-loop/Holliday Junction. Several studies have indicated that Rad54 might play a role in branch migration (Kim et al., 2002). Resolution of the Holliday Junction occurs post synapsis and is mediated by specialized helicases such as BLM, WRN (in humans) (Van Brabant et al., 2000; Orren et al., 2002), Mus81-Mms4 (Interthal and Heyer, 2000) and Sgs1 (in yeast) (Ira et al., 2003; Rockmill et al., 2003; Sugawara et al., 2004).

DNA synthesis during BIR proceeds differently from SSA or GC, as it is believed to involve formation a real replication fork with both leading and lagging strands. Support for this belief come from several lines of evidence. All 3 major replicative polymerases (δ, ε and α) involved in BIR (Lydeard et al., 2007) including the non-essential Pol32 subunit (Lydeard et al., 2007) participate in BIR DNA synthesis. BIR requires the replicative DNA helicases Cell Division Cycle (Cdc) 45, the GINS (Go, Ichi, Nii and San; five, one, two and three in Japanese) complex, McM (mini chromosome maintenance) 2-7 and C-terminal Domain (Ctd) 1. Cdc7 kinase, necessary for both initiation of DNA replication and post replication repair is also required for BIR. Therefore, almost all proteins in S-phase replication initiation are involved in initiating BIR. Also, kinetics of repair suggests that DNA is synthesized at a processive rate comparable to a S-phase replication fork. Such evidence supports the idea that BIR might be bonafide replication restart mechanism following DSB.

2.5 Significance of studying the molecular mechanism of BIR

Apart from its possible role in restarting collapsed replication forks; BIR is implicated in promoting a number of genomic instabilities. 1) BIR is proposed to elongate telomeres which are lost in the absence of telomerase or when telomeres are uncapped (McEachern and Haber, 2006). A BIR-recombination dependent mechanism, known as alternative lengthening of telomeres, has been proposed for telomere elongation in tumors in humans (Dunham et al., 2000). 2) BIR repair of DSBs by allelic or ectopic recombination leads to a loss of heterozygosity (LOH), if the homologous are polymorphic (Malkova et al., 2005; Bosco and Haber, 1998) and are especially dangerous as BIR involves extensive synthesis of DNA regions. 3) BIR or BIR-related mechanisms have been suggested to promote formation of copy number variation (alterations in genomic DNA that result in cell having abnormal number of copies of one or more sections of the DNA: these maybe deletions, insertions, duplications, triplications, inversions, etc.) in several genomic disorders and cancers (Payen et al., 2008; Lee et al., 2007; Hastings et al., 2007). The consequences described above are all hallmarks of carcinogenesis and are commonly encountered in many tumor cells. Hence BIR represents an important phenomenon responsible for the rescue of collapsed replication forks and in generation of genomic instability.

Maintaining genome stability is critical for cell survival and normal cell growth. Most human cancer cells show marks of genome instability ranging from high mutagenesis rates, to gross chromosomal rearrangements and aneuploidy (alterations in chromosome number; Kolodner et al., 1996). Traditionally cancer cells were divided into two fundamental classes of genetic instability (reviewed in Vogelstein et al., 1998):
1. Those showing increased rates of point mutations (base substitutions or single nucleotide deletions or insertions) and frameshift mutations; 2. Those having increase rates of chromosome instability including chromosomal translocations (involving fusions of different chromosomes or of non-contiguous segments of single chromosome), aneuploidy (alterations in chromosome number involving loss or gain of whole

chromosomes) and gene amplifications (amplicons containing 0.5-10 megabases of DNA which are different from duplications of large chromosome regions resulting from translocations or aneuploidy). Several cases have been described in which the two phenotypes may co-exist (Abdel-Rahman et al., 2001). Genome rearrangements may not be restricted to cancer but may also be a vital characteristic in a number of other diseases and evolution.

The molecular mechanisms that generate such instability or how it remains suppressed in normal cells remains unknown. Studies in the powerful eukaryotic model system yeast *S. Cerevisiae* have implicated several genes, including those functional in S-phase checkpoints, recombination and telomere protection as critical towards maintaining genomic stability. Human homologs of several of these genes have documented roles as tumor suppressors. Such demonstrations are in agreement with the suggestion that mechanisms that preserve genomic integrity in yeast are the same ones that go haywire in cancer.

Therefore understanding the underlying molecular mechanisms of DNA repair processes is critical. My research, in trying to unravel the molecular mechanisms of BIR in yeast, is important in understanding pathways of genomic instability and advancing knowledge towards more complex systems in higher eukaryotes, especially humans.

CHAPTER 3. MATERIALS AND METHODS

3.1 Materials

3.1.1 Strains

All the strains used along with their genotypes are shown in Table 3.1. All of the strains were originally derived from AM1003-9 (described in Deem et al., 2008). AM1003-9 is a disomic with the phenotype: *hmlΔ::ADE1/hmlΔ::ADE3 MATα-LEU2-tel/MATα-inc hmrΔ::HYG FS2Δ::NAT/FS2 leu2/leu2-3,112 thr4 ura3-52 ade3::GAL::HO ade1 met13.* In this strain sequences centromere distal to *MATα* portion of CHRIII were deleted leaving only 46bp homology to the donor chromosome ensuring a very low frequency of gene conversion, and therefore the high efficiency of BIR in repairing HO-endonuclease induced DSBs at *MATα*.

Strains used in assaying BIR-induced frameshift mutagenesis were derived from AM1291, AM1411 and AM1482 (described in Deem et al., 2011) carrying *lys2::ins* frameshift reporters. Single gene deletion mutants (*pif1Δ and rev3Δ*) were constructed by using two types of disruption-deletion cassettes having dominant drug resistance while maintaining isogenecity to AM1003-9. These were constructed either using PCR-derived *kanMX* (G418-KANAMYCIN) (Wach et al., 1994) cassette or PCR-derived *BSD* (Blasticidin S-Hydrochloride) cassette having specific flanking sequences homologous to the open reading frame of respective genes, followed by transformation and selection

on appropriate antibiotic media selecting for gene expressing drug resistance. *Pif1Δ* in AM1291, AM1411, AM1482, AM2268, made by *kanMX* disruption, were confirmed by PCR using a combination of oligonucleotides OL26, OL384 and OL27, OL399. Absence of *PIF1* was confirmed by PCR reaction using oligonucleotides OL399, OL1623. *Pif1Δ* in AM2161, AM2452 and AM2459 by BSD disruption were confirmed by PCR using a combination of oligonucleotides OL1733, OL399 and OL1734, OL384*. Rev3Δ* in AM2191, AM2161, AM2453 and AM2459 by BSD disruption were confirmed by PCR using a combination of oligonucleotides OL1733, OL1196 and OL1734, OL1198. Double mutants *pif1Δrev3Δ* were made using a combination of the above-mentioned cassettes and were similarly confirmed by PCR. *Pif1-m2* (point mutation altering the second ATG codon in the open reading frame of Pif1) strains were constructed by transforming AM1291, AM1411 and AM1482 with pJH1928 digested by Hind III to replace Pif1 by *pif1-m2*. These transformants were then confirmed by PCR amplification and digestion with XhoI endonuclease. (*Pif1-m2* mutation creates a new XhoI restriction site).

Strains used for assaying BIR induced base substitutions were derived from AM1003-9. AM2072 was constructed by deleting the WT *URA3* gene from its native position in chromosome V by *delitto perfetto* approach (Storici et al., 2001). This was achieved in two steps. First AM2048 was created by transformation of AM1003-9 by a DNA fragment obtained by PCR amplification of pCORE cassette (Storici et al., 2001). pCORE integration was confirmed by PCR using a combination of oligonucleotides OL103, OL1384 and OL104, OL1385. AM2072 was then derived by transformation of AM2048 by a mixture of complementary oligonucleotides OL293, OL294 having homology on either side of *URA3* gene. *URA3* deletion (i.e. pCORE deletion) was confirmed by PCR using oligonucleotides OL1384, OL1385. AM2110 was then derived from AM2072 by replacement of *HMRΔ::HPH* by a DNA fragment containing *HMRΔ::KAN* generated by PCR amplification of *kanMX* cassette (Wach et al., 1994). Base substitution reporter *ura3-29* (Scherbakova and Pavlov, 1993), marked by *HPH* cassette, was PCR amplified by 3 different combinations of oligonucleotides to transform AM2072. By this method,

three derivatives of AM2072 were created, bearing *ura3-29* reporter at three different positions. In particular, AM2452 was created by inserting ura3-*29* at *MATα-inc* gene ("*MAT"* position) by using OL1721, OL1722 oligonucleotides; AM2161 was created by inserting *ura3-29* inserted at the "16kb position" between *RSC6* and *THR4* using OL1516, OL1518 and AM2459 was created by inserting *ura3-29* at the "36kb position" between *SED4* and *ATG15* using OL1740, OL1741. All strains were confirmed by PCR and by phenotype.

Proofreading deficient mutants *pol3-5DV* (Jin et al., 2005) and *pol2-4* (Morrison et al., 1991) were constructed as described in Jin et al. (2005) and Morrison et al. (1991) respectively and confirmed by PCR and sequencing (primers used are described in Table 3.2). No-DSB control strains (strains lacking *GAL::HO* site) were obtained by plating each experimental strain on Leucine dropout galactose media to select for Leu^+ colonies. These Leu^+ colonies, resistant to *HO* endonuclease, contained *MATα-inc* allele that was transferred in *MATα* by gene conversion. Wild Type (WT) strains carrying frameshift reporters at 16kb and 36kb were used for determining the mode of synthesis associated with BIR. These strains were modified by transforming them with a plasmid carrying flanking sequences homologous to the donor copy (*MATα-inc* containing copy) of CHRIII, marked by BSD. This modification led to the increased length of the *MATα-inc* – containing chromosome, by which better separation of BIR product from the donor chromosomes by pulse field gel electrophoresis could be performed (Chapter 6).

Table 3.1 List of *Saccharomyces Cerevisiae* strains used in this study

Strain	Genotype	Source
AM1003-9	*MATα-LEU2-tel/MATα-inc ade1 met13 ura3-52 leu2-3,112/leu2-3,112 thr4 hmlΔ::ADE1/hmlΔ::ADE3 hmrΔ::HYG ade3::GAL-HO FS2Δ::NAT*	Deem et al., 2008
AM1284	AM1003-9, but lys2Δ THR4 LYS2	Barbara Coffey (Malkova Lab)
AM2048	AM1284, but *ura3::pCORE*	
AM2072	AM2048, but *ura3Δ*	This Study
AM2110	AM2072, but *hmr::KAN*	This Study
AM2161	AM2072, but *ura3-29* on CHRIII at the "16kb" position	This Study
AM2259	AM2161, but *MATα-inc-LEU2-tel/MATα-inc (NO-DSB)*	This Study
AM2260	AM 2161, but *MATα-inc-LEU2-tel/MATα-inc(NO-DSB)(similar to AM2259, but independent GC outcome*	This Study
AM2271	AM 2161, but *pol2-4*	This Study
AM2471	AM 2271, but *MATα-inc-LEU2-tel/MATα-inc (NO-DSB)*	This Study

Table 3.1 List of *Saccharomyces Cerevisiae* strains used in this study (continued)

Strain	Genotype	Source
AM2425	AM2161, but *pol3-5DV*	This Study
AM2472	AM2425, but *MATα-inc-LEU2-tel/MATα-inc (NO-DSB)*	This Study
AM2415	AM2161, but *pif1Δ::BSD*	This Study
AM2475	AM2415, but *MATα-inc-LEU2-tel/MATα-inc (NO-DSB)*	This Study
AM2461	AM2161, but *rev3Δ::BSD*	This Study
AM2476	AM2461, but *MATα-inc-LEU2-tel/MATα-inc (N0-DSB)*	This Study
AM2452	AM2110, but *MATa-LEU2-tel/MATα-inc::ura3-29*	This Study
AM2476	AM2452, but *MATα-inc::ura3-29-LEU2-tel/MATα-inc::ura3-29 (NO-DSB)*	This Study
AM2469	AM2452, but *pif1Δ::BSD*	This Study
AM2478	AM2469, but *MATα-inc::ura3-29-LEU2-tel/MATα-inc::ura3-29 (NO-DSB)*	This Study

Table 3.1 List of *Saccharomyces Cerevisiae* strains used in this study (continued)

Strain	Genotype	Source
AM2459	AM2110, but *ura3-29 on CHRIII at the "36kb" position*	This Study
AM2479	AM2459, but *MATα-inc-LEU2-tel/MATα-inc (NO-DSB)*	This Study
AM2454	AM2459, but *pif1Δ::BSD*	This Study
AM2480	AM2454, but *MATα-inc-LEU2-tel/MATα-inc (NO-DSB)*	This Study
AM2462	AM2459, but *rev3Δ::BSD*	This Study
AM2481	AM2462, but *MATα-inc-LEU2-tel/MATα-inc (NO-DSB)*	This Study
AM1411	AM1003-9, but *MATα-LEU2-tel/MATα-inc::lys2::Ins (A_4)*	Deem et al., 2011
AM1291	AM1003-9, but *lys2::Ins (A_4)* on CHRIII at the "16kb" position	Deem et al., 2011
AM1482	AM1003-9, but *lys2::Ins (A_4)* on CHRIII at the "36kb" position	Deem et al., 2011

Table 3.1 List of *Saccharomyces Cerevisiae* strains used in this study (continued)

Strain	Genotype	Source
AM1449	AM1291, but *MATα-inc-LEU2-tel/MATα-inc*	Deem et al., 2011
AM1473	AM1411, but *MATα-inc:: lys2::Ins (A_4)-LEU2-tel/MATα inc::lys2::Ins (A_4) (NO-DSB)*	Deem et al., 2011
AM1649	AM1482, but *MATα-inc-LEU2-tel/MATα-inc (NO-DSB)*	Deem et al., 2011
AM2193	AM1411, but *pif1Δ::KAN*	This study
AM2191	AM1291, but *pif1Δ::KAN*	This study
AM2198	AM1482, but *pif1Δ:: KAN*	This study
AM2247	AM2191, but *MATα-inc-LEU2-tel/MATα-inc (NO-DSB)*	This study
AM2257	AM2198, but *MATα-inc-LEU2-tel/MATα-inc (NO-DSB)*	This study
AM2455	AM2193, but *MATα-inc:: lys2::Ins (A4)-LEU2-tel/MATα-inc::lys2::Ins (A_4) (NO-DSB)*	This study
AM2243	AM1291, but *pif1-m2*	This study

Table 3.1 List of *Saccharomyces Cerevisiae* strains used in this study (continued)

Strain	Genotype	Source
AM2244	AM1482, but *pif1-m2*	This Study
AM2245	AM1482, but *pif1-m2*	This Study
AM2246	AM1411, but *pif1-m2*	This Study
AM2278	AM2246, but *MATα-inc::lys2::Ins (A_4) -LEU2-tel/MATα-inc::lys2::Ins (A_4) (NO-DSB)*	This Study
AM2261	AM2243, but *MATα-inc-LEU2-tel/MATα-inc (NO-DSB)*	This Study
AM2279	AM2244, but *MATα-inc-LEU2-tel/MATα-inc (NO-DSB)*	This Study
AM2268	AM1411, but *rev3Δ:: ura3*	Ira Lab, Baylor College of Medicine
AM2456	AM2268, but *MATα-inc::lys2::Ins (A_4) -LEU2-tel/MATα-inc::lys2::Ins (A_4) (NO-DSB)*	This Study
AM2409	AM2268, but *pif1Δ::KAN*	This Study
AM2457	AM2409, but *MATα-inc::lys2::Ins (A_4) -LEU2-tel/MATα-inc::lys2::Ins (A_4) (NO-DSB)*	This Study

Table 3.1 List of *Saccharomyces Cerevisiae* strains used in this study (continued)

Strain	Genotype	Source
AM2438	AM1482, but carrying additional inserted sequences in *MATα-inc* copy of CHRIII marked by BSD	This Study
AM2439	AM1291 but carrying additional inserted sequences in *MATα-inc* copy of CHRIII marked by BSD	This Study

Table 3.2 List of Primers used in strain construction in this study

Malkova Lab Database Name	5' to 3' sequence	Description
OL1279	TGATTCGGTAATCTCCGAGCAGAAGGAAGA ACGAAGGA AGGAGCACAGACTTAGATTGGTgagctcgttttcgacactgg	P1 to amplify ura3: pCORE fragment Caps: Genomic sequence LC: pCORE sequence
OL1280	CGGGTAATAACTGATATAATTAAATTGAAGCTCTAATTTG TGAGTTTAGTATACATGCATtccttaccattaagttgatc	P2 to amplify ura3: pCORE fragment Caps: Genomic sequence LC: pCORE sequence
OL1384	GAAGAATTAATTGAGGGCGGATTAC	P1 to confirm integration of ura3::pCORE fragment
OL1385	GGCCCAAGCCTTGTCCCAAGGCAGC	P2 to confirm integration of ura3::pCORE fragment
OL103	GCAGTTTCATTTGATGCTCGATGAG	P1 inside pCORE to determine presence of pCORE on CHRV
OL104	GGCACGGTGCAACACTCACTTC	P2 inside pCORE to determine presence of pCORE on CHRV
OL1293	GACCATCAAAGAAGGTTAATGTGGCTGTGGTTTCAGGGT CCATAAAGCTTCTTCAATTTAATTATATCAGTTATTACC CGGGAATCTCGGTCGTAATGAT	IRO1 to remove ura3::pCORE complementary to OL1294
OL1294	ATCATTACGACCGAGATTCCCGGGTAATAACTGATATAA TTAAATTGAAGAAGCTTTATGGACCCTGAAACCACAGCCAC ATTAACCTTCTTTGATGGTC	IRO2 to remove ura3::pCORE complementary to OL1293

Table 3.2 List of primers used in strain construction in this study (continued)

Malkova Lab Database Name	5' to 3' sequence	Description
OL1509	CAGCTGAAGCTTCGTACGC	P1 to amplify *kan-MX* fragment *(MX18 primer)*
OL1510	GCATAGGCCACTAGTGGATCTG	P2 to amplify *kan-MX* fragment *(MX19 primer)*
OL1516	TCTTTCTGCAATTATTGCACGCCTCCTCGTGAGTAGTGAC CGTGCGAACAAAAGAGTCATTACAACGAGGAAATAGAAGA agtcagtgagcgaggaagc	P1 to amplify and insert *ura3-29* into intergenic region 3' of *THR4* on CHRIII Caps:Genomic sequence LC: *ura3-29* sequence
OL1518	ATATTTGCTGCTATACTACCAAATGGAAAAATATAAGATAC ACAATATAGATAGTATTAAAAAAACGTGTATACGTTATT attgtactgagagtgcacc	P2 to amplify and insert *ura3-29* into intergenic region 3' of *THR4* on CHRIII Caps:Genomic sequence LC: *ura3-29* sequence
OL1545	CCACCTATGGTGCTACCACCTT	P1 to confirm integration of *ura3-29* into intergenic region 3' of *THR4* on CHRIII
OL1542	GCTTCCTCGCTCACTGACT	P2 inside ura3-29 to determine presence of *ura3-29* on CHRIII
OL1541	GGTGCACTCTCAGTACAAT	P1 inside ura3-29 to determine presence of *ura3-29* on CHRIII of *THR4* on CHRIII
OL1007	AAGACCACCGTCAGTGGCCAGACC	P2 to confirm integration of *ura3-29* into intergenic region 3'

Table 3.2 List of primers used in strain construction in this study (continued)

Malkova Lab Database Name	5' to 3' sequence	Description
OL1721	TATGTCTAGTATGCTGGATTTAAACTCATCTGTGATTTGTG GATTTAAAAGGTCTTTAATGGGTATTTTATTCATTTTTT agtcagtgagcgaggaagc	P1 to amplify and insert *ura3-29* at *MATα-inc* on CHRIII Caps: Genomic sequence LC: *ura3-29* sequence
OL1722	TGCTGCATTTTGTCCGCGTGCCATTCTTCAGCGAGCAGAG AAGACAAGACATTTTGTTTTACACCGGAGCCAAACTGTGA G attgtactgagagtgcacc	P2 to amplify and insert *ura3-29* at *MATα-inc* on CHRIII Caps: Genomic sequence LC: *ura3-29* sequence
OL1770	GGTAGTAGTGAGTTGAGATGTTGTTTGC	P1 to confirm integration of *ura3-29* at *MATα-inc* on CHRIII
OL633	CAAAAGAGGCAAGTAGATAAGGGT	P2 to confirm integration of *ura3-29* at *MATα-inc* on CHRIII
OL1740	AAATCGTAAATACATAGGCTGGGCCATATACACTA ACATGTGTCGTGACCAATGTGCAGC AGATAGACTTGCTCATTAAATagtcagtgagcgaggaagc	P1 to amplify and insert *ura3-29* between *SED4* and *ATG15* on CHRIII Caps: Genomic sequence LC: *ura3-29* sequence
OL1741	AACTGGAAATGCTTTCCCTTTTGCCCTATCATTATTTT CTTTCCGATGTTATGCTTATTATATC TGTGATTGATAAGAGAAattgtactgagagtgcacc	P2 to amplify and insert *ura3-29* between *SED4* and *ATG15* on CHRIII Caps: Genomic sequence LC: *ura3-29* sequence
OL1065	AGCACCATATATCGGATATCCGACGTC	P1 to confirm integration of *ura3-29* between *SED4* and *ATG15* on CHRIII

Table 3.2 List of primers used in strain construction in this study (continued)

Malkova Lab Database Name	5' to 3' sequence	Description
OL1066	TGCATCCTAGATGCAAAGGAGAAGC	P2 to confirm integration of *ura3-29* between *SED4* and *ATG15* on CHRIII
OL1511	GTGTGCTTCATTGGATGTTCGTAC	P1 to make sequencing fragment to characterize *ura3-29* base substitution mutations
OL1512	AAAAGGCCTCTAGGTTCCTTTGTT	P2 to make sequencing fragment to characterize *ura3-29* base substitution mutations
OL1513	CTGGAGTTAGTTGAAGCATTAGG	P1 to sequence *ura3-29* fragment made by OL1511 and OL1512
OL1514	ATTCGTAATGTCTGCCCATTCTGC	P2 to sequence *ura3-29* fragment made by OL1511 and OL1512
OL1226	ATTCCAATCAGTTATTCGAGGCCAG	P1 to amplify fragment to verify integration of *pol2-4* mutation by sequencing
OL1227	CACCATTGAAGGTGGATATAACAGT	P2 to amplify fragment to verify integration of *pol2-4* mutation by sequencing
OL1228	GTAGAAGCGCCACTTCATCG	P1 to sequence fragment made by OL1226 and OL1227 to verify *pol2-4* mutation

Table 3.2 List of primers used in strain construction in this study (continued)

Malkova Lab Database Name	5' to 3' sequence	Description
OL1719	TTATTCTAAGATGTGGTCTTCGGTATCCTGACCA CGAGGTTCGTCGGAAACCAATGAATGA ACTTGATTACTATTAGACTCgcgatatcgctagctcgagc	P1 to amplify *pif1::BSD* fragment
OL1720	ATGCCAAAGTGGATAAGATCAACATTGAATCATAT TATACCAAGAAGGCCATTTATCTGTA GTTTCAACAGTTTTCTTTTAagaggatccccgggaattca	P2 to amplify *pif1::BSD* fragment
OL1734	GCTCGAGCTAGCGATATCGC	P1 inside *BSD* to confirm presence of *BSD* on CHRIII
OL1733	TGAATTCCCGGGGATCCTCT	P2 inside *BSD* to confirm presence of *BSD* on CHRIII
OL384	GCTTCCTGTCAGCTTGGTTACTTT	P1 to confirm elimination of WT *pif1*
OL399	TTTAACGTCCGT TAACTTCCCCTT	P2 to confirm elimination of WT *pif1*
OL1717	TTACCAATCATTTAGAGATATTAATGCTTCTTCCCT TTGAACAGATTGATTATCTCTCAA GTA TCTTTCTGCTTTGACACGgcgatatcgctagctcgagc	P1 to amplify *rev3::BSD* fragment

Table 3.2 List of primers used in strain construction in this study (continued)

Malkova Lab Database Name	5' to 3' sequence	Description
OL1718	ATGTCGAGGGAGTCGAACGACACAATACAGAGCG ATACGGTTAGATCATCCTCTAAATCAG ACTATTTTAGAATCCAGCTAagaggatccccgggaattca	P2 to amplify *rev3::BSD* fragment
OL1198	GATATGACCCTGTCAAACAACTTTGA	P1 to confirm elimination of WT *rev3*
OL1196	GTTCCATTCCACTCAAATTTGGG	P2 to confirm elimination of WT *rev3*
OL1461	GGATAAGCCCGAATTGGGTGAAGTG	P1 to confirm integration of *ura3-29 (antisense/orientation2)* into intergenic region 3' of THR4 on CHRIII
OL1462	GGTGACTTCATCAGAACGGAAAGTAG	P2 to confirm integration of *ura3-29 (antisense/orientation2* into intergenic region 3' of THR4 on CHRIII
OL1735	TTGGCAGCAACAGGACTAGG	P2 inside ura3-29 to determine presence of *ura3-29* (antisense/orientation2)on CHRIII
OL382	GACAGAGGCATTGTGAGTTAGTCT	P1 to amplify *pif1::KAN* fragment
OL383	AATCAGGACGCTTCAAATGCCTTC	P2 to amplify *pif1::KAN* fragment

Table 3.2 List of primers used in strain construction in this study (continued)

Malkova Lab Database Name	5' to 3' sequence	Description
OL26	CCTCGACATCATCTGCCC	Used to confirm insertion of *kan-MX* (Wach et al., 1994) to delete gene function. Within TEF terminator, 174bp from the MX18 primer pointing towards the MX18 primer
OL27	CAGCGAGGAGCCGTAATTTT	Used to confirm insertion of *kan-MX* (Wach et al., 1994) to delete gene function. Within TEF terminator, 269bp from the MX19 primer pointing towards the MX19 primer
OL1621	AAATCGCAATTATGAATCAGGACG	P1 to make pif1 fragment for checking *pif1-m2* mutation (by further restriction digest by Xho1)
OL1622	GGAAGCAGTGACTGCAACATTCTC	P2 to make pif1 fragment for checking *pif1-m2* mutation (by further restriction digest by Xho1)
OL1104	AAATGTCACTGCAAATTATGCGGAAGAC	P1 to make 400-bp sequencing fragment to characterize LYS2::Ins frameshift mutations
OL1181	CCATCCACTTCTCATCTGAAAGACC	P2 to make 400-bp sequencing fragment to characterize LYS2::Ins frameshift mutations
OL1106	GTTCGTACCCCTCTCGAGAATA	P1 to sequence 400-bp *LYS2::Ins* fragment made with OL1104 and OL1181

3.1.2 Media and Growth Conditions

3.1.2.1 Media

Yeast strains were grown non-selectively in YEPD medium, consisting of 1% yeast extract, 2% Bacto peptone, 2% dextrose, and 0.004% adenine in 0.05N HCl. Galactose (a filter sterilized 20% w/v solution of galactose prepared in ddH_20) instead of dextrose was used to make YEP-Galactose medium. YEP-lactate medium (Glucose free medium), consisting of 1% yeast extract, 2% Bacto peptone media and 3.7% lactic acid was used to induce *GAL::HO* DSB. Synthetic media missing a one or two required nutrients were used for selection of yeast auxotrophic markers, and consisted of 1% yeast nitrogen base without amino acids, 2% dextrose, and amino acids as required for selection (Guthrie and Fink, 1991). Minimal media containing 5g/L of flouro-orotic acid (5-FOA) was used for selection of Ura^- cells. pH of all media was adjusted to 5.5 (except for 5-FOA that was adjusted below pH 5.0). Plate media was prepared similarly to liquid media, but contained 25 g/L of granulated agar. Antibiotic-containing media was prepared by addition of the drug of interest to the YEPD media in the following amounts: G418 0.3 g/L or 0.5 g/L; Nourseothricin sulphate 0.1 g/L; Hygromycin 0.3 g/L; Blasticidin 0.1 g/L or 0.2 g/L). Filter sterilized solutions of these drugs, dissolved in 5 mL of ddH_20 were added to autoclaved media that was cooled to 55° C before the addition.

3.1.2.2 Measurement of Growth

Growth of yeast strains in YEPD/YEP-lac was measured at Optical Density of 600 nm wavelength (SpectraMax M2, Molecular Devices).

3.2 Methods

3.2.1 Transformation Methods

3.2.1.1 One-Step Method of Transformation

Simple strain modifications including introduction of *pif1-m2* mutation, *KAN-MX* replacement, *pol3-5DV* mutation, and *pol2-4* mutation were carried out using One-step transformation method that was performed as follows. 1-5 ml of saturated yeast culture was grown overnight in liquid YEPD medium at 30° C. Cells were collected by centrifugation at 3000 rpm for 1 minute (min.) in a table top centrifuge and resuspended in 100 µl of one step buffer (dithiothreitol (100 mM), lithium acetate (0.2M) in Polyethleneglycol (40%)). Thirty micrograms of sonicated salmon sperm DNA (Agilent Technologies), denatured at 100° C was added to the cells, followed by addition of 50 ng-1 µg of DNA. The mixture was then incubated at 45° C for 30 min. Following incubation, cells were either plated on selective media, where only transformants were able to grow or plated on non-selective media (YEPD) followed by replica plating on antibiotic-containing media. Plates were incubated at 30° C for 2-4 days to provide sufficient time for growth. In some cases, to achieve selection of Ura^- transformants, cells were first allowed to grow on non-selective YEPD medium, followed by replica-plating on 5-fluoro-orotic acid media where only Ura^- transformants could grow. All transformants were confirmed by genetic markers and by PCR.

3.2.1.2 *Delitto Perfetto* Method of Transformation

Strains requiring removal of genetic markers or complex gene modification were constructed using *delitto perfetto* approach. This approach takes advantage of a CORE cassette containing two reporters: *KlURA3* (*URA3* gene from *Kluyveromyces lactis*) and a

kanMX4 reporter. The approach involves two steps. Step 1 involves targeted insertion of the CORE cassette at the locus of the region to be deleted. To achieve this, 5 ml of saturated yeast culture was grown overnight in liquid YEPD medium at 30° C. 1.5 ml from this suspension was then aliquoted into 50 ml of liquid YEPD medium followed by incubation with shaking at 30° C for 4 hours to obtain logarithmically growing cells (logarithmic growth was confirmed by O.D measurement ranging between 0.3-0.6). The entire culture was then centrifuged at 3000 rpm for 3 min. to harvest cells. The cells were washed with ddH_20 and centrifuged again, followed by washing with 0.1M Li acetate in 1XTE buffer (pH 7.5) and resuspended in 250 ml of 0.1M Li acetate in 1XTE buffer (pH 7.5). The transformation mix consisted of 50 µl of cells, resuspended in 0.1M Li Acetate in 1XTE(pH 7.5), 300 µl of 1XTE(pH 7.5) polyethylene glycol (50%), of 30 µg of sonicated and denatured salmon sperm DNA, and 50 ng-1 µg of transforming PCR DNA fragment, bearing pCORE cassette. The reaction mixture was incubated at 30° C for 30 min, followed by heat shock at 42° C for 15 min. with intermittent vortexing. The mixture was then plated onto non-selective YEPD media. This was followed by overnight incubation at 30° C and replica plating onto G418 antibiotic medium and/or Uracil dropout medium. The plates were incubated for 3-5 days at 30° C to achieve selective growth.

Step 2 involved removal of the pCORE cassette using a pair of oligonucleotides (IROs) leading to complete deletion of the targeted genetic locus or gene. This was achieved by a similar transformation protocol described; except that the transforming DNA was a mixture of two complementary denatures oligonucleotides (0.5 nmol; 100bp each). Following transformation, cells were plated on non-selective YEPD media and grown overnight at 30° C. Cells were replica plated to a 5-fluoro-orotic acid medium to enable selection of transfomants that lost the *URA3* marker. Transformants were confirmed by genetic markers and by PCR.

3.2.1.3 Plasmid Preparation

Competent *E.coli* cells (XL-1 Blue Cells - Stratagene Corporation) were transformed with various plasmids. In particular, from 0.1 to 50 ng of plasmid DNA was added to 100 µl of cells that were gently mixed and incubated on ice for 30 min. The mixture was then subjected to heat shock at 42° C for 45 sec and then incubated on ice for 2 min. 0.9 ml of Luria Broth (LB) media was added to the mixture and incubated on a rolling drum at 37° C for 1 hour. Cells were plated on Luria Broth media plates containing 100 µg/ml of ampicillin and then incubated again at 37° C for the overnight growth.

3.2.2 Yeast Recombinant DNA Techniques

3.2.2.1 PCR

Polymerase chain reaction (PCR) was used to amplify DNA fragments. The reaction mixture consisted of 50 µM each of the two PCR-specific oligonucleotide primers, dNTP (10mM), $MgCl_2$ (7.5mM), Go Taq Buffer (proprietary mixture), ddH_20, 10-50 ng of DNA template and 1 unit Taq-DNA polymerase (Promega Corporation or Sib Enzyme Ltd.). In certain cases 1X Buffer E (Genaxxon), a proprietary mixture of $MgCl_2$ and dNTP or Go-Taq Buffer (Sib Enzyme Ltd) were used. PCR amplification of long or difficult DNA fragments was carried out using 1X Ex-Taq buffer, 0.2mM dNTPs, 2.0mM $MgCl_2$, 50µM each of the two oligonucleotide primers specific to the appropriate sequences in each strand, between 10 and 50 ng template DNA, and 1U Ex-Taq polymerase (all from Takara Bio Company). Transformants were confirmed by PCR using whole cells as a source of DNA. PCR reactions were run on a BIORAD MyCycler PCR machine. A typical PCR cycle consisted of a denaturation step (performed at 94° C for 1 min.); 40 denaturing cycles at 94° C for 30 s, followed by an annealing step varying from 55C-60° C for 1 min., an extension step at 72° C for 1.5 min. and final extension at 72° C for 10 min.

3.2.2.2 Restriction Digestion

The method was performed using restriction enzymes (New England Bioloabs or Fermentas) with appropriate buffer (NEB or Fermentas catalog). Specifically, 1 µg of plasmid DNA was digested by restriction enzyme followed by incubation at 37° C for 2 hrs. Additional 5-10U of enzymes was used for genomic DNA digest with extended overnight incubation at 37° C. Restriction digests were confirmed using agarose gel electrophoresis.

3.2.3 DNA Purification

3.2.3.1 Glass Bead Genomic DNA Extraction

Five milliliter of saturated yeast culture grown overnight in liquid YEPD medium at 30° C was harvested by centrifugation at 3000 rpm for 5 min. The pellet was then suspended in a lysis buffer consisting of 1% sodium dodecyl sulfate, 10mM Tris (8.0), 1mM EDTA (pH 8.0). 600 µl of this mix was added to a microfuge tube containing 300 µl of sterile glass beads (Sigma-Aldrich) followed by addition of 400 µL of Tris-buffered 50% phenol, 48% chloroform, 2% isoamyl alcohol. The mixture was then vortexed for 1 min. on high speed, followed by 1 min. incubation on ice and then vortexed for an additional 1 min. The mixture was then centrifuged for 15 min. at 3000 rpm and the clear aqueous phase obtained is then transferred and mixed (by inverting several times) with 400 mL of Tris-buffered 50% phenol, 48% chloroform, 2% isoamyl alcohol, in a separate clean microfuge tube. The mixture was then centrifuged again. The aqueous phase was transferred to another tube and mixed with 50 µl of 3M sodium acetate (pH 6.5) followed by addition of 600 µL of isopropanol and followed by centrifugation. The DNA pellet was resuspended in 300 µL 1x TE buffer, treated with RNase (3 µL of 10 mg/mL) followed by incubation at 37°C for 30 min. The DNA was precipitated by addition of

30 µL of 3M ammonium acetate (5.5) followed by addition of 300 µl isopropyl alcohol and then centrifuged as previously. The DNA pellet obtained was washed with 300 µl of 80% ethanol and finally resuspended in 300 µL of TE.

3.2.3.2 Extraction of Genomic DNA for Pulse Field Gel Electrophoresis (PFGE)

Samples grown in 50ml liquid YEPD medium were centrifuged at 3000 rpm for 5 min. to harvest cells. Pellets were washed with 50mM EDTA (pH 8), centrifuged, and placed on ice after discarding the supernatant. Pellets were resuspened in 400 µL of a solution of SCE (1M sorbitol, O.1M sodium citrate (pH 5.8), 10mM EDTA containing 25 µL 2-mercaptoethanol and 0.005 gm zymolase (20T) and incubated briefly at 40° C. Five hundred microliters of cell suspension was mixed with 1% molten low-melting point agarose in SCE (Molecular Cloning: A Laboratory Manual III by Sambrook and Russel) cooled to 40° C and transferred into plug molds. Plugs were allowed to solidify at 4° C for approximately 10 min. and then expelled into 50 mL polypropylene tubes. Plugs were then covered in 5 mL of a solution of 0.5 M EDTA, 10mM Tris (pH 8.0), 7% 2-mercaptoethanol, 1 µL/mL of 10 mg/mL RNase and incubated at 37° C for 1 hr. After incubation, the solution was removed and replaced with 5 mL of solution of 1% N-lauroyl sarcozyl in 0.5M EDTA (pH 9.0) with 1 mg/mL proteinase K and incubated at 50° C over night. After incubation, the solution is removed and plugs are washed with 5 mL of 1XTE buffer storage at 4° C, or with 50 mL of 50% glycerol for long term at -20° C.

3.2.3.3 Plasmid Purification

Isolation of plasmids from *E. coli* was carried out using a Qiagen Maxiprep Kit (Qiagen). *E. coli* cells containing the plasmid were grown approximately for 12 hrs at 37° C in 5 ml LB medium containing 100 µg/ml of ampicillin. The inoculums were transferred to 250 ml of LB containing 50 µg/ml of ampicillin and grown for 16 hrs at 37° C. Cells were then harvested by centrifugation at 6000g at 4° C for 15 min. The pellet was resuspened in 20

ml of Buffer P1 (50mM Tris-HCl, 10mM EDTA (pH 8.0), 100 µg Rnase A). Twenty milliliters of Buffer P2 (200mM NaOH, 1% (w/v) SDS) was then added to this mixture and samples were gently inverted several times. This is followed by 5 min. incubation at room temperature after which 20 ml of chilled buffer P3 (3M potassium acetate (pH 5.5)) was added. The samples mixture was then mixed by gentle inversion several times. Samples were then centrifuged at 2000g for 30 min. at 4° C to remove cell debris. The supernatant, which contains the plasmid DNA was then applied to a Qiagen-tip 500 column, pre-equilibrated with 10 ml of QBT buffer (750mM $NaCl_2$, 50mM MOPS, 15% ethanol (pH 7.0)). This is followed by washing of the column with 30 mL Buffer QC (1 $NaCl_2$, 50mM Tris-HCl, 15% ethanol (pH 8.5) and elution of the plasmid in 15 ml of Buffer QF (1.25M $NaCl_2$, 50mM Tris-HCl, 15% ethanol (pH 8.5)). Plasmid DNA was then precipitated with isopropanol (0.7 volumes) and centrifuged at 15000g at 4° C for 30 min. This was followed by washing of the pellet with 70% ethanol and centrifugation. The DNA was resuspended in 200-400 µl TE Buffer and stored at -20° C.

3.2.4 Pulse Field Gel Electrophoresis

DNA plugs obtained by high molecular weight extraction (described in 3.2.3.2) were run on 1% low melt agarose (Fischer Scientific) or 1% low-endoosmosis (Biorad) gels in 0.5X TBE buffer (Molecular Cloning: a Laboratory Manual III by Sambrook and Russel) with a continuous circulation in the electrophoresis cell chamber. The following settings on the CHEF DR-II control module were used for resolution of CHRIII DSB repair products: 6V/cm, 10-35 s switch times, 40-48 hrs run time. Following 30 min. incubation in 0.5X TBE with ethidium bromide and 15 min. incubation in ddH_20 bands were visualized in UV light.

3.2.5 Southern Hybridization of PFGE

Full characterization of DSB repair products separated on PFGE gel was achieved by Southern Hybridization with specific probes as described (Southern, 1975). To achieve this, the agarose gel was exposed to 600 micro-joules of ultraviolet (UV) light using Stratalinker 2400 Crosslinker. Next, the gel was incubated in buffer containing 0.5M NaOH, 1.5M NaCl (pH 7.0) for 40 min. The gel was then transferred to another buffer containing 1M Tris-HCl, 1.5M NaCl (pH 7.0) and incubated for 30 min. DNA from the gel was transferred to nitrocellulose membrane (Amersham Hybond N^{+}) by upward capillary transfer method in 10X SSC buffer (Molecular Cloning: a Laboratory Manual III by Sambrook and Russel). Membranes were then probed by *ADE1* or *ADE3* specific probes labeled with Stratagene "Prime-It random primer labeling kit".

3.2.6 Analysis of DSB Repair Outcomes

3.2.6.1 Determination of DSB Repair Efficiency

To determine the efficiency of BIR, 5 ml inoculums were grown in YEPD media at 30° C overnight followed by a 1:10 dilution into YEP-lactate media and subsequent an overnight growth. Appropriate dilutions of cells were then plated on YEP-GAL plate media to induce DSB and also on YEPD plate media as control. These DSB repair outcomes were allowed to grow for 3-5 days by incubation at 30° C. The resulting colonies were then replica plated on appropriate dropout media to analyze the *ADE1, ADE3, HIS3 and LEU2* markers of these strains.

3.2.6.2 Statistical Analysis of DSB Repair Outcomes

At least 3 independent experiments were performed for each individual mutant to determine their effect on the efficiency of BIR. Results from individual experiments were

pooled into one group. The results from individual experiments were not statistically different as determined by Chi-square test. To determine the effect of mutations on the efficiency of BIR, all repair outcomes were divided into two groups: containing BIR repair outcomes (Ade^+Leu^-) and the others. Distributions between these two groups for mutants were then compared to those of WT to determine if the mutants affected the efficiency of BIR. The effect of mutations on other repair outcomes was determined similarly.

3.2.7 Mutagenesis Associated with DSB repair

3.2.7.1 Determination of Mutagenesis Rates

To determine the frequency of mutations, yeast strains were grown in Leucine dropout liquid medium for approximately 19 hrs at 30° C. The inoculums were then transferred into YEP-Lac medium by a 1:20 dilution and grown to logarithmic phase for approximately 16 hrs at 30° C. Twenty percent galactose was then added to the YEP-lac culture to a final concentration of 2%, followed by incubation for an additional 7 hrs at the 30° C. The exact same procedure was followed for analysis of No-DSB control strains.

Samples from individual cultures were diluted to obtain appropriate concentrations and then plated on Adenine drop-out and Adenine-Lysine double dropout plate media before (0h) and seven hours after the addition of Galactose (7h) to measure the frequency of Ade^+Lys^+ cells. (For Adenine dropout media, cells were plated to obtain single colonies, while concentrations of cells on Ade-Lys was adjusted based on expected frequency of Ade^+Lys^+) In any case, cells were not plated at concentrations above 1×10^8 cells/plate). Cells were grown at 30° C for 5-7 days.

The above experimental procedure is described for analyzing Lys^+ frameshift mutations. The exact same procedure was used to determine the rate of base substitution mutations except that adenine-uracil dropout media was used instead of adenine-lysine to obtain Ade^+Ura^+ cells.

3.2.7.2 Calculation of Mutation Rates

Spontaneous mutation frequencies were calculated based on the number of mutations accumulated over many cell generations. Mutation rates were calculated for spontaneous mutagenesis using the Drake Equation (Drake J, 1991). First, the rate of spontaneous mutagenesis was calculated by using mutation frequencies obtained at 0hr for experimental strains and No-DSB control strains using the formula: $\mu=0.434/\log(N\mu)$, where μ=rate of spontaneous mutagenesis, f=mutation frequency at 0hr (Ade^+Lys^+ or Ade^+Ura^+ cells) and N= the number of cells in culture at 0hr (Ade^+ cells). Spontaneous mutagenesis rates were determined for No-DSB control strains in similar fashion. For No-DSB control strains at *MAT position*, the median rates calculated from the above rates were divided by two to account for the presence of two *LYS2* reporters in these particular strains. The rates of BIR mutagenesis i.e. the rate of mutations after galactose DSB induction (μ_7) was calculated by modifying the Drake equation: $\mu_7=(f_7-f_0)$ where f_7 and f_0 are mutation frequencies at times 7hr and 0hr, respectively. In this case the modification to the Drake equation takes into account the fact that the experimental strains did not divide between 0hr and 7hr, while No-DSB controls underwent ≤ 1 division between 0hr and 7hr.

Rates of mutagenesis were reported as median values, where the 95% confidence limits for the median are calculated for the strains with a minimum of 6 individual experiments as shown in tables (4.1a, b 5.1a, b). For strains with < 6 experiments the range of the median was calculated. Median mutation rates were statistically compared using the Mann-Whitney U test (Mann and Whitney, 1947).

3.2.7.3 Analysis of Mutation Spectra

For analysis of Lys^+ frameshift mutations, a portion of the *LYS2* gene was sequenced from independent Lys^+ outcomes (OL1104 and OL1181 were used to make the fragment, OL1106 was used for sequencing; described in Table 3.2) Sequencing reactions were performed at the IUPUI sequencing Core Facility (ABI 3100 genetic analyzer) and at Functional Biosciences, Madison WI (ABI 3730xL DNA sequencer).

For experimental strains undergoing BIR repair, 7hr Lys^+ BIR events (confirmed as Ade^+ Leu^-) were used for sequencing. These strains did not divide between 0hr and 7hr time points (due to G2/M arrest) and frequency of Lys^+ at 7hr significantly exceeded that at 0hr. Therefore all Lys^+ events resulting from DSB repair experiments were considered independent. To ensure that the mutation spectrum represented among BIR outcomes was not biased, colonies from different Lys dropout plates and from different independent experiments were selected for sequencing. For No-DSB control strains, independent Lys^+ events were obtained by growing cultures from single cells in YEPD overnight and choosing only one Lys^+ event from each individual culture.

BIR repair yields a second copy of *lys2::ins* gene. The site of frameshift mutation among $Ade^+Leu^-Lys^+$ (BIR) events was determined by analyzing .abi files using Codon Code Aligner where 2 copies of *lys2::ins* gene can be separated (deconvolution) and aligned to reference sequence of WT parent strain. Such heterozygous events were different from homozygous events where BIR yielded only one copy of *lys2::ins* gene. For such sequences the site of frameshift mutation was determined by simply aligning the single *lys2::ins gene* copy to the reference sequence. Template switching events were analyzed by BLAST search method available in Codon Code Aligner.

A similar approach was followed for analysis of Ura^+ base substitutions. The site of Ura^+ base substitution was determined by analyzing .abi files to identify the nucleotide displaying superimposition of two peaks, resulting from two copies of the *ura3-29* gene.

CHAPTER 4. PATHWAYS OF MUTAGENESIS IN BREAK-INDUCED REPLICATION

4.1 Background

Genetic Information is passed on from one generation to another by chromosomal duplication of DNA in S-phase. Accurate replicative DNA polymerases and potent polymerase proofreading coupled with post-replicative mismatch repair mechanisms carry out this process. These mechanisms guarantee a high fidelity of DNA synthesis where only one out of every 10^9 nucleotides inserted is erroneous. This high accuracy of DNA replication ensures maintenance of genomic integrity through generations.

Recently our lab demonstrated that DNA synthesis associated with break-induced replication (BIR) was highly mutagenic (Deem et al., 2011). Here, BIR was shown to be highly mutagenic in copying DNA as a dramatic increase in rate of frameshift mutations was observed compared to S-phase DNA replication. To understand why such a high mutagenesis was observed in BIR, several components involved in S-phase DNA replication and repair were tested for their effect on BIR mutagenesis. Some of these components were found to be inefficient in BIR. It was shown that the proofreading activity of DNA polymerase Pol δ was less efficient in correcting BIR-related versus S-phase replication errors, implicating Pol δ as one of the polymerases responsible for many BIR frameshift mutations. Further it was revealed that although mismatch repair was functional in BIR, its efficiency in correcting frameshift mutations was lower when compared to S-phase replication. Also the DNA damage checkpoint response (as a part of G2/M cell cycle arrest) for cells undergoing BIR repair was found to stimulate an

increase in dNTP pools. These increased dNTP pools were also implicated as a prominent source of frameshift mutagenesis in BIR. In summary, these studies indicated that the high level of frameshift mutations occurring in BIR was due a low fidelity or mutagenic replication fork whose errors remain uncorrected. This mutagenic replication fork associated with BIR supposedly copied DNA with many defects, including reduced Pol δ replication fidelity and decreased MMR deficiency along with presence of increased nucleotide pools, all of which simultaneously led to a high rate of errors.

It was clear from these studies that the supposed mutagenic replication fork associated with BIR was different from the high fidelity S-phase replication fork. For a better understanding of this mutagenic replication fork, components non-essential to S-phase replication fork were tested for their effect on BIR mutagenesis. These included the 5’ to 3’ DNA helicase Pif1 and translesion polymerase Pol ζ (Rev3). In this chapter we first describe the phenomenon of BIR induced frameshift mutagenesis followed by effect of Pif1 and Rev3 on BIR mutagenesis.

4.2 Characterization of BIR associated Frameshift Mutagenesis

4.2.1 Experimental System

A disomic strain with a modified form of Chromosome III (CHRIII) was used as the experimental system *in Saccharomyces Cerevisiae* to assay BIR induced frameshift mutagenesis (described in Figure 4.1) (Deem et al., 2011). DSB was created at the *MATa* locus by the galactose inducible HO endonuclease (*GAL::HO*). This *MATa* containing recipient copy was truncated and fused to *LEU2* and telomeric sequences. The donor copy of CHR III is resistant to cleavage due to a mutation at the *Matα-* locus (*MATα-inc*). This *MATα-inc* containing copy of CHRIII is full length and serves as the template for DSB repair of the broken (recipient) *MATa* copy. Elimination of all but 46bp of homology on one side of the DSB site in the *MATa* copy ensured high efficiency of BIR i.e. the majority of DSBs introduced at *MATa* are repaired by BIR in this strain. Following a DSB, there is a 5'–3' resection in the broken (recipient) copy, followed by strand invasion of the 3' end into the full length, donor copy to initiate BIR.

To assay BIR associated frameshift mutagenesis, frameshift reversion reporters *lys2::ins* (Tran et al., 1997) were inserted at 3 positions in the *MATα-inc* containing copy; at *MATα-inc* ("*MAT*"), 16kb centromere distal from *MATα-inc* in the region between *RSC6* and *THR4* ("16kb") and 36kb centromere distal from *MATα-inc* in the region between *SED4* and *ATG16* ("36kb"). These reporters are alleles of *LYS2* gene with a 61bp insertion, which includes a homonucleotide run of 4 Adenines. The insertion of these reporters shifted the reading frame of *LYS2* by +1bp giving a Lys^- phenotype. A Lys^+ phenotype can result from a frameshift mutation that occurs in the 71bp region of the allele, which restores the reading frame. In all strains, *LYS2* was fully deleted from its native location in chromosome II.

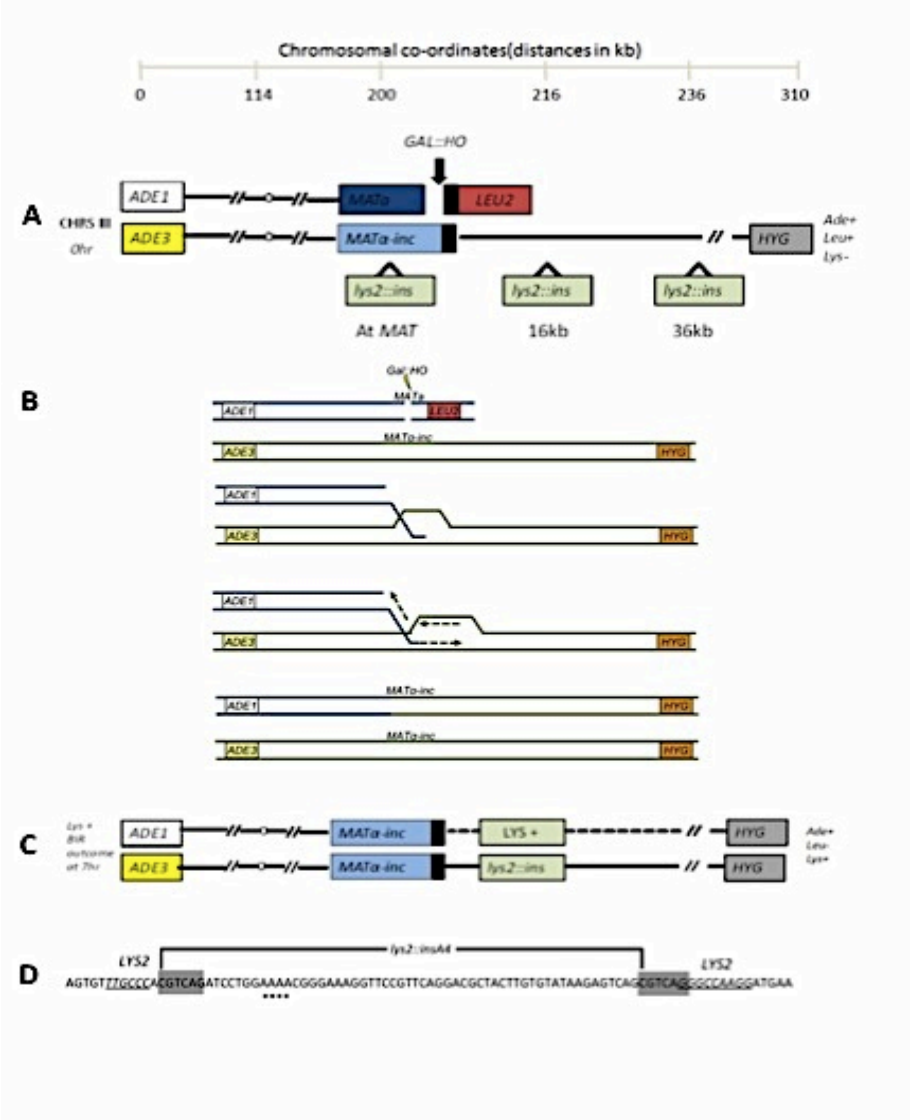

Figure 4.1 Experimental System to study BIR associated Frameshift Mutations.

Figure 4.1 Experimental System to study BIR associated Frameshift Mutations (from Deem et al., 2011). (A) Disomic Experimental system with modified Chromosome III (CHR III) used to study BIR. DSB was created at *MATa* by HO endonuclease induced by galactose. *MATa* copy of CHRIII is truncated by *LEU2* fused to telomeric sequences while *MATα-inc* has full length CHRIII. The *MATa* copy shares only 46bp homology with the *MATα-inc* copy (hatched lines). Majority of DSBs introduced at *MATa* are repaired by BIR (strand invasion followed by copying of the donor chromosome till its end). Frameshift reporters *lys2::ins* were inserted at 3 positions: at 0kb (*MATα-inc*), 16kb from *MATα-inc* and 36kb from *MATα-inc* (B) After 5'-3' resection following DSB, the broken (recipient) chromosome, invades into the homologous donor (template) chromosome and copies close to 100kb of DNA sequences from the donor chromosome to fully repair the broken chromosome. (C) BIR associated mutations are detected by Lys^+ phenotype, when an error in DNA copying of the template *lys2::ins* reporter is made, which restores the *LYS2* reading frame (Here 16kb position is shown). BIR associated mutations show $Ade^+Lys^+Leu^-$ phenotype. (D) Sequence of 60bp insert of *lys2::ins* constructs flanked by *LYS2* sequences. Asterisk indicates location of poly-A_4 run. 6bp direct repeats that border the inserted sequence on either side are indicated by gray shaded box. Nucleotides underlined on the right side of the gray shaded box indicate a mutation hotspot region, while those underlined on the left side indicate a -1bp quasipalindromic sequence of the mutation hotspot.

BIR associated frameshift mutagenesis was measured by plating appropriate dilutions of cell suspensions to get single colonies on Adenine and Adenine-Lysine dropout media before and 7hr after incubation in galactose containing media. The cells undergoing DSB repair by BIR were confirmed by an $Ade^{+}Lys^{+}Leu^{-}$phenotype. BIR efficiency in WT and mutant strains is shown in the Table 4.1a.

4.2.2 Rate of BIR-induced Frameshift Mutagenesis

For strains carrying *lys2::ins* frameshift reporters at 3 positions: *MAT*, 16kb and 36kb the rate of Lys^{+} frameshift mutations was determined following induction of DSB. On comparison to spontaneous Lys^{+} mutation rates i.e. Lys^{+} rates before DSB induction, we found that the rate of Lys^{+} mutations following DSB repair was much higher than the rate of spontaneous Lys^{+} mutations. As shown in Table 4.1a, the increase in mutagenesis was consistently observed for frameshift reporters at all 3 positions, where the rate of Lys^{+} frameshift mutagenesis (7hr) following DSB repair exceeded the rate of Lys^{+} frameshift mutagenesis before DSB repair (0hr) by 80-575 fold (see Figure 4.2). To accurately estimate spontaneous Lys^{+} mutations, No-DSB control strains lacking the *GAL::HO* cut site were used (refer materials and methods (3.1.1) for more details). Thus compared to spontaneous Lys^{+} rates shown in Table 4.1b (in No-DSB control strains) the rate of Lys^{+} mutations following DSB repair were observed to be 330-1200 fold higher.

A majority of the Lys^{+} mutations following DSB induction were due to DSB repair by BIR (confirmed by $Ade^{+}Lys^{+}Leu^{-}$ phenotype) (Refer Table 4.1a % BIR). Thus the dramatic increase in frameshift mutagenesis in strains with DSB compared to strains without DSB result from the error-prone DNA synthesis during BIR. Taken together, these results clearly demonstrate that BIR is highly mutagenic leading to a 330-1200 fold increase in the rate of frameshift mutations compared to S-phase replication.

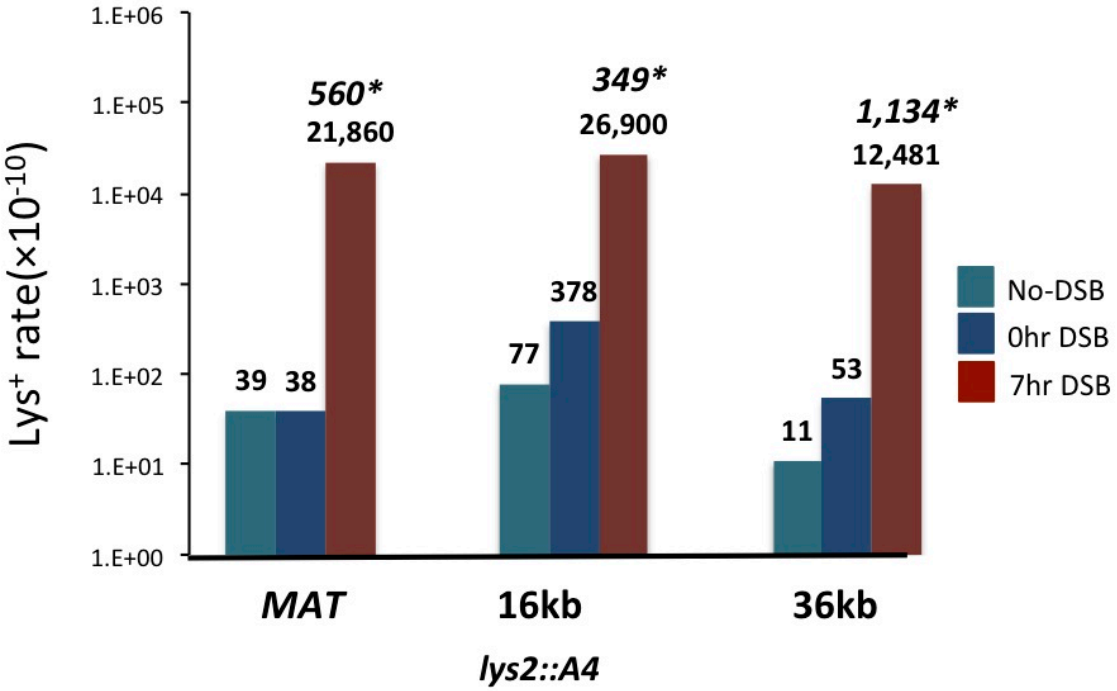

Figure 4.2. The Rate of BIR associated Frameshift Mutagenesis.
The rate of Lys+ frameshift mutations was determined before (0hr) and (7hr) after addition of galactose to media for WT strains carrying *lys2::ins* frameshift reporters at 3 positions, at *MATα-inc (MAT),* 16kb and 36kb centromere-distal to *MAT.* Rate of spontaneous Lys^+ mutations were determined using isogenic No-DSB control strains (No-DSB). Medians of Lys^+ mutagenesis rates are reported as Log_{10} scale (See Table 4.1a, b for confidence intervals/ranges and number of repeats). The fold increases in BIR mutation rate is indicated in italics. Statistically significant differences from the rates of spontaneous mutagenesis are indicated by asterisk.

Table 4.1a The Rate of DSB-associated Lys$^+$ mutations

The table represents the rate of DSB associated Lys$^+$ mutations in strains carrying WT Pif1, *pif1Δ* and *pif1-m2, rev3Δ and pif1Δrev3Δ*. DSB associated Lys$^+$ mutations for *lys2::ins* at positions, *MATα-inc* (0kb), 16kb from *MATα-inc* and 36kb from *MATα-inc* are shown here. Rates for Lys$^+$ mutations are given for time-points, 0hr and 7hr i.e. before and 7hr after addition of galactose). [a] Rates calculated at 0hr based on 0hr frequencies using the Drake equation (Drake J, 1991) (refer materials and methods for more details). At 7 hr, rates were calculated as (7hr frequency - 0hr frequency); [b] for strains with ≥ 6 experiments CI of median is given while for strains with < 6 experiments median range is given. Numbers in brackets [ ] represent repeats of experiments. [c] Statistically significant reduction of 7h median rate of mutant compared to 7h median rate of WT in strains with a DSB determined using the Mann-Whitney U test for p-value ≤ 0.05. [d] % BIR for 7h Lys$^+$ outcomes for strains with DSB sites was determined from 6-8 independent experiments. Abbreviations: NA-not available, NS-not significant.

Table 4.1a The Rate of DSB-associated Lys^+ Mutations

Position	Construct	*HO site*	Relevant Genotype	Rate of Lys^+ ($x10^{10}$) [a]				Fold below wt (p-value) [d]	% BIR
				Before galactose (0hr)		After galactose (frequency (7hr - 0hr))			
				Median	CI or range[b] [# Of repeats]	Median	CI or range[b] [# Of repeats]		
0 kb	A_4	DSB	WT	39	(32 - 62) [9]	20,140	(19,066 - 25,296) [9]	NA	94
0 kb	A_4	DSB	*pif1-m2*	23	(14 - 36) [8]	13,036	(9,777 - 16,162) [8]	1.5 (0.0055)	94
0 kb	A_4	DSB	*pif1Δ*	27	(11- 38) [8]	6,433	(3,583- 11,202) [8]	3.1 (0.0003)	95
0 kb	A_4	DSB	*rev3Δ*	15	(12-39) [6]	8,917	(4,227-14,164) [6]	2.3 (0.0028)	97
0kb	A_4	DSB	*pif1Δrev3Δ*	6	(3-10) [11]	232	(116-507) [11]	87	80
16 kb	A_4	DSB	WT	396	(127- 643) [13]	32,943	(12,792- 48,237) [13]	NA	70
16 kb	A_4	DSB	*pif1-m2*	84	(53 - 102) [12]	7,632	(5,908 -11,541) [12]	4.3 (0.0001)	75
16 kb	A_4	DSB	*pif1*	59	(40 - 104) [14]	1,347	(1,036- 1,580) [14]	24.5 (0.0001)	73
36 kb	A_4	DSB	*WT*	53	(27-112) [6]	12,481	(8,601 - 15,520) [6]	NA	80
36 kb	A_4	DSB	*pif1-m2*	14	(11- 18) [12]	2,410	(2,226 - 2,889) [12]	5.2 (0.009)	77
36 kb	A_4	DSB	*pif1Δ*	9	(5 - 23) [6]	27	(14- 47) [6]	462 (0.005)	90

Table 4.1b The Rate of Spontaneous Lys^+ mutations
The table represents the rate of Lys^+ mutations for spontaneous events estimated in strains with No-DSB. Rates are presented only for 0hr (there is no significant difference in rates between 0hr and 7hr for strains with No-DSB). [a] Rates calculated at 0 hr similarly as described in Table 4.1a; [b] for strains with ≥ 6 experiments CI of median is given while for strains with < 6 experiments median range is given. Numbers in brackets [ ] represent repeats of experiments. [d] % BIR was not determined for strains with No-DSB. Abbreviations ND: Not determined

Position	Construct	*HO* site	Relevant Genotype	Rate of Lys^+ ($x10^{10}$)[a]		% BIR
				Median	CI or range[b] [# of repeats]	
0 kb	A_4	No	WT	73	(10 - 446) [6]	N.D.
0 kb	A_4	No	*pif1-m2*	83	(13- 188) [6]	N.D
0 kb	A_4	No	*pif1Δ*	21	(13-54) [5]	N.D
0 kb	A_4	No	*rev3Δ*	13	(11-17) [6]	N.D.
0 kb	A_4	No	*rev3Δpif1Δ*	16	(13-21) [4]	N.D
16 kb	A_4	No	*WT*	81	(33 - 340) [10]	N.D.
16 kb	A_4	No	*pif1-m2*	108	(88 -138) [6]	N.D.
16 kb	A_4	No	*pif1Δ*	53	(33- 75) [6]	N.D
36 kb	A_4	No	*WT*	11	(7 - 54) [4]	N.D
36 kb	A_4	No	*pif1-m2*	22	(7-35) [4]	N.D
36 kb	A_4	No	*pif1Δ*	9	(6 -39) [5]	N.D

.

4.3 Genetic Control of BIR associated Frameshift Mutagenesis

4.3.1 The Role of Pif1 helicase

Pif1 is a 5' to 3' DNA helicase, encoded by the Pif1 gene of *S. Cerevisiae*, having dual functions and localization (Lahaye, 1991). Pif1 was originally isolated as gene involved in maintenance and repair of mtDNA although the exact mechanism remains unknown to date (Foury and Van Dyk, 1995; Foury and Kolodynsk, 1983).

In the nucleus, the helicase activity of Pif1 is required for removing telomerase from telomeric sequences (Schulz and Zakian, 1994; Zhou et al., 2000; Boule et al., 2005) and also from DSBs (Schulz and Zakian, 1994; Mangahas et al., 2001; Myung K, 2001). This is critical because telomerase can hinder DSB repair by adding telomeric repeats to a broken chromosome, which prevents the break from engaging in recombination repair. Addition of telomere to a DSB is deleterious since it creates a chromosome deficient in genetic information from the site of the break to the normal end of the chromosome. Thus *Pif1* is important for DSB repair as it inhibits telomerase mediated telomere addition to DSBs.

G-quadruplex structures may form from G-rich sequences enriched at DSB sites, telomeric regions, ribosomal DNA (rDNA) and at transcriptional regulatory sites (Hupper JL, 2010). These G4 structures are known to be detrimental to the progress of replication and may also lead to rearrangements (Lipps and Rhodes, 2009). The helicase activity of Pif1 was found to be important for unwinding such G-quadruplex structures *in vitro* (Sanders, 2010; Ribeyre et al., 2011) and *in vivo* (Paeschke et al., 2011).

In addition Pif1 acts within the rDNA in a locus specific manner to help maintain the replication fork barrier (Ivessa et al., 2000). Pif1 also has more global functions in S-phase DNA replication where it co-operates with Pol δ and Dna2 in Okazaki fragment

maturation. It also has repair functions as it localizes to DNA damage foci and reduces accumulation of toxic recombination intermediates, which are formed by the Sgs1 helicase in *top3* (topoisomerase III) cells (Bochman et al., 2010).

Overall Pif1 is a non-essential helicase, which is not a component of S-phase replisome; rather it is recruited to the replication fork as and when it is necessary (Paeschke et al., 2011; reviewed in Bochman et al., 2010). Nevertheless it plays an important role in assisting replication through protein/DNA regions that are difficult to replicate and also in DSB repair, and is important for maintaining genomic stability.

4.3.1.1 The Effect of Pif1 on the efficiency of BIR

Our first goal was to test the role of Pif1 in BIR where we hypothesized that Pif1 is required for an efficient BIR. This was achieved by testing the efficiency of BIR in Pif1-defective cells. Recent literature suggested that nuclear function of Pif1 could be eliminated via a complete deletion of Pif1, *pif1Δ* (eliminating activity of Pif1 in nucleus and mitochondria), or through a point mutation *pif1-m2* (altering second AUG site in the open reading frame), eliminating activity of Pif1 in the nucleus.

The experimental system described earlier in Section 4.2.1 was used to determine the efficiency of BIR (Figure 4.3). Strains carrying *lys2::ins* frameshift reporters at all 3 positions, *MAT*, 16kb and 36kb away from *MAT* were analyzed for the efficiency of BIR, estimated by determining the frequency of $Ade^{+}Leu^{-}$ outcomes among the total number of DSB repaired outcomes following *HO* induction (please refer materials and methods (3.2.6.1) for more details). In this way for WT strains at MAT, the frequency of $Ade^{+}Leu^{-}$ events was determined to be 81% (Table 4.2). For the same position, the frequency of $Ade^{+}Leu^{-}$ events was reduced to 72.1% in *pif1-m2* strains and to 57% in *pif1Δ* strains. Similarly at 16kb, the frequency of $Ade^{+}Leu^{-}$ events was reduced from 76% in WT strains to 60.6 % in *pif1-m2* and 54.6% in *pif1Δ* strains. At 36kb too, the frequency of $Ade^{+}Leu^{-}$ events was reduced, from 70% in WT to 58% in *pif1-m2* and 52.5% in *pif1Δ.* Statistical analysis showed that the reduction of $Ade^{+}Leu^{-}$ frequency only in *pif1Δ* was significant from WT but comparable among all 3 positions. These results thus show that the frequency of $Ade^{+}Leu^{-}$ events was reduced from nearly 80% in WT to nearly 50% in cells defective in Pif1 (*pif1Δ*).

DSB repaired outcomes selected by an $Ade^{+}Leu^{-}$ phenotype consisted of not only BIR repaired outcomes but also chromosomal translocations (invasion of broken chromosome into other non-homologous chromosomes (see Figure 4.3). Further analysis (by Dr. Malkova) demonstrated that up to 30% of the remaining $Ade^{+}Leu^{-}$ outcomes in *pif1Δ* were chromosomal rearrangements including translocations.

In summary, all our results taken together demonstrate that the efficiency of BIR is reduced from nearly 80% in WT to nearly 22% in Pif1 defective cells. Thus elimination of *PIF1* reduces the efficiency of BIR by approximately 3.3 fold.

The decrease in BIR efficiency observed in the absence of Pif1 was simultaneously accompanied by an increase in the frequency of other DSB stabilizing outcomes. The frequency of gross chromosomal rearrangements (including half crossovers and chromosomal translocations) was increased from nearly 8% in WT to nearly 50% in Pif1 defective cells (Table 4.2). Chromosomal loss events were also observed with a higher frequency (nearly 15-20%) in Pif1 defective cells (see Figure 4.3 for descriptions).

These results therefore demonstrate that Pif1 is required for the high efficiency of BIR. The fact that a substantial amount of BIR (22%) can still continue in Pif1$^-$ background made it possible to test the role of Pif1 in BIR mutagenesis further.

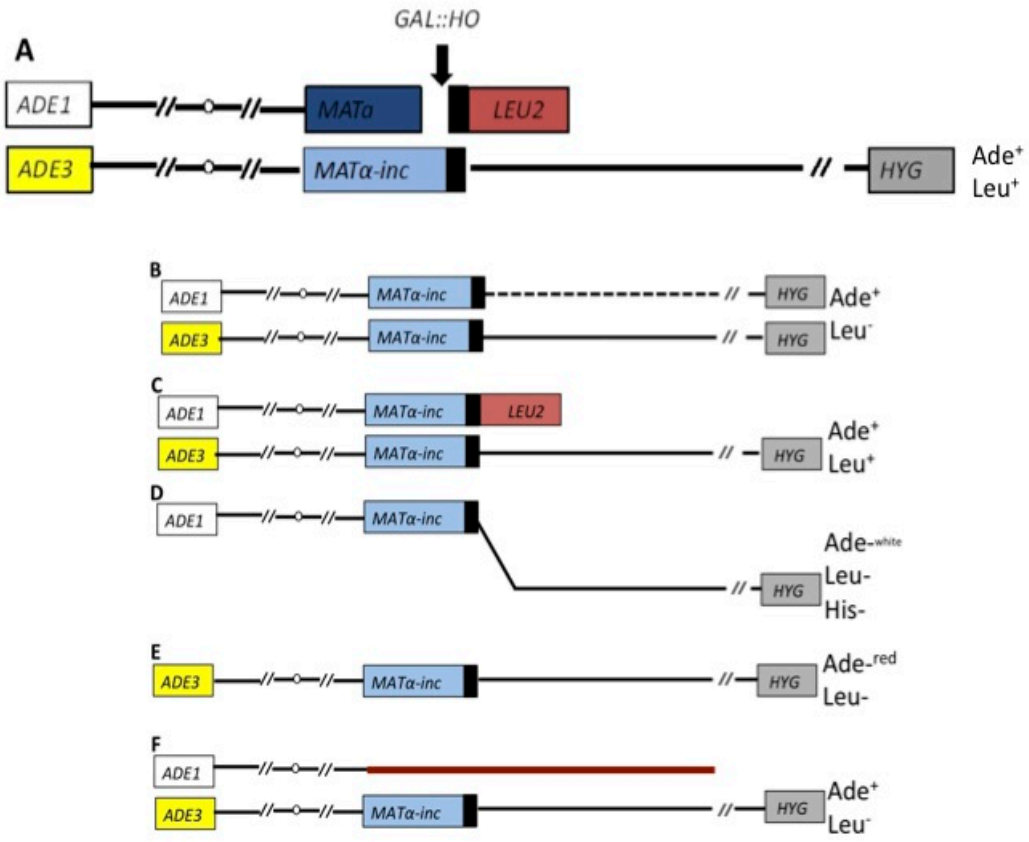

Figure 4.3 HO induced DSB repair outcomes from disomic Experimental System.
The experimental strain described in Figure 4.1 along with its HO induced DSB repair outcomes are shown here. (A) Represents the parent strain, which in this case could be WT, *pif1Δ* or *pif1-m2.* (B) BIR repair outcome. (C) GC repair outcome. (D) HCO outcome resulting from fusion of left half of truncated chromosome and right half of full-length chromosome. (E) Chromosome loss when HO cut site is not repaired and truncated chromosome is lost. (F) Chromosomal translocation resulting from repair of the broken chromosome by any non-homologous chromosome. For repair outcomes (B-F) phenotypes are indicated on the right.

Table 4.2 HO induced DSB repair outcomes in WT and Pif1 defective cells (*pif1Δ* or *pif1-m2*)

Position	Genotype	Total outcomes (Colonies) scored	Number of DSB repaired Outcomes with Phenotype indicated (%)				p -value
			BIR (Ade+Leu-	GC (Ade+Leu+	HCO (Ade-^{white}Leu^{-}His^{-}	CL (Ade-^{red}Leu^{-}	
MAT	*WT*	98	80 (81.6)	2 (2)	8 (8)	8 (8)	N.A
	pif1Δ	100	57 (57)*	3 (3)	21 (21)	19 (19)	0.002
	pif1-m2	97	70	4	18	5	NS
16kb	*WT*	100	76 (76)	15 (15)	8 (8)	1 (1)	NA
	pif1Δ	97	53 (54.6)*	12 (12.3)	22 (22.6)	10 (10.3)	0.0004
	pif1m2	99	60 (60.6)	27 (27.2)	11 (11.1)	1 (1)	N.S
36kb	*WT*	100	70 (70)	20 (20)	8 (8)	2 (2)	N.A
	pif1Δ	97	51 (52.5)*	10 (10.3)	22 (22.6)	14 (14.4)	< 0.0001
	pif1-m2	100	58 (58)	19 (19)	21 (21)	2 (2)	N.S.

Abbreviations: Ade^{-red} =Ade^{-} His^{+} red colonies denoting the *ade1ADE3* genotype; Ade^{-white}=Ade^{-}His^{-} white colonies denoting the *ADE1ade3.* Genotype; GC= gene conversion; BIR= break-induced replication; HCO=half-crossover; WT= wild type; [a] at least some events could be GCRs. Asterisk* indicates statistically significant difference in the efficiency of BIR from isogenic WT strains. p-values based on $p < 0.05$ determined by Chi-square Analysis.

4.3.1.2 The Role of Pif1 in BIR Frameshift Mutagenesis

The role of Pif1 in BIR mutagenesis was tested by introducing *pif1-m2* and *pif1Δ* in disomic BIR strains (described in Figure 4.1) carrying frameshift reporters at all 3 positions *MAT*, 16kb and 36kb away from *MAT*. To determine the effect of Pif1 on BIR frameshift mutagenesis, the rates of DSB induced Lys^+ mutagenesis in pif1 defective cells (i.e. *pif1-m2* and *pif1Δ*) were compared the rates of DSB induced Lys^+ mutagenesis in WT. A similar experimental approach (as in Section 4.2.1) was followed to determine the level of DSB-induced Lys^+ mutagenesis in *pif1-m2* and *pif1Δ* strains.

First, in the *pif1-m2* background at MAT position, the rate of DSB induced Lys^+ frameshift mutations were reduced by 1.5 times compared to WT as shown in Table 4.1a (see Figure 4.4). DSB induced Lys^+ mutations were also reduced at 16kb in *pif1-m2* by 4.3 times and at 36kb by 5 times compared to WT. A majority of these DSB induced Lys^+ frameshift mutations result from error-prone DNA synthesis during BIR (^{e} determined by the % of BIR in Table 4.1a). Therefore our data suggests that *pif1-m2* made frameshift mutations progressively less frequent in BIR, starting from the point of initiation at MAT to as far as 36kb away, when compared to WT.

Next, Lys^+ frameshift mutation rates were analyzed in strains carrying full deletion of *PIF1*. For strains at *MAT*, carrying *pif1Δ,* the rate of DSB induced Lys^+ mutations were reduced by 3 times compared to WT (Table 4.1a, Figure 4.4). For strains at 16kb, the rate of DSB induced Lys^+ mutations were strongly decreased by over 24 times in *pif1Δ* compared to WT. For *pif1Δ* strains at 36kb, the rate of DSB induced Lys+ mutations reduced dramatically, by 492 times compared to WT, becoming almost comparable to spontaneous levels.

Thus we saw that the effect of *pif1Δ* was higher than the effect of *pif1-m2* on mutagenesis in BIR. Overall frameshift mutations in BIR were very few in *pif1Δ*

compared to WT, especially at 36kb. Taken together, these results demonstrate that Pif1 is responsible for a large part of frameshift mutations associated with BIR.

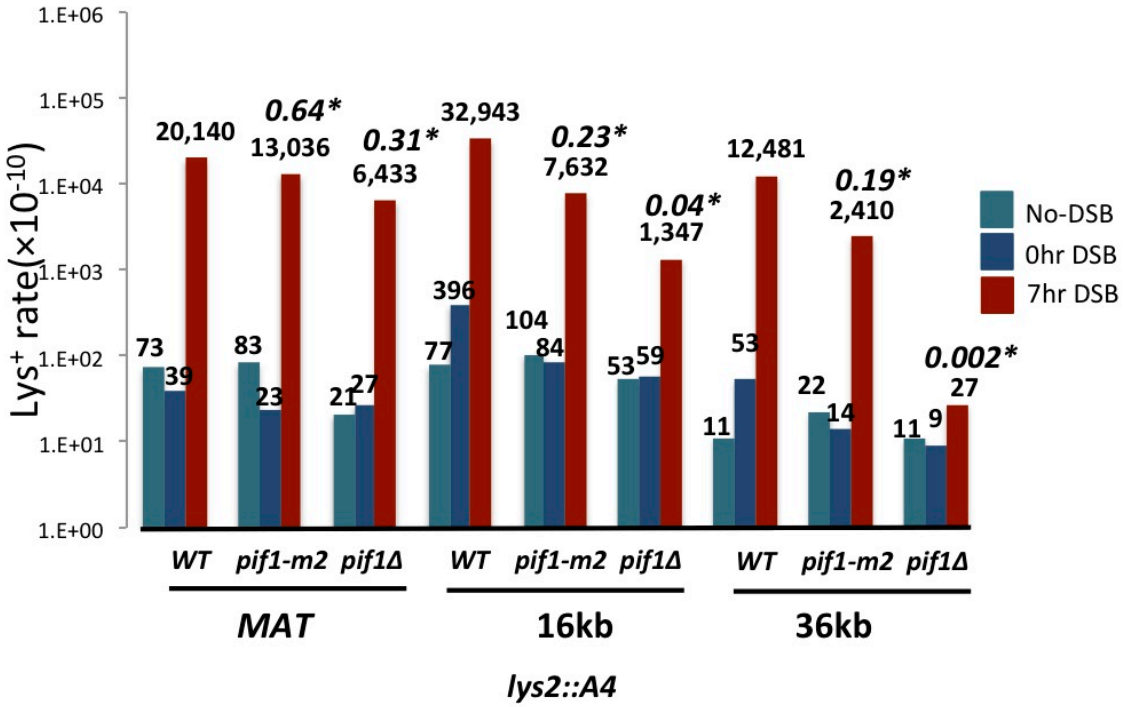

Figure 4.4 The Role of Pif1 in BIR associated frameshift mutagenesis.
The rate of Lys^+ frameshift mutations was determined before (0hr) and (7hr) after addition of galactose to media for WT, *pif1-m2 and pif1Δ* strains carrying *lys2::ins* frameshift reporters at 3 positions *MATα-inc (MAT)*, 16kb and 36kb centromere-distal to *MAT.* The fold decrease in BIR mutagenesis rates in mutants as compared to WT (in case of statistically significant difference) is indicated in italics. Statistically significant differences from WT are indicated by an asterisk. Other abbreviations and statistical details are similar to those described in the legend for Figure 4.2.

4.3.2 The Role of Translesion Polymerase Pol ζ

In 4.3.1.2 we saw that *pif1Δ* had a smaller effect on frameshift mutagenesis at *MAT* when compared to other positions. Therefore, we hypothesized that another pathway of mutagenesis may exist in the absence of Pif1. We speculated that such a pathway of mutagenesis maybe either be associated with a defective replication fork or assisted by accumulation of damaged DNA (as discussed in Northam et al., 2010; Pavlov et al., 2006; Strathern et al., 1995; Yang et al., 2008).

Our speculation was based on the idea that the *MAT* locus, the site where BIR initiates after a DSB, is persistently associated with ssDNA in the form of a displacement (D) loop, due to the slow initiation of BIR (Jain et al., 2001; Malkova et al., 2005). This bare ssDNA at MAT becomes a potential source of DNA damage or mutagenesis. In S-phase replication, such DNA damage (in the form of adducts or lesions) which can potentially stall or collapse DNA replication forks can be avoided by specialized DNA polymerases known as translesion polymerases such as Pol ζ. Pol ζ can bypass such DNA damage lesions by incorporating a nucleotide opposite to the lesion instead of repairing it. Pol ζ, is a low fidelity polymerase as it lacks 3’ to 5’ exonuclease proofreading activity (McCulloch and Kunkel, 2008). Therefore even though it helps replication to continue past damaged DNA, its synthesis is highly error-prone and promotes mutagenesis.

Pol ζ is also not usually associated with S-phase replisome and is required on an as needed basis for events such as damaged DNA replication. However it participates in DSB repair and is also responsible for mutagenesis in DSB repair (Holleback and Strathern, 1997). Therefore we hypothesized that Pol ζ could be associated with the mutagenic replication fork in BIR and promotes mutagenesis close to the site of BIR initiation in *pif1Δ* strains.

4.3.2.1 The Effect of Rev3 on BIR Frameshift Mutagenesis

To test the role of Pol ζ in BIR associated frameshift mutagenesis, strains carrying frameshift reporters at *MAT* with full deletion of *REV3* (Rev3, encodes the catalytic subunit of yeast Pol ζ) were used. We determined the effect of *rev3Δ* on BIR mutagenesis at *MAT* by comparing the rate of DSB induced Lys^+ mutagenesis in *rev3Δ* cells to the rate of DSB induced Lys^+ mutagenesis in WT.

For the *rev3Δ* background at *MAT*, the rate of Lys^+ frameshift mutagenesis was reduced 2 times compared to WT (as shown in Table 4.1a; Figure 4.5). This result showed that Rev3 is responsible for some frameshift mutagenesis in BIR at *MAT*. This led us to believe that the remaining high frequency of mutations observed at *MAT* position in the *pif1Δ* strains were probably made by a Rev3 dependent pathway. To test this possibility, *rev3Δ* was introduced in *pif1Δ* strains carrying frameshift reporters at *MAT*. We determined the effect of this double mutant *rev3Δpif1Δ* on mutagenesis at *MAT*, by comparing the rate of DSB induced Lys^+ mutations between *rev3Δpif1Δ* and WT.
The rate of Lys^+ frameshift mutations was reduced severely, by nearly 87 times in *rev3Δpif1Δ* compared to WT (as shown in Table 4.1a). Thus the high frequency of BIR frameshift mutagenesis observed in WT, and the mutagenesis remaining in *pif1Δ* was synergistically reduced in *rev3Δpif1Δ* suggesting that *rev3Δ* eliminated mutagenesis occurring in *pif1Δ*.

Therefore our results demonstrate that a Rev3 (Pol ζ) dependent pathway exists in BIR, observed in the absence of Pif1, which is responsible for a signficant portion of frameshift mutations occurring close to the initiation of BIR.

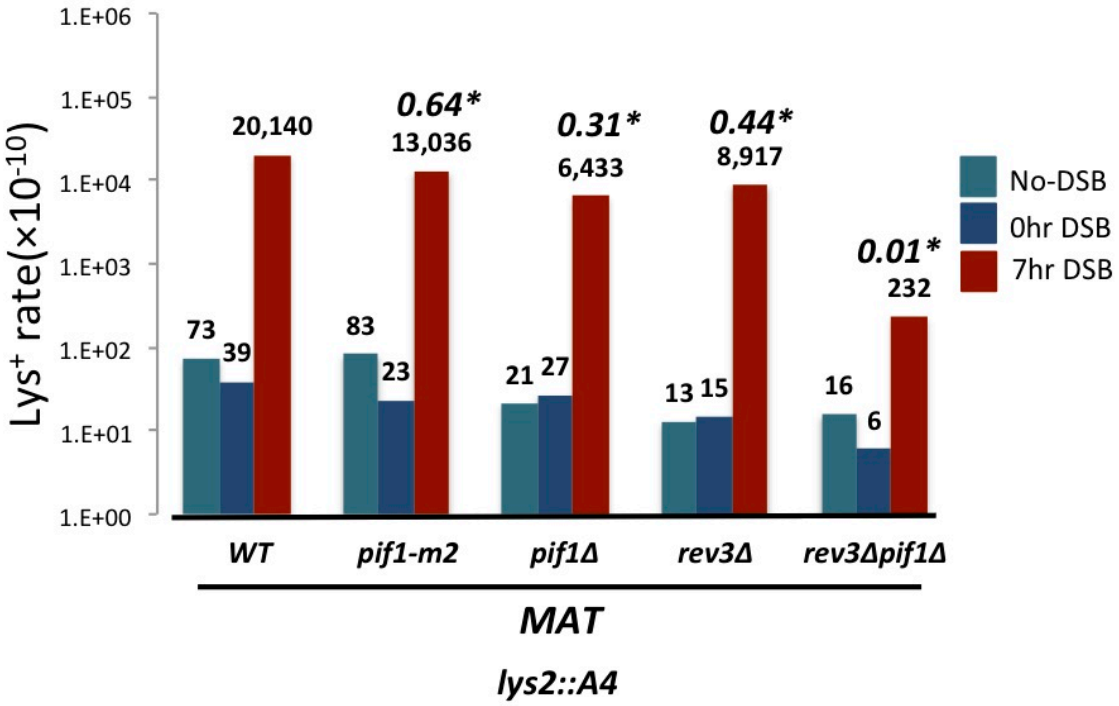

Figure 4.5 The Role of Rev3 in BIR associated frameshift mutagenesis in the absence of *PIF1***.** The rate of Lys+ frameshift mutations was determined before (0hr) and (7hr) after addition of galactose to media for WT, *pif1-m2 and pif1Δ*, *rev3Δ* and *pif1Δrev3Δ* strains carrying *lys2::ins* frameshift reporters at *MATα-inc (MAT).* The fold decrease in BIR mutagenesis rates in mutants as compared to WT (in case of statistically significant difference) is indicated in italics. Statistically significant differences from WT are indicated by an asterisk. Other abbreviations and statistical details are similar to those described in the legend for Figure 4.2.

4.3.3 Analysis of DSB induced Lys$^+$ Mutation Spectra

Next, we analyzed DSB induced Lys$^+$ outcomes at MAT by sequencing 400bp of the *LYS2* gene containing the *lys2::ins* frameshift reporter. Lys$^+$ outcomes obtained in WT, *rev3Δ, pif1Δ* and *rev3Δpif1Δ* strains were sequenced. We observed that 100% of Lys$^+$ outcomes in WT (25/25) were simple -1bp deletions (Table 4.3) (For example in Table 4.4a Strain ID 1411.8.36 shows A deletion at position 78). All of these -1bp deletions in WT were concentrated in the sequence AGGGCCAAGG (Figure 6), which consisted of several small homonucleotide runs where one of the small homonucleotide runs could promote replication slippage.

One hundred percent of Lys$^+$ outcomes in *rev3Δ* background (29/29) were also simple -1bp deletions (Table 4.3), similar to WT as shown in Table 4.4b. These -1bp deletions observed in *rev3Δ* background were clearly Pif1 dependent since *pif1Δ* eliminated *rev3Δ* independent Lys$^+$ mutations (As described earlier in Section 4.3.1.2; Figure 4.5).

Next, we observed that Lys+ outcomes in the *pif1Δ* strain background were of two types; 29% (11/37) of Lys$^+$ mutations were simple -1bp deletions and the remaining 71% of Lys$^+$ mutations (26/37) were complex events with 3-23bp deletions and 2-25bp insertions (Table 4.3). Among these complex mutations, 80% (21/26) of insertions were templated from sequences located upstream in the *lys2* reporter. For example in Table 4.4c Strain ID 2193G1 shows an 8bp deletion (green) and 7bp insertion (red) between the loci 78-85. We found that this 7bp insertion was copied from sequences located in the *lys2* reporter itself between the loci 42-48 (orange). These insertions appeared to have been synthesized by switching between template sequences where the nascent strand dissociated from donor template at C (before the 7bp deletion (green)), invaded into the G in the sequence GACTTGC (orange) copied this sequence, which led to the formation of an inverted repeat (red insertion), dissociated from C in the copied sequence GACTTGC (orange) and returned back to G (after the 7bp deletion). Interestingly, small regions of micro-homologies (1-6bp) were found near the junctions

of template switching (In this case AGCGTC before the deletion (green) complementary to TCGCAG before the template switching sequence (orange)). These Lys^+ template-switching events observed here in the *pif1Δ* background were Rev3 dependent since *rev3Δ* eliminated Lys^+ mutations in *pif1Δ* strains. Taken together these results indicate the role of Rev3 (Pol ζ) in promoting template switching in BIR initiated events. Physical analysis of these Lys^+ outcomes associated with template switching, observed in the *pif1Δ* background (by PFGE and Southern hybridization) revealed that they were frequently associated with gross chromosomal rearrangements (approximately 60% (9/15 analyzed so far)) as shown in Figure 4.6.

We observed that Lys^+ outcomes in the double mutant *rev3Δpif1Δ*, which occurred 100 times less frequent than in WT, were of two types. 33% of these outcomes (6/18) were simple -1bp deletions while remaining 67% (12/18) were complex mutations with 3-16bp deletions and 5-15bp insertions (Table 4.3). Interestingly, 60% of these complex mutations consisted of insertions having GT rich sequences and were of a specific pattern GTGGGTGTGGTGTGT (For example in Table 4.4d Strain ID 2409 contained a 15bp insertion consisting of GT rich sequences). These GT rich sequences were found to be identical to sequences in telomere regions in some chromosomes. We speculate that these sequences are inserted by telomerase mediated DNA synthesis. Such events are quite possible in the absence of Pif1, a known negative regulator of telomerase at DSB sites. Another possibility is that these sequences may be inserted by template switching to telomeric regions by an unknown DNA polymerase.

Table 4.3 Summary of Types of BIR induced Lys^+ mutations at *MAT.*
Lys^+ outcomes in WT, *pif1Δ, rev3Δ and pif1Δrev3Δ* strains carrying frameshift reporter *lys2::ins*. Lys^+ outcomes were classified as either simple mutations consisting of -1bp deletions or complex mutations consisting of large indels (See Table 4.4 for detailed analysis). Numbers in parenthesis represent percentages of total sequences analyzed.

Position	Genotype	Types of Mutations (%)		Total Analyzed
		Simple Mutations (-1bpdel)	Complex Mutations	
MAT	*WT*	25 (100)	-	25
	rev3Δ	29 (100)	-	29
	pif1Δ	11 (29)	26 (71)	37
	pif1Δrev3Δ	6 (33)	12 (67)	18

Table 4.4 Sequencing analysis of BIR induced Lys$^+$ mutations at *MAT* for (a) WT, (b) *rev3Δ*, (c) *pif1Δ and* (d) *pif1Δrev3Δ* strains. A portion of the *LYS2* coding sequence containing the 61 nucleotide insert (*lys2::ins*; positions 13-74) is shown above each table. In the sequence the gray box indicates the direct repeats flanking the 61bp insert. The underlined italics *GGGCCAAGG* (on the right) indicate the frameshift mutation hotspot and *TTGCC*, its partial -1bp quasipalindromic sequence (on the left). For all strains BIR induced Lys$^+$ outcomes are aligned with the original reference sequence (WT *lys2::ins* sequence) to identify the site of mutation. Sequences (nucleotides) shaded in green represented deleted sequences while those in red represent insertions. Italicized sequences in orange represent regions from where the insertions were found to be templated. BIR induced Lys$^+$ sequences were classified as either heterozygotes (having two copies of *lys2* gene) or homozygotes (where only one copy of *lys2* is retained). For each outcome the number of indels (insertions plus deletions) that results in Lys$^+$ frameshift mutation is described along with the position of mutation. For Lys$^+$ outcomes resulting from template switching events, the loci of templated sequences are indicated.

Table 4.4a Sequencing Analysis of BIR induced Lys^{+} mutations at *MAT* (WT)

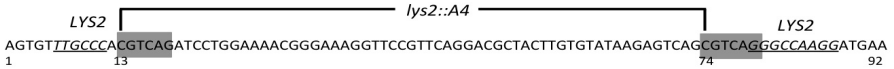

Strain ID:	Sequence:	Mutation Type	No of Indels	Locus of Mutation	Locus of Template Switching
1411.8.36	Original: AGTGTTTGCCCACGTCAGATCCTGGAAAACGGGAAAGGTTCCGTTCAGGACGCTACTTGTGTATAAGAGTCAGCGTCAGGGCCAAGGATGAA Outcome: AGTGTTTGCCCACGTCAGATCCTGGAAAACGGGAAAGGTTCCGTTCAGGACGCTACTTGTGTATAAGAGTCAGCGTT GGGCCAAGGATGAA	heterozygote	1bpdel	78	N.D.
1411.8.44	Orignal: AGTGTTTGCCCACGTCAGATCCTGGAAAACGGGAAAGGTTCCGTTCAGGACGCTACTTGTGTATAAGAGTCAGCGTCAGGGCCAAGGATGAA Outcome: AGTGTTTGCCCACGTCAGATCCTGGAAAACGGGAAAGGTTCCGTTCAGGACGCTACTTGTGTATAAGAGTCAGCGTCAGG CCAAGGATGAA	heterozyote	1bpdel	81	N.D.
1411.8.45	Original: AGTGTTTGCCCACGTCAGATCCTGGAAAACGGGAAAGGTTCCGTTCAGGACGCTACTTGTGTATAAGAGTCAGCGTCAGGGCCAAGGATGAA Outcome: AGTGTTTGCCCACGTCAGATCCTGGAAAACGGGAAAGGTTCCGTTCAGGACGCTACTTGTGTATAAGAGTCAGCGTCAGGGCCA GGATGAA	heterozygote	1bpdel	85	N.D.
1411.8.01	Original: AGTGTTTGCCCACGTCAGATCCTGGAAAACGGGAAAGGTTCCGTTCAGGACGCTACTTGTGTATAAGAGTCAGCGTCAGGGCCAAGGATGAA Outcome: AGTGTTTGCCCACGTCAGATCCTGGAAAACGGGAAAGGTTCCGTTCAGGACGCTACTTGTGTATAAGAGTCAGCGTCAGGGCCAA GATGAA	heterozygote	1bpdel	87	N.D.
1411.8.38	Original: AGTGTTTGCCCACGTCAGATCCTGGAAAACGGGAAAGGTTCCGTTCAGGACGCTACTTGTGTATAAGAGTCAGCGTCAGGGCCAAGGATGAA Outcome: AGTGTTTGCCCACGTCAGATCCTGGAAAACGGGAAAGGTTCCGTTCAGGACGCTACTTGTGTATAAGAGTCAGCGTCAGGGC AAGGATGAA	heterozygote	1bpdel	82	N.D.
1411.11.02	Original: AGTGTTTGCCCACGTCAGATCCTGGAAAACGGGAAAGGTTCCGTTCAGGACGCTACTTGTGTATAAGAGTCAGCGTCAGGGCCAAGGATGAA Outcome: AGTGTTTGCCCACGTCAGATCCTGGAAAACGGGAAAGGTTCCGTTCAGGACGCTACTTGTGTATAAGAGTCAGCGTCAGGGCCA GGATGAA	heterozygote	1bpdel	85	N.D.
1411.8.48	Original: AGTGTTTGCCCACGTCAGATCCTGGAAAACGGGAAAGGTTCCGTTCAGGACGCTACTTGTGTATAAGAGTCAGCGTCAGGGCCAAGGATGAA Outcome: AGTGTTTGCCCACGTCAGATCCTGGAAAACGGGAAAGGTTCCGTTCAGGACGCTACTTGTGTATAAGAGTAAGCGTAAGG CCAAGGATGAA	homozygote	1bpdel	81	N.D.
1411.8.49	Original: AGTGTTTGCCCACGTCAGATCCTGGAAAACGGGAAAGGTTCCGTTCAGGACGCTACTTGTGTATAAGAGTCAGCGTCAGGGCCAAGGATGAA Outcome: AGTGTTTGCCCACGTCAGATCCTGGAAAACGGGAAAGGTTCCGTTCAGGACGCTACTTGTGTATAAGAGTAAGCGTAAGG CCAAGGATGAA	heterozygote	1bpdel	81	N.D.
1411.8.42	Original: AGTGTTTGCCCACGTCAGATCCTGGAAAACGGGAAAGGTTCCGTTCAGGACGCTACTTGTGTATAAGAGTCAGCGTCAGGGCCAAGGATGAA Outcome: AGTGTTTGCCCACGTCAGATCCTGGAAAACGGGAAAGGTTCCGTTCAGGACGCTACTTGTGTATAAGAGTCAGCGTCAGG TTAAGGATGAA	heterozygote	3bpdel+2bpins =-1del	81-83	N.D.
1411.8.43	Original: AGTGTTTGCCCACGTCAGATCCTGGAAAACGGGAAAGGTTCCGTTCAGGACGCTACTTGTGTATAAGAGTCAGCGTCAGGGCCAAGGATGAA Outcome: AGTGTTTGCCCACGTCAGATCCTGGAAAACGGGAAAGGTTCCGTTCAGGACGCTACTTGTGTATAAGAGTCAGCGTCAGGGCC AGGATGAA	heterozygote	1bpdel	85	N.D.
1411.7.93	Original: AGTGTTTGCCCACGTCAGATCCTGGAAAACGGGAAAGGTTCCGTTCAGGACGCTACTTGTGTATAAGAGTCAGCGTCAGGGCCAAGGATGAA Outcome: AGTGTTTGCCCACGTCAGATCCTGGAAAACGGGAAAGGTTCCGTTCAGGACGCTACTTGTGTATAAGAGTCAGCGTCAGGGCCAA GATGAA	heterozygote	1bpdel	87	N.D.

Table 4.4a Sequencing Analysis of BIR induced Lys^{+} mutations at *MAT* (WT) (continued)

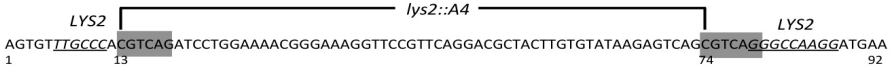

Strain ID:	Sequence:	Mutation Type	No of Indels	Locus of Mutation	Locus of Template Switching
1411.7.1	Orignal: AGTGTTTGCCCACGTCAGATCCTGGAAAACGGGAAAGGTTCCGTTCAGGACGCTACTTGTGTATAAGAGTCAGCGTCAGGGCCAAGGATGAA Outcome: AGTGTTTGCCCACGTCAGATCCTGGAAAACGGGAAAGGTTCCGTTCAGGACGCTACTTGTGTATAAGAGTCAGCGTCAGG CCAAGGATGAA	hererozygote	1bpdel	81	N.D.
1411.7.2	Original: AGTGTTTGCCCACGTCAGATCCTGGAAAACGGGAAAGGTTCCGTTCAGGACGCTACTTGTGTATAAGAGTCAGCGTCAGGGCCAAGGATGAA Outcome: AGTGTTTGCCCACGTCAGATCCTGGAAAACGGGAAAGGTTCCGTTCAGGACGCTACTTGTGTATAAGAGTCAGCGTCAGGGC AAGGATGAA	hererozygote	1bpdel	82	N.D.
1411.7.3	Original: AGTGTTTGCCCACGTCAGATCCTGGAAAACGGGAAAGGTTCCGTTCAGGACGCTACTTGTGTATAAGAGTCAGCGTCAGGGCCAAGGATGAA Outcome: AGTGTTTGCCCACGTCAGATCCTGGAAAACGGGAAAGGTTCCGTTCAGGACGCTACTTGTGTATAAGAGTCAGCGTCAGGGCCAA GATGAA	hererozygote	1bpdel	87	N.D.
1411.7.4	Original: AGTGTTTGCCCACGTCAGATCCTGGAAAACGGGAAAGGTTCCGTTCAGGACGCTACTTGTGTATAAGAGTCAGCGTCAGGGCCAAGGATGAA Outcome: AGTGTTTGCCCACGTCAGATCCTGGAAAACGGGAAAGGTTCCGTTCAGGACGCTACTTGTGTATAAGAGTCAGCGTCAGGGCC AGGATGAA	hererozygote	1bpdel	85	N.D.
1411.7.73	Original: AGTGTTTGCCCACGTCAGATCCTGGAAAACGGGAAAGGTTCCGTTCAGGACGCTACTTGTGTATAAGAGTCAGCGTCAGGGCCAAGGATGAA Outcome: AGTGTTTGCCCACGTCAGATCCTGGAAAACGGGAAAGGTTCCGTTCAGGACGCTACTTGTGTATAAGAGTCAG ATCAGGGCCAAGGATGAA	heterozygote	2bpdel+1bpdel =-1del	74-75	N.D.
1411.7.81	Orignal: AGTGTTTGCCCACGTCAGATCCTGGAAAACGGGAAAGGTTCCGTTCAGGACGCTACTTGTGTATAAGAGTCAGCGTCAGGGCCAAGGATGAA Outcome: AGTGTTTGCCCACGTCAGATCCTGGAAAACGGGAAAGGTTCCGTTCAGGACGCTACTTGTGTATAAGAGTCAGCGTCAGG CCAAGGATGAA	heterozygote	1bpdel	81	N.D.
1411.7.89	Original: AGTGTTTGCCCACGTCAGATCCTGGAAAACGGGAAAGGTTCCGTTCAGGACGCTACTTGTGTATAAGAGTCAGCGTCAGGGCCAAGGATGAA Outcome: AGTGTTTGCCCACGTCAGATCCTGGAAAACGGGAAAGGTTCCGTTCAGGACGCTACTTGTGTATAAGAGTCAGCGTCAGGGCC AGGATGAA	heterozygote	1bpdel	85	N.D.
1411.7.74	Original: AGTGTTTGCCCACGTCAGATCCTGGAAAACGGGAAAGGTTCCGTTCAGGACGCTACTTGTGTATAAGAGTCAGCGTCAGGGCCAAGGATGAA Outcome: AGTGTTTGCCCACGTCAGATCCTGGAAAACGGGAAAGGTTCCGTTCAGGACGCTACTTGTGTATAAGAGTCAGCCTCCGGGC AAGGATGAA	heterozgygote	1bpdel	83	N.D.
1411.7.82	Orignal: AGTGTTTGCCCACGTCAGATCCTGGAAAACGGGAAAGGTTCCGTTCAGGACGCTACTTGTGTATAAGAGTCAGCGTCAGGGCCAAGGATGAA Outcome: AGTGTTTGCCCACGTCAGATCCTGGAAAACGGGAAAGGTTCCGTTCAGGACGCTACTTGTGTATAAGAGTCAGCGTCAGG CCAAGGATGAA	heterozygote	1bpdel	81	N.D.
1411.7.90	Original: AGTGTTTGCCCACGTCAGATCCTGGAAAACGGGAAAGGTTCCGTTCAGGACGCTACTTGTGTATAAGAGTCAGCGTCAGGGCCAAGGATGAA Outcome: AGTGTTTGCCCACGTCAGATCCTGGAAAACGGGAAAGGTTCCGTTCAGGACGCTACTTGTGTATAAGAGTCAGCGTCAGGGCC AGGATGAA	heterozygote	1bpdel	85	N.D.

Table 4.4a Sequencing Analysis of BIR induced Lys^{+} mutations at *MAT* (WT) (continued)

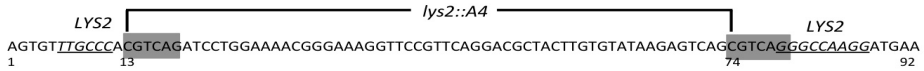

Strain ID:	Sequence:	Mutation Type	No of Indels	Locus of Mutation	Locus of Template Switching
1411.7.75	Orignal: AGTGTTTGCCCACGTCAGATCCTGGAAAACGGGAAAGGTTCCGTTCAGGACGCTACTTGTGTATAAGAGTCAGCGTCAGGGCCAAGGATGAA Outcome: AGTGTTTGCCCACGTCAGATCCTGGAAAACGGGAAAGGTTCCGTTCAGGACGCTACTTGTGTATAAGAGTCAGCGTCAGG CCAAGGATGAA	heterozygote	1bpdel	81	N.D.
1411.7.83	Orignal: AGTGTTTGCCCACGTCAGATCCTGGAAAACGGGAAAGGTTCCGTTCAGGACGCTACTTGTGTATAAGAGTCAGCGTCAGGGCCAAGGATGAA Outcome: AGTGTTTGCCCACGTCAGATCCTGGAAAACGGGAAAGGTTCCGTTCAGGACGCTACTTGTGTATAAGAGTCAGCGTCAGG CCAAGGATGAA	heterozygote	1bpdel	81	N.D.
1411.7. 91	Orignal: AGTGTTTGCCCACGTCAGATCCTGGAAAACGGGAAAGGTTCCGTTCAGGACGCTACTTGTGTATAAGAGTCAGCGTCAGGGCCAAGGATGAA Outcome: AGTGTTTGCCCACGTCAGATCCTGGAAAACGGGAAAGGTTCCGTTCAGGACGCTACTTGTGTATAAGAGTCAGCGTCAGG CCAAGGATGAA	heterozgyote	1bpdel	81	N.D.
1411.7.76	Original: AGTGTTTGCCCACGTCAGATCCTGGAAAACGGGAAAGGTTCCGTTCAGGACGCTACTTGTGTATAAGAGTCAGCGTCAGGGCCAAGGATGAA Outcome: AGTGTTTGCCCACGTCAGATCCTGGAAAACGGGAAAGGTTCCGTTCAGGACGCTACTTGTGTATAAGAGTCAGCCTCCGGGC AAGGATGAA	heterozygote	1bpdel	83	N.D.

Table 4.4b Sequencing Analysis of BIR induced Lys^{+} mutations at *MAT* (*rev3Δ*)

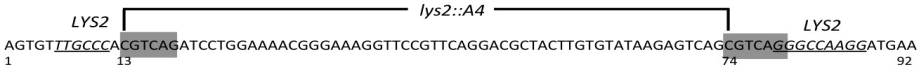

Strain ID:	Sequence:	Mutation Type	No of Indels	Locus of Mutation	Locus of Template Switching
2268B6	Original: AGTGTTTGCCCACGTCAGATCCTGGAAAACGGGAAAGGTTCCGTTCAGGACGCTACTTGTGTATAAGAGTCAGCGTCAGGGCCAAGGATGAA Outcome: AGTGTTTGCCCACGTCAGATCCTGGAAAACGGGAAAGGTTCCGTTCAGGACGCTACTTGTGTATAAGAGTCAGCGTCAGGGCCAAG ATGAA	heterozygote	1bpdel	87	N.D
2268B8	Original: AGTGTTTGCCCACGTCAGATCCTGGAAAACGGGAAAGGTTCCGTTCAGGACGCTACTTGTGTATAAGAGTCAGCGTCAGGGCCAAGGATGAA Outcome: AGTGTTTGCCCACGTCAGATCCTGGAAAACGGGAAAGGTTCCGTTCAGGACGCTACTTGTGTATAAGAGTCAGCGTCAGGGCCA GGATGAA	heterozyote	1bpdel	85	N.D
2268B9	Original: AGTGTTTGCCCACGTCAGATCCTGGAAAACGGGAAAGGTTCCGTTCAGGACGCTACTTGTGTATAAGAGTCAGCGTCAGGGCCAAGGATGAA Outcome: AGTGTTTGCCCACGTCAGATCCTGGAAAACGGGAAAGGTTCCGTTCAGGACGCTACTTGTGTATAAGAGTCAGCGTCAGGGCCA GGATGAA	heterozygote	1bpdel	85	N.D
2268B10	Original: AGTGTTTGCCCACGTCAGATCCTGGAAAACGGGAAAGGTTCCGTTCAGGACGCTACTTGTGTATAAGAGTCAGCGTCAGGGCCAAGGATGAA Outcome: AGTGTTTGCCCACGTCAGATCCTGGAAAACGGGAAAGGTTCCGTTCAGGACGCTACTTGTGTATAAGAGTCAGCGTCAGGGCCA GGATGAA	heterozygote	1bpdel	85	N.D
2268D5	Original: AGTGTTTGCCCACGTCAGATCCTGGAAAACGGGAAAGGTTCCGTTCAGGACGCTACTTGTGTATAAGAGTCAGCGTCAGGGCCAAGGATGAA Outcome: AGTGTTTGCCCACGTCAGATCCTGGAAAACGGGAAAGGTTCCGTTCAGGACGCTACTTGTGTATAAGAGTCAGCGTCAGGGCCA GGATGAA	heterozygote	1bpdel	85	N.D
2268C1	Original: AGTGTTTGCCCACGTCAGATCCTGGAAAACGGGAAAGGTTCCGTTCAGGACGCTACTTGTGTATAAGAGTCAGCGTCAGGGCCAAGGATGAA Outcome: AGTGTTTGCCCACGTCAGATCCTGGAAAACGGGAAAGGTTCCGTTCAGGACGCTACTTGTGTATAAGAGTCAGCGTCAGGGCCA GGATGAA	heterozygote	1bpdel	85	N.D
2268C2	Original: AGTGTTTGCCCACGTCAGATCCTGGAAAACGGGAAAGGTTCCGTTCAGGACGCTACTTGTGTATAAGAGTCAGCGTCAGGGCCAAGGATGAA Outcome: AGTGTTTGCCCACGTCAGATCCTGGAAAACGGGAAAGGTTCCGTTCAGGACGCTACTTGTGTATAAGAGTCAGCGTCAGGGCCA GGATGAA	heterozygote	1bpdel	85	N.D
2268C3	Original: AGTGTTTGCCCACGTCAGATCCTGGAAAACGGGAAAGGTTCCGTTCAGGACGCTACTTGTGTATAAGAGTCAGCGTCAGGGCCAAGGATGAA Outcome: AGTGTTTGCCCACGTCAGATCCTGGAAAACGGGAAAGGTTCCGTTCAGGACGCTACTTGTGTATAAGAGTCAGCGTCAGGGCCA GGATGAA	heterozygote	1bpdel	85	N.D
2268C4	Original: AGTGTTTGCCCACGTCAGATCCTGGAAAACGGGAAAGGTTCCGTTCAGGACGCTACTTGTGTATAAGAGTCAGCGTCAGGGCCAAGGATGAA Outcome: AGTGTTTGCCCACGTCAGATCCTGGAAAACGGGAAAGGTTCCGTTCAGGACGCTACTTGTGTATAAGAGTCAGCGTCAGGGCCA GGATGAA	heterozygote	1bpdel	85	N.D
2268C5	Original: AGTGTTTGCCCACGTCAGATCCTGGAAAACGGGAAAGGTTCCGTTCAGGACGCTACTTGTGTATAAGAGTCAGCGTCAGG GCCAAGGATGAA Outcome: AGTGTTTGCCCACGTCAGATCCTGGAAAACGGGAAAGGTTCCGTTCAGGACGCTACTTGTGTATAAGAGTCAGCGTCAGGTCAGGGCCAAGGATGAA	heterozygote	5bpins	81-85	N.D
2268C6	Original: AGTGTTTGCCCACGTCAGATCCTGGAAAACGGGAAAGGTTCCGTTCAGGACGCTACTTGTGTATAAGAGTCAGCGTCAGGGCCAAGGATGAA Outcome: AGTGTTTGCCCACGTCAGATCCTGGAAAACGGGAAAGGTTCCGTTCAGGACGCTACTTGTGTATAAGAGTCAGCGTCAGGGCCAAG ATGAA	heterozygote	1bpdel	87	N.D

Table 4.4b Sequencing Analysis of BIR induced Lys^{+} mutations at *MAT* (*rev3Δ*) (continued)

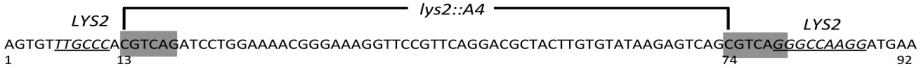

Strain ID:	Sequence:	Mutation Type	No of Indels	Locus of Mutation	Locus of Template Switching
2268C7	Original: AGTGTTTGCCCACGTCAGATCCTGGAAAACGGGAAAGGTTCCGTTCAGGACGCTACTTGTGTATAAGAGTCAGCGTCAGGGCCAAGGATGAA Outcome: AGTGTTTGCCCACGTCAGATCCTGGAAAACGGGAAAGGTTCCGTTCAGGACGCTACTTGTGTATAAGAGTCAGCGTCAGGGCCA GGATGAA	heterozygote	1bpdel	85	N.D
2268C9	Original: AGTGTTTGCCCACGTCAGATCCTGGAAAACGGGAAAGGTTCCGTTCAGGACGCTACTTGTGTATAAGAGTCAGCGTCAGGGCCAAGGATGAA Outcome: AGTGTTTGCCCACGTCAGATCCTGGAAAACGGGAAAGGTTCCGTTCAGGACGCTACTTGTGTATAAGAGTCAGCGTCAGGGCCA GGATGAA	heterozygote	1bpdel	85	N.D
2268C10	Original: AGTGTTTGCCCACGTCAGATCCTGGAAAACGGGAAAGGTTCCGTTCAGGACGCTACTTGTGTATAAGAGTCAGCGTCAGGGCCAAGGATGAA Outcome: AGTGTTTGCCCACGTCAGATCCTGGAAAACGGGAAAGGTTCCGTTCAGGACGCTACTTGTGTATAAGAGTCAGCGTCAGGGCCA GGATGAA	heterozygote	1bpdel	85	N.D
2268C11	Original: AGTGTTTGCCCACGTCAGATCCTGGAAAACGGGAAAGGTTCCGTTCAGGACGCTACTTGTGTATAAGAGTCAGCGTCAGGGCCAAGGATGAA Outcome: AGTGTTTGCCCACGTCAGATCCTGGAAAACGGGAAAGGTTCCGTTCAGGACGCTACTTGTGTATAAGAGTCAGCGTCAGGGCCA GGATGAA	heterozygote	1bpdel	85	N.D
2268C12	Original: AGTGTTTGCCCACGTCAGATCCTGGAAAACGGGAAAGGTTCCGTTCAGGACGCTACTTGTGTATAAGAGTCAGCGTCAGGGCCAAGGATGAA Outcome: AGTGTTTGCCCACGTCAGATCCTGGAAAACGGGAAAGGTTCCGTTCAGGACGCTACTTGTGTATAAGAGTCAGCGTCAGGGCCA GGATGAA	heterozygote	1bpdel	85	N.D
2268D1	Original: AGTGTTTGCCCACGTCAGATCCTGGAAAACGGGAAAGGTTCCGTTCAGGACGCTACTTGTGTATAAGAGTCAGCGTCAGGGCCAAGGATGAA Outcome: AGTGTTTGCCCACGTCAGATCCTGGAAAACGGGAAAGGTTCCGTTCAGGACGCTACTTGTGTATAAGAGTCAGCGTCAGGGCCA GGATGAA	heterozygote	1bpdel	85	N.D
2268D2	Original: AGTGTTTGCCCACGTCAGATCCTGGAAAACGGGAAAGGTTCCGTTCAGGACGCTACTTGTGTATAAGAGTCAGCGTCAGGGCCAAGGATGAA Outcome: AGTGTTTGCCCACGTCAGATCCTGGAAAACGGGAAAGGTTCCGTTCAGGACGCTACTTGTGTATAAGAGTCAGCGTCAGGGCCAAG ATGAA	heterozygote	1bpdel	87	N.D

Table 4.4c Sequencing Analysis of BIR induced Lys^{+} mutations at *MAT* (*pif1Δ*)

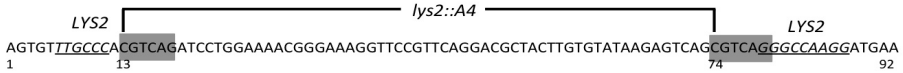

Strain ID	Sequence:	Mutation Type	No of Indels	Locus of Mutation	Locus of Template Switching
2193C2	Original: AGTGTTTGCCCACGTCAGATCCTG*GAAAACGGG*AAAGGTTCCGTTCAGGACGCTACTTGT GTATAAGAGTCAGCGTCAGGGCCAAGGATGAA Outcome: AGTGTTTGCCCACGTCAGATCCTGGAAAACGGGAAAGGTTCCGTTCAGGACGCTACTTGTCCCGTTTTC AGTCAGCGTCAGGGCCAAGGATGAA	heterozygote	4bpdel+9bpins =+5bpins	61-70	25-33
2193C7	Original: AGTGTTTGCCCACGTCAGATCCTGGAAAACGGGAAAGGTTCCGTTCAGGACGCTACTTGTGTATAAGAGTCAGCGTCAGGGCCAAGGATGAA Outcome: AGTGTTTGCCCACGTCAGATCCTGGAAAACGGGAAAGGTTCCGTTCAGGACGCTACTTGTGTATAAGAGTCAGCGTCAG GCCAAGGATGAA	heterozygote	1bpGdel	81	N.D
2193C8	Original: AGTGTTTGCCCACGTCAGATCCTGGA*AAACGGG*AAAGGTTCCGTTCAGGACGC TACTTGTGTATAAGAG TCAGCGTCAGGGCCAAGGATGAA Outcome: AGTGTTTGCCCACGTCAGATCCTGGAAAACGGGAAAGGTTCCGTTCAGGACGCTAT**CCCGTTT**TTTAGGGGTCAGCGTCAGGGCCAAGGATGAA	homozygote	16bpdel+8bpins =+2ins	56-71	27-33
2193C9	Original: AGTGTTTGCCCACGTCAGATCCTGGAAAACGGGAAAGGTTCCGTTCAGGACGCTACTTGTGTATAAGAGTCAGCGTCAGGGCCAAGGATGAA Outcome:AGTGTTTGCCCACGTCAGATCCTGGAAAACGGGAAAGGTTCCGTTCAGGACGCTACTTGTGTATAAGAGT AGCGTCAGGGCCAAGGATGAA	heterozygote	1bpCdel	71	N.D
2193C10	Original: AGTGTTTGCCCACGTCAGATCCTGGAAAACGGGAAAGGTTCCGTTCAGGACGCTACTTGTGTATAAGAGTCAGCGTCAGG GCCAAGGATG AA Outcome: AGTGTTTGCCCACGTCAGATCCTGGAAAACGGGAAAGGTTCCGTTCAGGACGCTACTTGTGTATAAGAGTCAGCGTCAGGAAGCGTATAAAAAA	homozygote	10bpdel+12bpins =+2ins	81-91	N.D.
2193C11	Original: *GTTTCAAAGTGTTTGCCCACG*TCAGATCCTGGAAAACGGGAAAGGTTCCGT TCAGGACGCTACTTGTGTA TAAGAGTCAGCGTCAGGGCCAAGGATGAAGAA Outcome: GTTTCAAAGTGTTTGCCCACGTCAGATCCTGGAAAACGGGAAAGGTTCCGTCGTGGGCAAACACTTTGAAACTAAGAGTCAGCGTCAGGGCCAAGGATGAAGAA	homozygote	19bpdel+21bpins =+2ins	45-65	(-6)-14
2193Z1	Original: *TTTGTTAGGACGTT*CTCCAAAGAACTACAGTTTCAAAGTGTTTGCCCACGTCAGATCCTGGAAAACGGGAAA GGTTCCGTTCAGGACGCTACTTG TGTATAAGA Outcome: TTTGTTAGGACGTTCTCCAAAGAACTACAGTTTCAAAGTGTTTGCCCACGTCAGATCCTGGAAAACGGGAAAAAAAATTGGAG**AACGTCCTAACAAA**TGTATAAGA	heterozygote	23bpdel+25bpins =+2ins	35-59	(-38)-25
2193Z11	Original: AGTGTTTGCCCACGTCAGATCCTGGAAAACGGGAAAGGTTCCGTTCAGGACGCTACTTGTGTATAAGAGTCAGCGTCAGGGCCAAGGATGAA Outcome: AGTGTTTGCCCACGTCAGATCCTGGAAAACGGGAAAGGTTCCGTTCAGGACGCTACTTGTGTATAAGAGTCAGCGTC CTGCCAAGGATGAA	homozygote	3bpdel+2bpins =-1del	78-81	N.D
2193F4	Original: AGTGTTTG*CCCACGTCAGATCCT*GGAAAACGGGAAAGGTTCC GTTCAGGACGCTA CTTGTGTATAAGAGTCAGCGTCAGGGCCAAGGATGAA Outcome: AGTGTTTGCCCACGTCAGATCCTGGAAAACGGGAAACGTTCCAGGATCTGACGTGGGCAAGTGTATAAGAGTCAGCGTCAGGGCCAAGGATGAA	homozygote	13bpdel+15bpins =+2ins	43-58	9--23
2193F7	Original: AGTGTTTG*CCCACGTCAGATCCT*GGAAAACGGGAAAGGTTCC GTTCAGGACGCTA CTTGTGTATAAGAGTCAGCGTCAGGGCCAAGGATGAA Outcome: AGTGTTTGCCCACGTCAGATCCTGGAAAACGGGAAAGGTTCCAGGATCTGACGTGGGCAAGTGTATAAGAGTCAGCGTCAGGGCCAAGGATGAA	heterozygote	13bpdel+15bpins =+2ins	43-58	9--23

Table 4.4c Sequencing Analysis of BIR induced Lys^{+} mutations at *MAT* (*pif1Δ*) (continued)

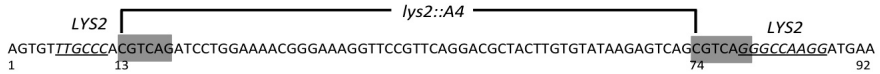

Strain ID	Sequence:	Mutation Type	No of Indels	Locus of Mutation	Locus of Template Switching
2193F9	Original: AGTGTTTGCCCACGTCAGATCCTGGAAAACGGGAAAGGTTCCGTTCAGGACGCTACTTGTGTATAAGAGTCAGCGTCAGGGCCAAGGATGAA Outcome: AGTGTTTGCCCACGTCAGATCCTGGAAAACGGGAAAGGTTCCGTTCAGGACGCTACTTGTGTATAAGAGTCAGCGTCAGG CCAAGGATGAA	heterozygote	1bpGdel	81	N.D
2193F11	Original: AGTGTTTGCCCACGTCAGATCCTGGAAAACGGGAAAGGTTCCGTTCAGGACGCTACTTGTGTATAAGAGTCAGCGTCAGGGCCAAGGATGAA Outcome: AGTGTTTGCCCACGTCAGATCCTGGAAAACGGGAAAGGTTCCGTTCAGGACGCTAC CCCGTTTAAGAGTCAGCGTCAGGGCCAAGGATGAA	homozygote	4bpdel+3bpinsl =-1bpde	57-60	31-33
2193F12	Original: AGTGTTTGCCCACGTCAGATCCTGGAAAACGGGAAAGGTTCCGTTCAGGACGCT ACTTGTGTATAAGA GTCAGCGTCAGGGCCAAGGATGAA Outcome: AGTGTTTGCCCACGTCAGATCCTGGAAAACGGGAAAGGTTCCGTTCAGGACGCTTTCCCGTTTTAAAAGGGTCAGCGTCAGGGCCAAGGATGAA	heterozygote	8bpdel+10bpins =+2ins	55-64	26-35
2193G1	Original: AGTGTTTGCCCACGTCAGATCCTGGAAAACGGGAAAGGTTCCGTTCAGGACGCTACTTGTGTATAAGAGTCAGCGTCAGGGCCAAGGATGAA Outcome: AGTGTTTGCCCACGTCAGATCCTGGAAAACGGGAAAGGTTCCGTTCAGGACGCTACTTGTGTATAAGAGTCAGCGTC CTGAACGGGATGAA	heterozygote	8bpdel+7bpins =-1del	78-85	42-48
2193G3	Original: AGTGTTTGCCCACGTCAGATCCTGGAAAACGGGAAAGGTTCCGTTCAGGACGCTACTTGTGTATAAGAGTCAGCGTCAGGGCCAAGGATGAA Outcome: AGTGTTTGCCCACGTCAGATCCTGGAAAACGGGAAAGGTTCCGTTCAGGACGCTACTTGTGTATAAGAGT GAA	homozygote	19bpdel	71-89	N.D
2193B2	Original: AGTGTTTGCCCACGTCAGATCCTGGAAAACGGGAAAGGTTCCGTTCAGGACGCTACTTGTGTATAAGAGTCAGCGTCAGGGCCAAGGATGAA Outcome: AGTGTTTGCCCACGTCAGATCCTGGAAAACGGGAAAGGTTCCGTTCAGGACGCTACTTGTGTATAAGAGT AGCGTCAGGGCCAAGGATGAA	heterozygote	1bpCdel	71	N.D
2193B11	Original: AGTGTTTGCCCACGTCAGATCCTGGAAAACGGGAAAGGTTCCGTTCAGGACGCTACTTGTGTATAAGAGTCAGCGTCAGGGCCAAGGATGAA Outcome: AGTGTTTGCCCACGTCAGATCCTGGAAAACGGGAAAGGTTCCGTTCAGGACGCTACTTGTGTATAAGAGT AGCGTCAGGGCCAAGGATGAA	heterozygote	1bpCdel	71	N.D.
2193B4	Original: AGTGTTTGCCCACGTCAGATCCTGGAAAACGGGAAAGGTTCCGTTCAGGACGCTAC TTGTGTATAA GAGTCAGCGTCAGGGCCAAGGATGAA Outcome: AGTGTTTGCCCACGTCAGATCCTGGAAAACGGGAAAGGTTCCGTTCAGGACGCTACCCCGTTTTCCAG GAGTCAGCGTCAGGGCCAAGGATGAA	heterozygote	11bpdel+13bpins =+2ins	57-69	21-33
2193B5	Original: AGTGTTTGCCCACGTCAGATCCTGGAAAACGGGAAAGGTTCCGTTCAGGACGCTACTTGTGTATAAGAGTCAGCGTCAGGGCCAAGGATGAA Outcome: AGTGTTTGCCCACGTCAGATCCTGGAAAACGGGAAAGGTTCCGTTCAGGACGCTACTTGTGTATAAGAGTCAG CTTGC GGCCAAGGATGAA	homozygote	6bpdel+5bpins =-1del	75-81	N.A.
2193B6	Original: AGTGTTTGCCCACGTCAGATCCTGGAAAACGGGAAAGGTTCCGTTCAGGACGCT ACTTGTG TATAAGAGTCAGCGTCAGGGCCAAGGATGAA Outcome: AGTGTTTGCCCACGTCAGATCCTGGAAAACGGGAAAGGTTCCGTTCAGGACGCTTTCCCGTTTTAAAAGAGTCAGCGTCAGGGCCAAGGATGAA	homozygote	7bpdel+9bpins =+2ins	55-63	27-35
2193B7	Original: AGTGTTTGCCCACGTCAGATCCTGGAAAACGGGAAAGGTTCCGTTCAGGACGCTACTTGTGTATAAGAGTCAGCGTCAGGGCCAAGGATGAA Outcome: AGTGTTTGCCCACGTCAGATCCTGGAAAACGGGAAAGGTTCCGTTCAGGACGCTACTTGTGTAT CGTCCTGAACG GACCAAGGATGAA	heterozygote	15bpdel+11bpins =-4del	65-80	42-52

Table 4.4c Sequencing Analysis of BIR induced Lys^{+} mutations at *MAT* (*pif1Δ*) (continued)

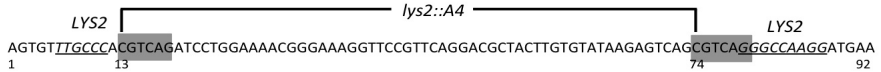

Strain ID	Sequence:	Mutation Type	No of Indels	Locus of Mutation	Locus of Template Switching
2193B8	Original: AGTGTTTGCCCACGTCAGATCCTGGAAAACGGGAAAGGTTCCGTTCAGGACGCTACTTGTGTATAAGAGTCAGCGTCAGGGCCAAGGATGAA Outcome: AGTGTTTGCCCACGTCAGATCCTGGAAAACGGGAAAGGTTCCGTTCAGGACGCTACTTGTGTATAAGAGT AGCGTCAGGGCCAAGGATGAA	heterozygote	1bpCdel	71	N.D
2193B9	Original: TTCAAAGTGTTTGCCCACGTCAGATCCTGGAAAACGGGAAAGGTTCCGTTCAGG ACGCTACTTGTG TATAAGAGTCAGCGTCAGGGCCAAGGATGAA Outcome: TTCAAAGTGTTTGCCCACGTCAGATCCTGGAAAACGGGAAAGGTTCCGTTCAGGGCAAACACTTTGAATATCAGAGTCAGCGTCAGGGCCAAGGATGAA	homozygote	12bpdel+14bpins =+2ins	51-64	(-4) - 10
2193B1	Original: AGTGTTTGCCCACGTCAGATCCTGGAAAACGGGAAAGGTTCCGTTCAGGACGCTACT TGTGTATAA GAGTCAGCGTCAGGGCCAAGGATGAA Outcome: AGTGTTTGCCCACGTCAGATCCTGGAAAACGGGAAAGGTTCCGTTCAGGACGCTACTCCCGTTTTCCAGAGTCAGCGTCGGGCCCAAGGATGAA	homozygote	8bpdel+10bpins =+2ins	58-68	24-33
2193B12	Original: AGTGTTTGCCCACGTCAGATCCTGGAAAACGGGAAAGGTTCCGTTCAGGACGCTACTTGTGTATAAGAGTCAGCGTCAGGGCCAAGGATGAA Outcome: AGTGTTTGCCCACGTCAGATCCTGGAAAACGGGAAAGGTTCCGTTCAGGACGCTACTTGTGTATAAGAGTCAGCGTCAAG CCAAGGATGAA	homozygote	3bpdel+2bpins =-1del	79-81	N.D
2193C1	Original: AGTGTTTGCCCACGTCAGATCCTGGAAAACGGGAAAGGTTCCGTTCAGGACGCTACTTGTGTATAAGAGTCAGCGTCAGGGCCAAGGATGAA Outcome: AGTGTTTGCCCACGTCAGATCCTGGAAAACGGGAAAGGTTCCGTTCAGGACGCTACTTGTGTATAAGAGTCAGCGTCAAG CCAAGGATGAA	homozygote	3bpdel+2bpins =-1del	79-81	N.D
2193C9	Original: AGTGTTTGCCCACGTCAGATCCTGGAAAACGGGAAAGGTTCCGTTCAGGACGCTACTTGTGTATAAGAGTCAGCGTCAGG GCCAAGGATGAA Outcome: AGTGTTTGCCCACGTCAGATCCTGGAAAACGGGAAAGGTTCCGTTCAGGACGCTACTTGTGTATAAGAGTCAGCGTCAGGAAGCGTATAAGAAA	homozygote	10bpdel+12bpins =+2ins	81-90	N.A.
2193C10	Original: AGTGTTTGCCCACGTCAGATCCTGGAAAACGGGAAAGGTTCCGTTCAGGACGCTACTTGTGTATAAGAGTCAGCGTCAGG GCCAAGGATGAA Outcome: AGTGTTTGCCCACGTCAGATCCTGGAAAACGGGAAAGGTTCCGTTCAGGACGCTACTTGTGTATAAGAGTCAGCGTCAGGAAGCGTATAAAAAA	homozygote	10bpdel+12bpins =+2ins	81-90	N.A.
2193C3	Original: AGTGTTTGCCCACGTCAGATCCTGGAAAACGGGAAAGGTTCCGTTCAGGACGCTACTTGTGTATAAGAGTCAGCGTCAGGGCCAAGGATGAA Outcome: AGTGTTTGCCCACGTCAGATCCTGGAAAACGGGAAAGGTTCCGTTCAGGACGCTACTTGTGTATAAGAGTCCTGAACGGAA CAAGGATGAA	homozygote	11bpdel+10bpins =-1del	72-82	39-48
2193C4	Original: AGTGTTTGCCCACGTCAGATCCTGGAAAACGGGAAAGGTTCCGTTCAGGACGCTACTTGTGTATAAGAGTCAGCGTCAGGGCCAAGGATGAA Outcome: AGTGTTTGCCCACGTCAGATCCTGGAAAACGGGAAAGGTTCCGTTCAGGACGCTACTTGTGTATAAGAGTG GCGTCAGGGCCAAGGATGAA	homozygote	2bpdel+1bins =-1del	71-72	N.D.
2193C12	Original: AGTGTTTGCCCACGTCAGATCCTGGAAAACGGGAAAGGTTCCGTTCAGGACGCTACTTGTGTATAAGAGTCAGCGTCAG GGCCAAGGATGAA Outcome: AGTGTTTGCCCACGTCAGATCCTGGAAAACGGGAAAGGTTCCGTTCAGGACGCTACTTGTGTATAAGACGGAACCTTTCCCGGCCAAGGATGAA	homozgote	11bpdel+13bpins =+2ins	69-82	31-43
2193C5	Original: AGTGTTTGCCCACGTCAGATCCTGGAAAACGGGAAAGGTTCCGTTCAGGACGCTACTTGTGTATAAGAGTCAGCGTCAGGGCCAAGGATGAA Outcome: AGTGCTTGCCCTCGTCAGATCCTGGAAAACGGGAAAGGATCCGTTCAGGACGCTACTTGTGTATAAGAGTAACCACCTGACAAAAGAG GAA	homozygote	19bpdel+18bpins =-1del	71-89	N.A
2193Z3	Original: AGTGTTTGCCCACGTCAGATCCTGGAAAACGGGAAAGGTTCCG TTCAGGACGCTACTTGTGTATAAGAGTCAGCGTCAGGGCCAAGGATGAA Outcome: AGTGTTTGCCCACGTCAGATCCTGGAAAACGGGAAAGGTTCCGGGATCTGACGTGGGCTTGTGTATAAGAGTCAGCGTCAGGGCCAAGGATGAA	homozygote	12bpdel+14bpins =+2ins	52-66	17-30

Table 4.4c Sequencing Analysis of BIR induced Lys^{+} mutations at *MAT* (*pif1Δ*) (continued)

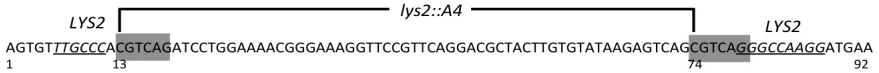

Strain ID	Sequence:	Mutation Type	No of Indels	Locus of Mutation	Locus of Template Switching
2193Z11	Original : AGTGTTTGCCCACGTCAGATCCTGGAAAACGGGAAAGGTTCCGTTCAGGACGCTACTTGTGTATAAGAGTCAGCGTCAGGGCCAAGGATGAA Outcome: AGTGTTTGCCCACGTCAGATCCTGGAAAACGGGAAAGGTTCCGTTCAGGACGCTACTTGTGTATAAGAGTCAGCGTC CTGCCAAGGATGAA	homozygote	5bpdel+4bpins =-1del	78-80	N.D.
2193Z4	Original: AGTGTTTGCCCACGTCAGATCCTGGAAAACGGGAAAGGTTCCGTTCAGGACGCTACTTGTGTATAAGAGTCAGCGTCAGGGCCAAGGATGAA Outcome: AGTGTTTGCCCACGTCAGATCCTGGAAAACGGGAAAGGTTCCGTTCAGGACGCTACTTGTGTATAAGAGTCAGCGTCAGG CCAAGGATGAA	homozygote	1bpdel	81	N.D.
2193Z12	Original: AGTGTTTGCCCACGTCAGATCCTGGAAAACGGGAAAGGTTCCGTTCAGGACGCTACTTGTGTATAAGAGTCAGCGTCAGGGCCAAGGATGAA Outcome: AGTGTTTGCCCACGTCAGATCCTGGAAAACGGGAAAGGTTCCGTTCAGGACGCTACTTGTGTATAAGAGTCAGCGTCAGG CCAAGGATGAA	heterozygote	1bpdel	81	N.D.
2193Z5	Original: AGTGTTTGCCCACGTCAGATCCTGGAAAACGGGAAAGGTTC*CGTTCAGG*ACGCTACTTGTGTATAAGAGTCAGCGTCAGGGCCAAGGATGAA Outcome: AGTGTTTGCCCACGTCAGATCCTGGAAAACGGGAAAGGTTCCGTTCAGGACGCTACTTGTGTATAAGAGTCAGCGT CCTGAACGGGATGAA	heterozygote	8bpdel+7bpins =-1del	78-85	42-48
2193F1	Original: AGTGTTTGCCCACGTCAGATCCTGGAAAACGGGAAAGGTTCC*GTTCA*GGACGCTACTTGTGTATAAGAGTCAGCGTCAGGGCCAAGGATGAA Outcome: AGTGTTTGCCCACGTCAGATCCTGGAAAACGGGAAAGGTTCCGTTCAGGACGCTACTTGTGTATAAGAGTCA TGAACGGGCCAAGGATGAA	homozygote	6bpdel+5bpins =-1del	73-78	43-47
2193Z6	Original: AGTGTTTGCCCACGTCAGATCCTGGAAAAC*GGG*AAAGGTTCCGTTCAGGACGCTACT TGTGTATAAGAGTCAGCGTCAGGGCCAAGGATGAA Outcome: AGTGTTTGCCCACGTCAGATCCTGGAAAACGGGAAAGGTTCCGTTCAGGACGCTACT**CCC**CCGTATAAGAGTCAGCGTCAGGGCCAAGGATGAA	heterozygote	3bpdel+5bpins =+2ins	58-62	31-33
2193F2	Original: AGTGTTTGCCCACGTCAGATCCTGGAAAACGGGAAAGGTTCCGTTCAGGACGCTACTTGTGTATAAGAGTCAGCGTCAGGGCCAAGGATGAA Outcome: AGTGTTTGCCCACGTCAGATCCTGGAAAACGGGAAAGGTTCCGTTCAGGACGCTACTTGTGTATAAGAGTCAGCGTCAGG CCAAGGATGAA	heterozygote	1bpdel	81	N.D.
2193Z7	Original: AGTGTTTGCCCACGTCAGATCCTGGAAAACGGGAAAGGTTCCGTTCAGGACGCTACTTGTGTATAAGAGTCAGCGTCAGGGCCAAGGATGAA Outcome: AGTGTTTGCCCACGTCAGATCCTGGAAAACGGGAAAGGTTCCGTTCAGGACGCTACTTGTGTATAAGAGTC CTGTCAGGGCCAAGGATGAA	homozygote	3bpdel+2bpins =-1del	72-74	N.A.
2193Z8	Original: AGTGTTTGCCCACGTCAGATCCTGGAAAACGGGAAAGGTTCCGTTCAGGACGCTACTTGTGTATAAGAGTCAGCGTCAGGGCCAAGGATGAA Outcome: AGTGTTTGCCCACGTCAGATCCTGGAAAACGGGAAAGGTTCCGTTCAGGACGCTACTTGTGTATAAGAGTCAGCGTCAGG CCAAGGATGAA	homozygote	1bpdel	81	N.D.
2193Z9	Original: AGTGTTTGCCCACGTCAGATCCTGGAAAACGGGAAAGGTTCCGTTCAGGACGCTACTTGTGTATAAGAGTCAGCGTCAGGGCCAAGGATGAA Outcome: AGTGTTTGCCCACGTCAGATCCTGGAAAACGGGAAAGGTTCCGTTCAGGACGCTACTTGTGTATAAGAGTCAGCGTCGGGGC AAGGATGAA	homozygote	1bpdel	83	N.D.
2193Z10	Original: AGTGTTTGCCCACGTCAGATCCTGGAAAACGGGAAAGGTTCC*GTTCA*GGACGCTACTTGTGTATAAGAGTCAGCGTCAGGGCCAAGGATGAA Outcome: AGTGTTTGCCCACGTCAGATCCTGGAAAACGGGAAAGGTTCCGTTCAGGACGCTACTTGTGTATAAGAGTCA TGAACGGGCCAAGGATGAA	heterozygote	6bpdel+5bpins =-1del	73-78	43-47

Table 4.4d Sequencing Analysis of BIR induced Lys^{+} mutations at *MAT* (*rev3Δpif1Δ*)

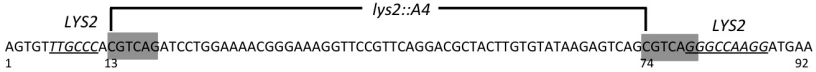

Strain ID:	Sequence:	Mutation Type	No of Indels	Locus of Mutation	Locus of Template Switching
2409B5	Original: AGTGTTTGCCCACGTCAGATCCTGGAAAACGGGAAAGGTTCCGTTCAGGACGCTACTTGTGTATAAGAGTCAGCGTCAGGGCCAAGGATGAA Outcome: AGTGTTTGCCCACGTCAGATCCTGGAAAACGGGAAAGGTTCCGTTCAGGACGCTACTTGTGT GTGGGTGTGGTGTGTGGGCCAAGGATGAA	homozygote	16bpdel+15bpins =-1bpdel	63-78	telomeres
2409B6	Original: AGTGTTTGCCCACGTCAGATCCTGGAAAACGGGAAAGGTTCCGTTCAGGACGCTACTTGTGTATAAGAGTCAGCGTCAGGGCCAAGGATGAA Outcome: AGTGTTTGCCCACGTCAGATCCTGGAAAACGGGAAAGGTTCCGTTCAGG GTGTGTGGGTGTATAAGAGTCAGCGTCTGGGCCAAGGATGAA	heterozygote	9bpdel+8bpins =-1bpdel	50-58	telomeres
2409B7	Original: AGTGTTTGCCCACGTCAGATCCTGGAAAACGGGAAAGGTTCCGTTCAGGACGCTACTTGTGTATAAGAGTCAGCGTCAGGGCCAAGGATGAA Outcome: AGTGTTTGCCCACGTCAGATCCTGGAAAACGGGAAAGGTTCCGTTCAGGACGCTACTTGTGT GTGGGTGTGGTGTGTGGGCCAAGGATGAA	homozygote	16bpdel+15bpins =-1del	63-78	telomeres
2409B8	Original: AGTGTTTGCCCACGTCAGATCCTGGAAAACGGGAAAGGTTCCGTTCAGGACGCTACTTGTGTATAAGAGTCAGCGTCAGGGCCAAGGATGAA Outcome: AGTGTTTGCCCACGTCAGATCCTGGAAAACGGGAAAGGTTCCGTTCAGGACGCTACTTGTGT GTGGGTGTGGTGTGTGGGCCAAGGATGAA	homozygote	16bpdel+15bpins =-1del	63-78	telomeres
2409B12	Original: AGTGTTTGCCCACGTCAGATCCTGGAAAACGGGAAAGGTTCCGTTCAGGACGCTACTTGTGTATAAGAGTCAGCGTCAGGGCCAAGGATGAA Outcome: AGTGTTTGCCCACGTCAGATCCTGGAAAACGGGAAAGGTTCCGTTCAGGACGCTACTTGTGTATAAGAGTCAGCGTCAGGGCCAA ACTGAA	homozygote	3bpdel+2bpins =-1del	86-88	N.D.
2409C1	Original: AGTGTTTGCCCACGTCAGATCCTGGAAAACGGGAAAGGTTCCGTTCAGGACGCTACTTGTGTATAAGAGTCAGCGTCAGGGC CAAGGATGAA Outcome: AGTGTTTGCCCACGTCAGATCCTGGAAAACGGGAAAGGTTCCGTTCAGGACGCTACTTGTGTATAAGAGTCAGCGTCAGGGCGTCAGGGCCAAGGATGAA	homozygote	8bpins=+8ins	83-90	N.A
2409C5	Original: AGTGTTTGCCCACGTCAGATCCTGGAAAACGGGAAAGGTTCCGTTCAGGACGCTACTTGTGTATAAGAGTCAGCGTCAGGGCCAAGGATGAA Outcome: AGTGTTTGCCCACGTCAGATCCTGGAAAACGGGAAAGGTTCCGTTCAGGACGCTACTTGTGTATAAGAGTCAGCGTCAGG CCAAGGATGAA	heterozygote	1bpdel	81	N.D.
2409C6	Original: AGTGTTTGCCCACGTCAGATCCTGGAAAACGGGAAAGGTTCCGTTCAGGACGCTACTTGTGTATAAGAGTCAGCGTCAGGGCCAAGGATGAA Outcome: AGTGTTTGCCCACGTCAGATCCTGGAAAACGGGAAAGGTTCCGTTCAGGACGCTACTTGTGT GTGGGTGTGGTGTGT GGGCCAAGGATGAA	homozygote	16bpdel+15bpins =-1del	63-78	telomeres
2409C7	Original: AGTGTTTGCCCACGTCAGATCCTGGAAAACGGGAAAGGTTCCGTTCAGGACGCTACTTGTGTATAAGAGTCAGCGTCAGGGCCAAGGATGAA Outcome: AGTGTTTGCCCACGTCAGATCCTGGAAAACGGGAAAGGTTCCGTTCAGGACGCTACTTGTGT GTGGGTGTGGTGTGT GGGCCAAGGATGAA	homozygote	16bpdel+15bpins =-1del	63-78	telomeres
2409C9	Original: AGTGTTTGCCCACGTCAGATCCTGGAAAACGGGAAAGGTTCCGTTCAGGACGCTACTTGTGTATAAGAGTCAGCGTCAGGGCCAAGGATGAA Outcome: AGTGTTTGCCCACGTCAGATCCTGGAAAACGGGAAAGGTTCCGTTCAGGACGCTACTTGTGTATAAGAGTCAGCGTCAGGGCCA GGATGAA	homozygote	1bpdel	85	N.D.
2409C10	Original: AGTGTTTGCCCACGTCAGATCCTGGAAAACGGGAAAGGTTCCGTTCAGGACGCTACTTGTGTATAAGAGTCAGCGTCAGGGCCAAGGATGAA Outcome: AGTGTTTGCCCACGTCAGATCCTGGAAAACGGGAAAGGTTCCGTTCAGGACGCTACTTGTGT GTGGGTGTGGTGTGT GGGCCAAGGATGAA	heterozygote	16bpdel+15bpins =-1del	63-78	telomeres

Table 4.4d Sequencing Analysis of BIR induced Lys^{+} mutations at *MAT* (*rev3Δpif1Δ*) (continued)

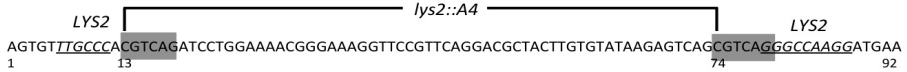

Strain ID:	Sequence:	Mutation Type	No of Indels	Locus of Mutation	Locus of Template Switching
2409C12	Original: AGTGTTTGCCCACGTCAGATCCTGGAAAACGGGAAAGGTTCCGTTCAGGACGCTACTTGTGTATAAGAGTCAGCGTCAGGGCCAAGGATGAA Outcome: AGTGTTTGCCCACGTCAGATCCTGGAAAACGGGAAAGGTTCCGTTCAGGACGCTACTTGTGT GTGGGTGTGGTGTGT GGGCCAAGGATGAA	heterozygote	16bpdel+15bpins =-1del	63-78	telomeres
2409D2	Original: AGTGTTTGCCCACGTCAGATCCTGGAAAACGGGAAAGGTTCCGTTCAGGACGCTACTTGTGTATAAGAGTCAGCGTCAGGGCCAAGGATGAA Outcome: AGTGTTTGCCCACGTCAGATCCTGGAAAACGGGAAAGGTTCCGTTCAGGACGCTACTTGTGTATAAGAGTCAGCGTCAGGGCCA GGATGAA	homozygote	1bpdel	85	N.D.
2409D4	Original: AGTGTTTGCCCACGTCAGATCCTGGAAAACGGGAAAGGTTCCGTTCAGGACGCTACTTGTGTATAAGAGTCAGCGTCAGGG CCAAGGATGAA Outcome: AGTGTTTGCCCACGTCAGATCCTGGAAAACGGGAAAGGTTCCGTTCAGGACGCTACTTGTGTATAAGAGTCAGCGTCAGGGTAGGGCCAAGGATGAA	homozygote	5bpins	82-86	N.A
2409A9	Original: AGTGTTTGCCCACGTCAGATCCTGGAAAACGGGAAAGGTTCCGTTCAGGACGCTACTTGTGTATAAGAGTCAGCGTCAGGGCCAAGGATGAA Outcome: AGTGTTTGCCCACGTCAGATCCTGGAAAACGGGAAAGGTTCCGTTCAGGACGCTACTTGTGTATAAGAGTCAGCGTCAGGGCCAAG ATGAA	homozygote	1bpdel	87	N.D.
2409A3	Original: AGTGTTTGCCCACGTCAGATCCTGGAAAACGGGAAAGGTTCCGTTCAGGACGCTACTTGTGTATAAGAGTCAGCGTCAGGGCCAAGGATGAA Outcome: AGTGTTTGCCCACGTCAGATCCTGGAAAACGGGAAAGGTTCCGTTCAGGACGCTACTTGTGTATAAGAGTCAGCGTCAGGGCCA GGATGAA	homozygote	1bpdel	85	N.D.
2409B3	Original: AGTGTTTGCCCACGTCAGATCCTGGAAAACGGGAAAGGTTCCGTTCAGGACGCTACTTGTGTATAAGAGTCAGCGTCAGGG CCAAGGATGAA Outcome: AGTGTTTGCCCACGTCAGATCCTGGAAAACGGGAAAGGTTCCGTTCAGGACGCTACTTGTGTATAAGAGTCAGCGTCAGGGGCCAAGGATGAA	homozygote	2bpins	82-83	N.D.
2409A4	Original: AGTGTTTGCCCACGTCAGATCCTGGAAAACGGGAAAGGTTCCGTTCAGGACGCTACTTGTGTATAAGAGTCAGCGTCAGGGC CAAGGATGAA Outcome: AGTGTTTGCCCACGTCAGATCCTGGAAAACGGGAAAGGTTCCGTTCAGGACGCTACTTGTGTATAAGAGTCAGCGTCAGGGCAGGGCCAAGGATGAA	homozygote	5bpins	83-87	N.A
2409B4	Original: AGTGTTTGCCCACGTCAGATCCTGGAAAACGGGAAAGGTTCCGTTCAGGACGCTACTTGTGTATAAGAGTCAGCGTCAGGGC CAAGGATGAA Outcome: AGTGTTTGCCCACGTCAGATCCTGGAAAACGGGAAAGGTTCCGTTCAGGACGCTACTTGTGTATAAGAGTCAGCGTCAGGGCAGGGCCAAGGATGAA	heterozygote	5bpins	83-87	N.A
2409A8	Original: AGTGTTTGCCCACGTCAGATCCTGGAAAACGGGAAAGGTTCCGTTCAGGACGCTACTTGTGTATAAGAGTCAGCGTCAGGGCCAAGGATGAA Outcome: AGTGTTTGCCCACGTCAGATCCTGGAAAACGGGAAAGGTTCCGTTCAGGACGCTACTTGTGTATAAGAGTCAGCGTCAGGGCCA GGATGAA	homozygote	1bpdel	85	N.D.

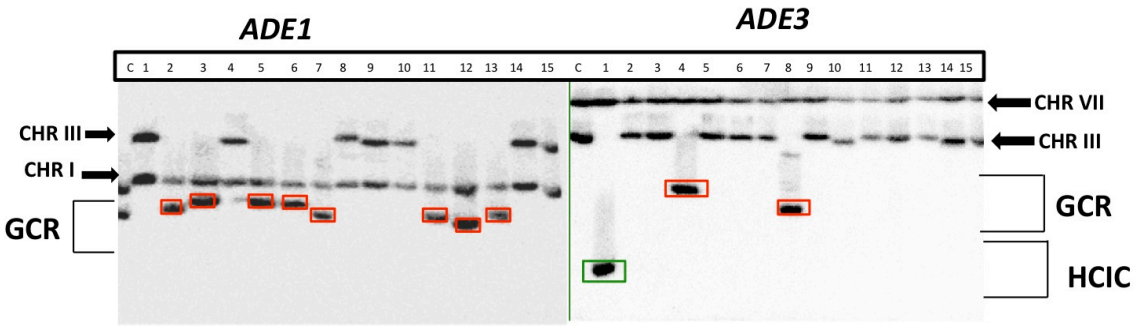

Figure 4.6 Structural Analysis of BIR-induced Lys$^+$ outcomes in *pif1Δ.*
Southern blot Analysis of PFGE Gel containing BIR induced Lys$^+$ outcomes in *pif1Δ* strains with (A) *Ade1* specific probe in and (B) *Ade3* specific probe**.** *Ade1* specific probe hybridizes to truncated CHRIII and CHRI while *Ade3* specific probe hybridizes to full-length donor CHRIII and CHRVII. Lane C in both (A) and (B) show DNA from AM2193 (*lys2::ins* strain at MAT with *pif1Δ*) where HO site was not cleaved. Lanes 1-15 represent BIR induced Lys$^+$ outcomes from AM2193 following DSB at HO. Lys$^+$ outcomes associated with gross chromosomal rearrangements are shown in red box, while HCIC events are shown in green box. Abbreviations: CHR: Chromosome; GCR: Gross Chromosomal Rearrangements; HCIC: Half Crossover Induced secondary Cascades.

4.4 Discussion

4.4.1 Pif1 and Rev3 characterize two Pathways of Mutagenesis

The results of this research demonstrate the existence of two pathways of mutagenesis associated with BIR: Pif1-dependent and Rev3-dependent (Figure 4.7 A-C). The absence of the 5' to 3' helicase Pif1 i.e. *pif1Δ* eliminated more than 75%, 95% and 99% of frameshift mutations in BIR at MAT, 16kb and 36kb positions respectively. In the absence of Pif1 BIR efficiency decreased from 85% in $Pif1^+$ strains to 22% in $Pif1^-$ strains. Evidently the effect of *pif1Δ* on the efficiency of BIR is less dramatic compared to its effect on BIR frameshift mutagenesis at least some positions (16kb and 36kb). Therefore, we propose that reduction in frameshift mutations at 16kb and 36kb is not only because of reduction in BIR itself but also due to BIR being less mutagenic in the absence of *PIF1*. Based on these observations, we now propose that in the absence of *PIF1* a highly efficient but mutagenic BIR pathway (Figure 4.7 E-F) can be switched to a less efficient but accurate BIR pathway (Figure 4.7 D). This suggests that Pif1 is important for making BIR both efficient and mutagenic.

The smaller effect of *pif1Δ* on BIR frameshifts at MAT suggested that an alternative pathway of mutagenesis exists in BIR. The effect of this alternative pathway, supposedly driven by Rev3, was observed when deletion of both *PIF1* and *REV3* eliminated more than 99% of mutations at MAT, confirming the existence of Pif1-independent, Rev3-dependent pathway of BIR mutagenesis. Thus it can be concluded that Pol ζ (Rev3) and Pif1 define two pathways of mutagenesis in BIR. While Pol ζ makes mutations during the initiation of BIR close to the DSB site, Pif1 makes mutations not only close to the DSB site but also further along the path of BIR DNA synthesis.

Lys^+ mutations observed in the *rev3Δ* background were all -1bp deletions and dependent on Pif1. It is known that -1bp deletions are frequently produced by mistakes

of DNA polymerase δ (Jin et al., 2005). The -1bp deletions also frequently result from a mismatch repair defect (Tran et al., 2007). The published data obtained previously in our lab (Deem et al., 2011), suggested that many BIR errors are made by Pol δ and are inefficiently corrected by mismatch repair. Here we speculate that Pif1 may be responsible for lowering the fidelity of mismatch repair as a result of which Pol δ errors are left uncorrected and lead to high mutagenesis in BIR.

Further we observed that complex Lys^+ mutations, consisting of large deletions and insertions in the *pif1Δ* background were promoted by Pol ζ (Rev3). We propose that, pausing of BIR driven by Pol δ leads to dissociation of nascent strand from its template and to a switch from Pol δ to Pol ζ. Next, Pol ζ promotes template switching mediated by micro- homologies, which leads to large insertions and insertions (Figure 4.7 E). The Lys^+ events observed in the *pif1Δ* background revealed regions of micro-homology (1-6bp) at the junctions of template switching. It is possible that in the absence of the helicase activity of Pif1, the preferred replicative polymerase Pol δ is unable to continue further synthesis of the invading nascent strand leading to a stall (Figure 4.7 G). Under these conditions, the non-essential polymerase, Pol ζ (Rev3) assumes this responsibility. Pol ζ, known to be a low processivety polymerase, then promotes frequent dissociation of the nascent strand from the donor template after extending synthesis from incompletely paired bases (revealed by junctions of micro-homology) to produce Lys^+ mutations. Interestingly, a majority of these Lys^+ template-switching events observed in the *Pif1Δ* background were associated with gross chromosomal rearrangements.

4.4.2 Genomic Instability in absence of Pif1

The data shown in Section 4.3.1.1 (based on events not selected as Lys^+ mutations) demonstrates that elimination of *PIF1* decreased the efficiency of BIR and led to a significant increase in the frequency of gross chromosomal rearrangements. The percentage of these GCRs, which consisted of half-crossovers and chromosomal

translocation events, was increased from 3-5% in WT to nearly 50% in Pif1$^-$ background. It is known that half-crossovers are fusion events between the left half of the broken chromosome and right half of the donor chromosomes (Figure 4.7 L) (with the remaining two halves being lost; also described in Figure 4.3), while chromosomal translocation events are caused by strand invasion of the broken chromosome into a non-homologous chromosome (Figure 4.7 K). Such translocation events were also observed following BIR initiation in *rad51Δ* strains where more than 80% of repair outcomes were found to be invasions into non-homologous chromosomes due to lack of homology pairing in the absence of Rad51 (Van Hulle et al., 2008). Presumably an impairment in DNA synthesis or aberrant processing of BIR intermediates leads to such kinds of events (Figure 4.7 G). A third class of events called secondary half crossovers or half crossover-induced cascades (HCICs) were also observed in the absence of Pif1, where the remaining half of the donor chromosome can stabilize itself by a translocation and can initiate cascades of genomic instability (Figure 4.7 M). These half crossovers are analogous to non-reciprocal translocations, implicated in the initiation of cascades of genomic instability in mammalian tumor cells.

Taken together, our results strongly suggest that Pif1 promotes a highly efficient and mutagenic BIR, and the elimination of *PIF1* leads to inefficient, but accurate BIR, and also promotes formation of chromosomal rearrangements resulting from accumulation of unprocessed BIR intermediates in the *pif1Δ* background (Figure 4.7 K, L, M).

4.4.3 BIR: a stepping-stone towards MMBIR?

Recently, a BIR related GCR mechanism known as micro-homology mediated BIR (MMBIR) has appeared as a major cause of copy number variations (CNVs), implicated in various human diseases and cancer (Hastings et al., 2009; Payen et al., 2008). MMBIR has been described in phenomena such as chromothripsis, which describes genomic instability as a one step event involving shattering of one chromosome followed by

multiple complex chromosomal rearrangements and mutations (Liu et al., 2011). This pathway initiated as a DSB or collapsed replication fork, proceeds similar to BIR, and is associated with frequent template switching between DNA sequences that share only micro-homologies. Even though BIR uses extensive homology for its initiation while MMBIR relies only on micro-homologies, both these processes depend on Pol32 (Payen et al., 2008). The exact mechanism by which this MMBIR is initiated although remains unclear. The mechanisms described in this chapter explaining template switching leading to chromosomal translocations; rearrangements and associated mutations may probably explain if BIR, a DNA repair process can be channeled into MMBIR, a potential genome destabilizing phenomenon (Figure 4.7 H-I, J).

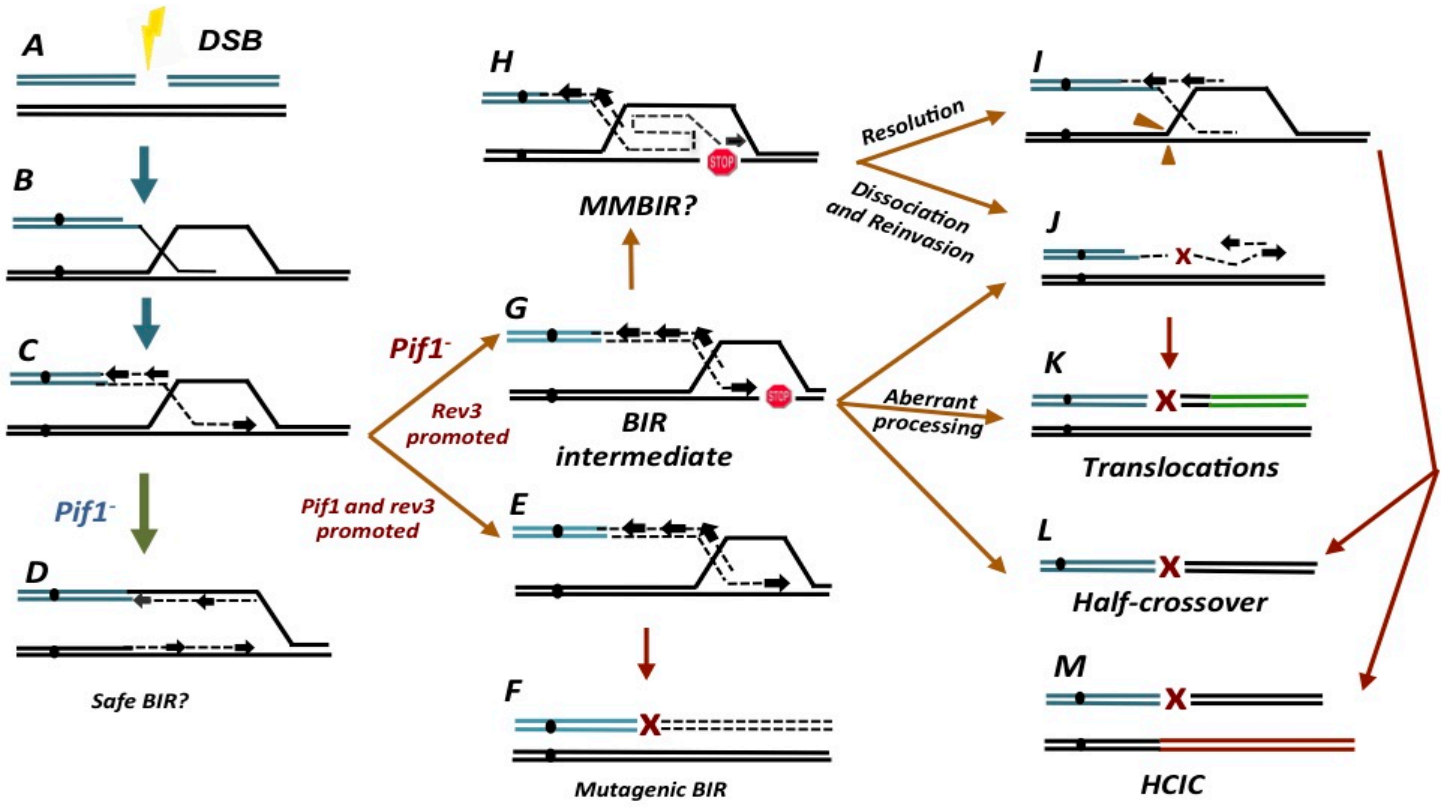

Figure 4.7 Model of Genomic Instability induced by Pif1 and Rev3 in BIR.
Graphic representation of possible pathways of genomic instability. Green Arrow indicates progress to a possible safe BIR pathway while orange, red arrows indicate progression towards potential genome destabilizing events. X indicates mutation while the stop sign indicates stalling of replication fork

CHAPTER 5. BASE SUBSTITUTION MUTAGENESIS ASSOCIATED WITH BREAK-INDUCED REPLICATION

5.1 Background

In the previous chapter, the phenomenon of BIR associated frameshift mutations was described. Even though frameshift mutations are the more dangerous kind of point mutations as they practically always eliminate gene function, base substitution mutations are more common, comprising almost 90% of all point mutations. A base substitution mutation results from mis-incorporation of a nucleotide followed by mismatch extension without proofreading. A large majority of these base substitution mutations are silent (no effect on gene function). Nevertheless, a significant fraction of diseased or cancer genomes contain missense or non-sense type of base substitutions that can effectively change or eliminate gene function.

The demonstration of high frequency of frameshift mutations in BIR hinted that base substitutions might be similarly induced. While frameshift mutations are presumably generated from misalignment of DNA strands due to strand slippage, base substitutions result from misincorporation of incorrect nucleotide events. This suggests that differences in the mechanisms promoting the two types of mutations may exist. Yet it has been shown that an increase in the rate of frameshift mutations correlates with an increase in base substitution errors during normal replication (Kunkel and Bebenek, 2000; McCulloch and Kunkel, 2008). In this light, investigating the phenomenon of base

substitutions in BIR became extremely important and forms the overall goal of the research presented in this chapter.

5.2 Characterization of BIR associated base substitutions

5.2.1 Experimental System

To assay base substitution mutagenesis associated with BIR, the disomic experimental system, similar to the one described in Chapter 4 was used, except that these strains carried base substitution reporter *ura 3-29* instead of *lys2::ins* frameshift reporters. Base substitution reporter *ura3-29* (Shcherbakova and Pavlov, 1993) is an allele of the *URA3* gene resulting from a single base substitution (T→C) in *URA3*. Insertion of this reporter results in a Ura^- phenotype. A Ura^+ phenotype can be restored by 3 types of base substitution mutations C→T transition, C→A or C→G transversions. Similar to the experimental system in Chapter 4, a series of isogenic strains were created where the reporter was inserted at 3 different loci, at *MAT*, 16kb and 36kb. In each strain WT *URA3* gene was completely deleted from its native position in Chromosome V.

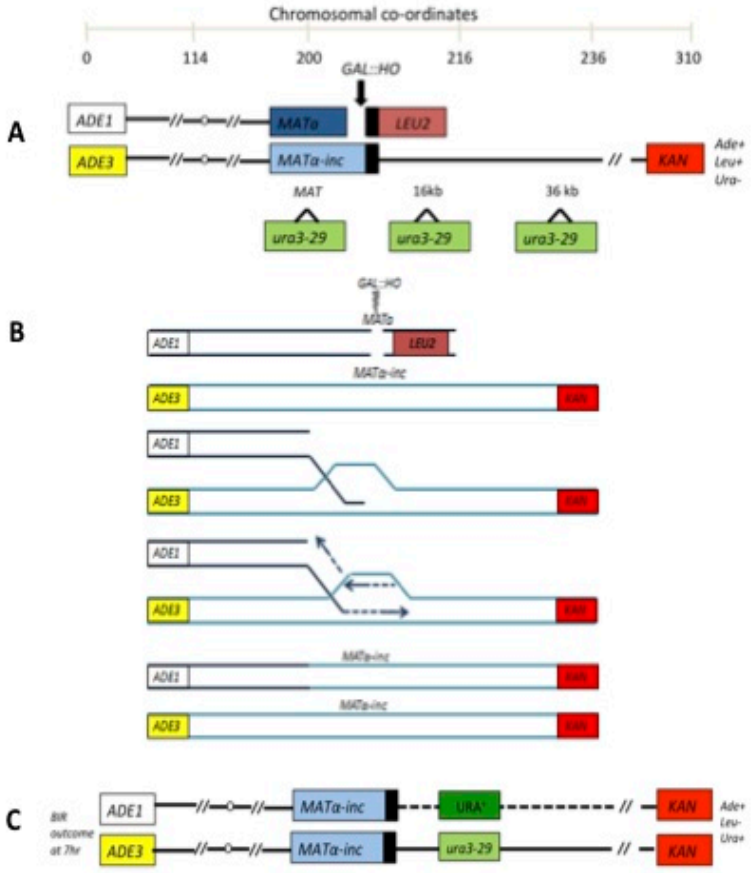

Figure 5.1 Experimental System to study BIR associated Base Substitution Mutations.

Figure 5.1 Experimental System to study BIR associated base substitution mutations. (A) Disomic Experimental system with modified CHRIII used to study BIR. DSBs were created at *MATa* by HO endonuclease induced by galactose*. MATa* copy of CHRIII is truncated and fused to *LEU2 and* telomeric sequences and hence shared only 46 bp homology with the donor copy. The *MATα-inc copy is* full length and resistant to cutting by HO. DSBs introduced at *MATa* were repaired by BIR initiated by strand invasion followed by copying of the donor chromosome till its end. To assay base substitution mutagenesis associated with BIR, base substitution reporter *ura 3-29* was inserted at different distances from *MATα-inc*: at 0kb (at *MATα-inc*), at 16kb and at 36kb. (B) Introduction of DSB promotes 5'-3' resection generating ssDNA in the broken molecule. This broken molecule, assisted by one-ended homology initiates BIR by invading into homologous donor chromosome and copies close to 100kb of DNA sequences from the donor chromosome to fully repair the broken chromosome. (C) BIR associated base substitution mutations are detected by a Ura^+ phenotype when an error in DNA synthesis, that reverts the base substitution reporter, is made in the second copy of the *ura3-29* reporter.

5.2.2 The Rate of BIR-induced base substitutions

To determine if BIR was responsible for promoting base substitution mutations, we determined the rate of DSB induced Ura^+ base substitutions following DSB induction for strains carrying base substitution reporter *ura3-29* at all 3 positions: *MAT*, 16kb and 36kb. By comparing with the rate to the spontaneous Ura^+ mutation rates i.e. Ura^+ rate before DSB induction, we observed that the rate of DSB induced Ura^+ mutations was higher than the rate of spontaneous Ura^+ mutations. The increase in mutagenesis was consistently observed for base substitution reporters located at all 3 positions i.e. rate of DSB induced Ura^+ mutations (7hr) exceeded the rate of spontaneous Ura^+ mutations (0hr) by 577 fold at MAT, 145 fold at 16kb and 300 fold at 36kb as shown in Table 5.1a. No-DSB control strains lacking *GAL::HO* DSB site were used to determine accurate spontaneous mutagenesis rates shown in Table 5.1b. In this way we observed that the rate of DSB induced Ura^+ base substitutions was higher than the rate of spontaneous Ura^+ base substitutions by 655 times at MAT, 419 times at 16kb and 1431 times at 36kb (Figure 5.2). The majority of DSB induced Ura^+ mutations following DSB induction observed in our experimental strains were due to DSB repair by BIR. Thus the high increase in base substitution mutations in strains with DSB compared to strains without DSB result from error prone DNA synthesis during BIR.

Therefore, our results show that base substitutions are 400-1400 times more likely to happen during BIR than in spontaneous S-phase replication and demonstrate that BIR is highly mutagenic in promoting base substitution mutations.

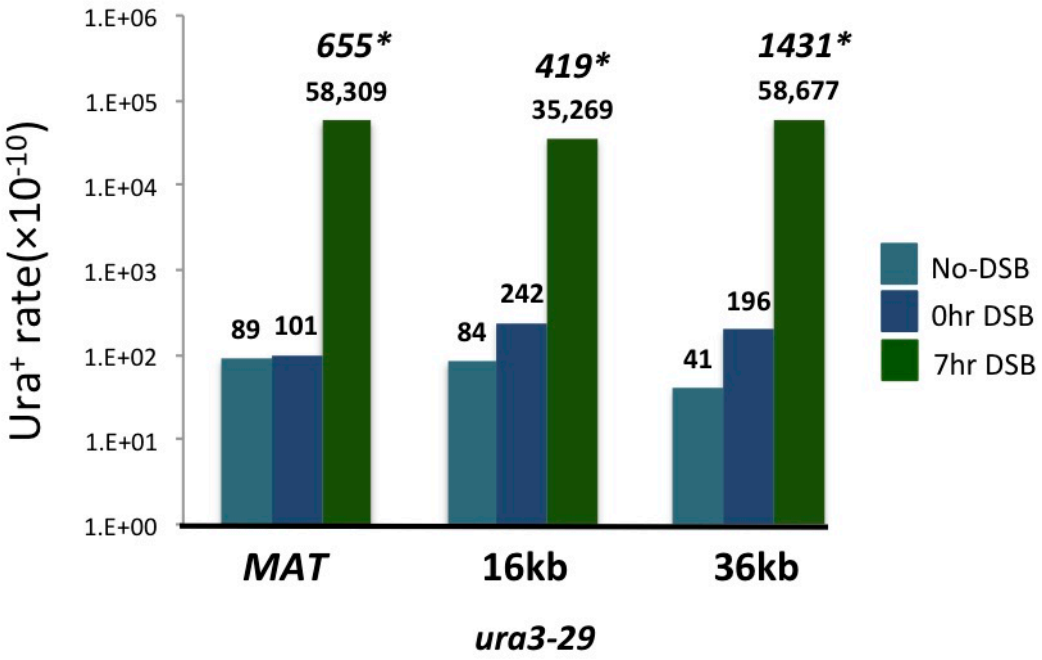

Figure 5.2 The Rate of BIR associated Base Substitution Mutagenesis.
The rate of Ura^+ substitution mutations was determined before (0hr) and (7hr) after addition of galactose to media for WT strains carrying *ura3-29* base substitution reporters at 3 positions *MATα-inc (MAT),* 16kb and 36kb centromere-distal to *MAT.* Rate of spontaneous Ura^+ mutations were determined using isogenic No-DSB control strains (No-DSB). Medians of mutagenesis rates are reported as Log_{10} scale (see Table 5.1a,b for confidence intervals/ranges and number of repeats). The fold increase in BIR mutation rate is indicated in italics. Statistically significant differences from the rates of spontaneous mutagenesis are indicated by an asterisk.

Table 5.1a The Rate of DSB induced Ura$^+$ mutations.
This table represents the rate of DSB associated Ura$^+$ mutations in strains carrying WT, *ura3-29*, WT (ori2 of *ura3-29*) *pif1Δ*, *pol2-4, pol3-5DV* and *rev3Δ*. DSB associated Ura$^+$ mutations for *ura3-29* at positions, *MATα-inc* (0kb), 16kb from *MATα-inc* and 36kb from *MATα-inc* are shown here. Rates for Ura$^+$ mutations are given for time-points, 0hr and 7hr i.e. before and 7hr after addition of galactose. [a]Rates calculated at 0hr are based on 0hr frequencies using the Drake equation (Drake J, 1991) (see materials and methods for more details). At 7hr, rates were calculated as (7hr frequency - 0hr frequency); [b] for strains with ≥ 6 experiments CI of median is given while for strains with < 6 experiments median range is given. Numbers in brackets [ ] represent repeats of experiments. [c] Statistically significant reduction of 7hr median rate of mutant compared to 7hr median rate of WT in strains with a DSB determined using the Mann-Whitney U test for p-value ≤ 0.0 5 Abbreviations: NA-not available, NS-not significant.

Table 5.1a The Rate of DSB induced Ura$^+$ mutations

Position	HO site	Relevant Genotype	Rate of Ura$^+$ (x10^{10}) [a]				Fold below wt (p-value) [d]
			Before galactose (0hr)		After galactose (frequency (7hr -0hr))		
			Median	CI or range[b] [# of repeats]	Median	CI or range[b] [# of repeats]	
MAT	DSB	*WT*	101	(61-168) [6]	58,309	(34,386-64,279) [6]	N.A.
MAT	DSB	*pif1Δ*	93	(85-127) [4]	143,872	(77,886-206,053) [4]	0.405 (p=0.0028)
16kb	DSB	*WT*	242	(120-252) [9]	35,269	(23,231-57,758) [9]	N.A.
16kb	DSB	*pol2-4*	396	(301-688) [4]	52,258	(27,013-71,940) [4]	N.S
16kb	DSB	*pif1Δ*	190	(127-187) [8]	11,372	(8,225-13,744) [8]	3 (p=0.001)
16kb	DSB	*pol3-5DV*	1,806	(230-5,633) [5]	63,928	(29,094-235,248) [5]	0.55 (p=0.0420)
16kb	DSB	*rev3Δ*	60	(36-124) [8]	7,438	(949-18,417) [8]	4.7 (p=0.036)
16k	DSB	*WT (ori2)*	2,159	(1,509-2,315) [6]	199,280	(161,957-307,706) [6]	0.176 (p=0.0004)
36kb	DSB	*WT*	196	(90-799) [6]	58,677	(29,144-73,057) [6]	N.A.
36kb	DSB	*rev3Δ*	57	(49-362) [5]	10,561	(10,044-24,918) [5]	5.55 (p=0.0043)
36kb	DSB	*pif1Δ*	116	(12-131) [6]	1,503	(61-2,553) [6]	39 (p=0.002)

Table 5.1b The Rate of Spontaneous Ura^{+} mutations.
This table represents the rate of Ura^{+} mutations for spontaneous events estimated in strains with No-DSB. Rates are presented only for 0hr (there is no significant difference in rates between 0hr and 7hr for strains with No-DSB). [a] Rates calculated at 0hr similarly as described in Table 5.1a; [b] For strains with ≥ 6 experiments CI of median is given while for strains with < 6 experiments median range is given. Numbers in brackets [ ] represent repeats of experiments.

Position	*HO* site	Relevant Genotype	Rate of Ura+ ×(10^{10}) [a]	
			Median	CI or range [b] [no of repeats]
MAT	No	*WT*	89	(65-252) [5]
MAT	No	*pif1Δ*	146	(93-229) [4]
16 kb	No	*WT*	84	(31-106) [8]
16kb	No	*pol2-4*	346	(302-659) [4]
16kb	No	*pif1Δ*	60	(16-125) [6]
16kb	No	*pol35-DV*	1,259	(929-2,971) [4]
16kb	No	*rev3Δ*	38	(15-54) [5]
16kb	No	*WT(ori2)*	2,087	(923-3,417) [3]
36kb	No	*WT*	41	(34-47) [6]
36kb	No	*rev3Δ*	38	(15-376) [4]
36kb	No	*pif1Δ*	63	(46-70) [6]

5.2.3 Sequencing Analysis of BIR-induced base substitution mutations

During S-phase replication, the *ura3-29* reporter can revert to Ura^+ by 3 types of base substitution mutations C→T, C→G, C→A. We were interested to know what types of Ura^+ base substitution reversions were produced in this reporter during BIR.

DSB induced Ura^+ mutations were analyzed in BIR for strains carrying *ura3-29* base substitution reporter at all 3 positions in the donor chromosome: at *MAT*, 16kb and 36kb and also spontaneous Ura^+ mutations in respective No-DSB control strains by sequencing 324bp of the *ura3-29* reporter gene. Out of the total 19 spontaneous Ura^+ mutations analyzed at *MAT*, 10 were C→ A while 9 were C→T type of reversions. The third type C→G was not observed in the cases analyzed so far. Among the 29 DSB induced Ura^+ mutations analyzed at MAT, 19 were C→A, 9 were C→T while 2 were C→G types of reversions. No statistically significant difference was observed for the types of reversions between spontaneous and BIR induced Ura^+ mutations at this position.

At 16kb, out of the 36 spontaneous Ura^+ mutations analyzed, 21 were C→A, 10 were C→T, and 5 were C→G type of reversions. This distribution of mutations was statistically different ($p=0.0045$) from the distribution of BIR induced Ura^+ reversions which included 47 C→A and 11 C→T reversions (out of total 58 analyzed). Thus we see that BIR-induced base substitutions were different from spontaneous base substitutions at 16kb, with C→A reversions being more frequent in BIR.

Sequencing analysis at 36kb revealed that 16/24 BIR induced Ura^+ base substitutions were C→T while 8/24 were C→A type of reversions. Hence compared to other positions, a statistically different distribution of mutations ($p=0.0034$ from MAT and $p < 0.0001$ from 16kb) was observed in BIR at 36kb where C→T reversions were more frequent.

Overall, we conclude that the types of BIR induced Ura$^+$ base substitution in the *ura3-29* reporter were similar to spontaneous base substitutions at *MAT* and different at 16kb where C→A types were more frequent. Among BIR induced Ura+ base substitutions at different positions, the types of reversions at 36kb, consisting of mainly C→T were different from types of reversions at *MAT* and at 16kb. Hence the difference that we observed between the types of base substitutions produced in BIR at 36kb compared to other positions suggests that the component(s) responsible for BIR base substitutions at this position maybe different from those at *MAT* or at 16kb positions.

Table 5.2 Sequencing Analysis of Ura^+ base substitutions
Types of BIR induced Ura^+ reversions of the *ura3-29* reporter are shown for strains carrying the reporter at *MAT*, 16kb and 36kb.Types of BIR induced Ura^+ mutations are compared to those of spontaneous Ura^+ mutations. Chi-Square Analysis based on p-value ≤ 0.05 determines statistically significant difference. Statistically significant difference from the types of spontaneous Ura^+ mutations is indicated by* (p=0.0045). Types of BIR induced Ura^+ mutations are also compared between different positions. Statistically significant difference in the distribution of BIR mutations between different positions is indicated by ** (p=0.0034 from MAT and p < 0.0001 from 16kb). Numbers in parenthesis indicate percentage of total events analyzed. Abbreviations: N.D. not determined, N.O. not observed.

Position	Type of Events	Type of Reversion Number of events (%)			Total Analyzed
		C→T	C→A	C→G	
MAT	Spontaneous	9 (47)	10 (52)	N.O.	19
	BIR	9 (31)	19 (65)	2 (6)	30
16kb	Spontaneous	10 (27)	21 (58)	5 (13)	36
	BIR	11 (19)	47*(81)	N.O.	58
36kb	Spontaneous	N.D	N.D	N.D.	N.D.
	BIR	16** (67)	8 (33)	N.O.	24

5.3 Genetic Control of BIR associated base substitutions

5.3.1 The Role of Polymerases in BIR base substitutions.

Analysis of BIR frameshift mutations showed that BIR is associated with a significantly higher level of polymerase errors than normal replication (Deem et al., 2011). DNA polymerase errors occurring during synthesis are usually corrected by 3'-5' exonuclease proofreading activity possessed by Pol δ and Pol ε, which during S-phase replication, promote lagging and leading strand synthesis respectively (McElhinny et al., 2008; Pursell et al., 2007). Previously our lab demonstrated that an increase in BIR frameshift mutagenesis was observed in a mutant lacking the proofreading activity of Pol δ (Deem et al., 2011). This observation led to conclusion that the majority of errors that led to frameshift mutations in BIR were made by Pol δ.

To determine the role of polymerases Pol δ and Pol ε in producing base substitutions associated with BIR, two exonuclease deficient mutations were introduced in strains carrying *ura3-29* reporter at position 16kb. The *pol3-5DV* and *pol2-4* eliminated the 3'-5' proofreading activity of Pol δ and Pol ε respectively.

5.3.1.1 The Role of Pol δ in BIR base substitutions

We observed that in *pol3-5DV* strains (lacking proofreading activity of Pol δ) the rate of spontaneous Ura^+ base substitution mutations were increased by 14 times as compared to the level observed in wild type strains as shown in Table 5.1b (Figure 5.3). This was consistent with previous observations made by others for spontaneous mutagenesis (Jin et al., 2005). Importantly, we observed that BIR induced Ura^+ base substitution mutagenesis was also increased 1.81 times in *pol3-5DV* strains compared to the already high mutagenesis in WT (as shown in Table 5.1a, Figure 5.3). These results suggest that proofreading activity of Pol δ works in BIR and can correct BIR induced base substitution

errors. Most importantly, since Pol δ predominantly proofreads its own errors, a significant increase of BIR base substitutions associated with BIR in *pol3-5DV* indicates that Pol δ is responsible for many of the base substitutions associated with BIR.

5.3.1.2 The Role of Pol ε in BIR base substitutions

Previously it was shown that eliminating the proofreading activity of Pol ε via *pol2-4* is associated with an increase of spontaneously induced base substitution mutagenesis by 15 times over WT level (Pavlov and Shcherbakova, 1995). Therefore, we tested the effect of *pol2-4* on the level of spontaneous and BIR-induced base substitution mutagenesis in our experimental system. We observed that the rate of spontaneously induced Ura^+ base substitutions was 346 (per 10^{10} nucleotides as shown in Table 5.1b) and was not statistically different from spontaneous levels in observed in WT as shown in Table 5.1b (Figure 5.3). Next, we determined the level of BIR induced base substitution mutagenesis in *pol2-4* and observed that this rate of 52258 (per 10^{10} nucleotides as shown in Table 5.1a) was also not statistically different from the WT rate (as shown in Table 5.1a).

Hence based on these results we conclude that *pol2-4* had no effect on BIR induced base substitutions.

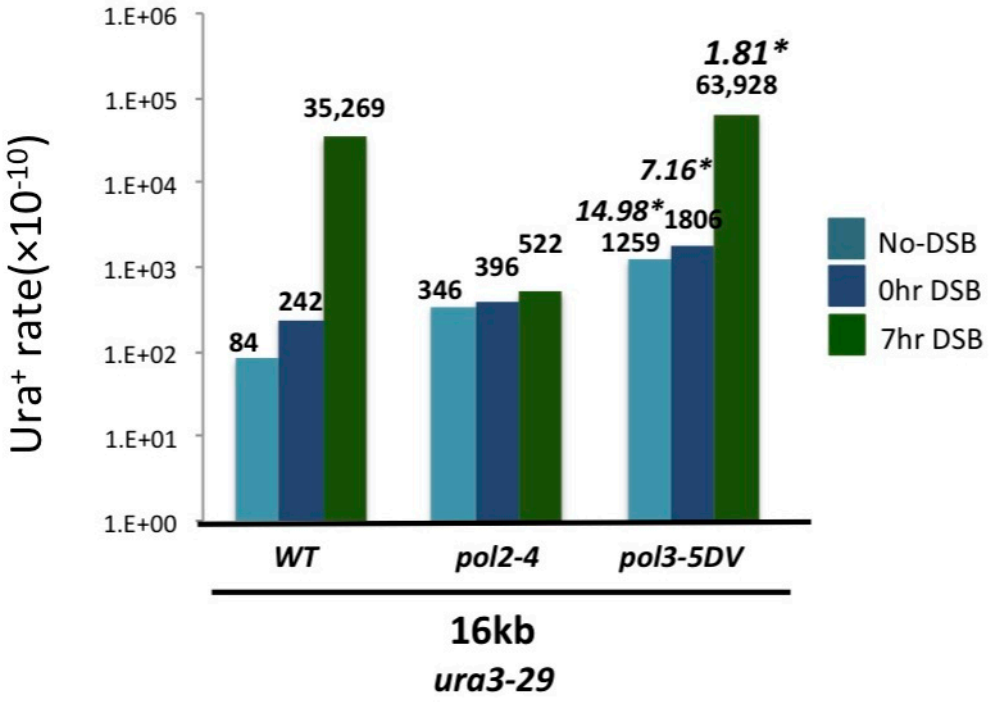

Figure 5.3 The Role of Pol ε and Pol δ in BIR associated base substitutions**.**
The rate of Ura$^+$ base substitution mutations was determined before (0hr) and (7hr) after addition of galactose to media for WT, *pol2-4* and *pol3-5DV* strains carrying *ura3-29* base substitution reporter at 16kb centromere-distal to *MAT.* The fold difference in BIR mutagenesis rates in mutants as compared to WT (in case of statistically significant difference) is indicated in italics Statistically significant differences from WT are indicated by an asterisk. Other abbreviations and statistical details are similar to those described in the legend for Figure 5.2.

5.3.2 The Role of Pif1 in BIR base substitutions

In the previous Chapter (4) we demonstrated that Pif1 is responsible for making BIR mutagenic where a Pif1 dependent pathway was found to promote frameshift mutations in BIR. Here the role of Pif1 in promoting BIR base substitutions is determined. To achieve this goal, strains carrying *ura3-29* reporters at all 3 positions and bearing a full deletion of *PIF1,* (*pif1Δ)* were used. The effect of Pif1 on BIR base substitution mutations was estimated by comparing the rates of DSB induced Ura^+ base substitutions between *pif1Δ* and WT strains.

AT *MAT* position, we observed that the rate of DSB induced Ura^+ mutations in pif1Δ strains were 2.5 times higher compared to the rate in WT as shown in Table 5.1a (Figure 5.4). At the 16kb position, DSB induced Ura^+ mutations were reduced by 3 times in *pif1Δ* as compared to WT. At 36kb, *pif1Δ* reduced the rate of Ura^+ base substitutions severely, by 39 times compared to WT.

Taken together our results demonstrate that Pif1 has a position dependent effect on BIR induced base substitutions. In *pif1Δ* base substitutions became more frequent at MAT while less frequent at 16kb and 36kb. Thus we observed the effect of the Pif1 mutagenesis pathway on base substitutions in BIR and saw that it was different from its effect on frameshift mutations, determined previously.

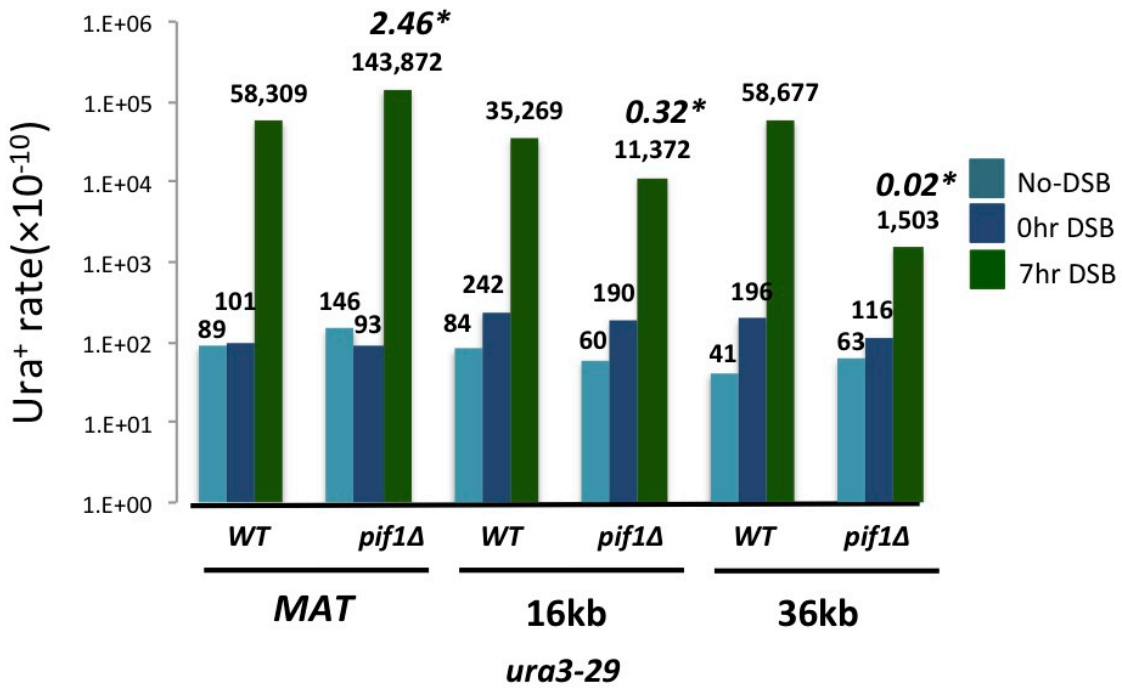

Figure 5.4 The Role of Pif1 in BIR associated base substitutions.
The rate of Ura$^+$ frameshift mutations was determined before (0hr) and (7hr) after addition of galactose to media for WT and *pif1Δ* strains carrying *ura3-29* base substitution reporters at 3 positions *MATα-inc (MAT)* 16kb and 36kb centromere-distal to *MAT.* The fold difference in BIR mutagenesis rates in mutants as compared to WT (in case of statistically significant difference) is indicated in italics. Statistically significant differences from WT are indicated by an asterisk. Other abbreviations and statistical details are similar to those described in the legend for Figure 5.2.

5.3.3 The Role of Pol ζ (Rev3) in BIR base substitutions

Through recent literature it is known that yeast Pol ζ has low fidelity and is particularly error prone for generating spontaneous base substitutions (Quah et al., 1980; Sabioneda et al., 2005). It was also shown to be responsible for mutagenesis associated with DSB repair where it had lower fidelity for base substitution errors compared to frameshifts (Hollback and Strathern, 1997; Hirano and Sugimoto, 1998). In the previous chapter we demonstrated that Pol ζ is responsible for a significant fraction of frameshift mutations occurring in BIR, where deletion of *REV3* (which encodes the catalytic subunit of Pol ζ) eliminated majority of *pif1Δ* independent mutagenesis at MAT. These results showed that a Rev3-dependent pathway of mutagenesis existed in BIR.

To test the role of Pol ζ (Rev3) in promoting base substitutions, strains carrying *ura3-29* reporters at 16kb and 36kb with full deletion of *REV3* were used. First spontaneously induced Ura^+ base substitutions were unaffected by *rev3Δ* when compared to WT in our experimental strains (Table 5.1b). To determine the effect of *rev3Δ* on BIR induced base substitutions, the rate of DSB induced Ura^+ base substitutions was compared between *rev3Δ* and WT strains. At 16kb, *rev3Δ* reduced the rate of DSB induced Ura+ base substitutions by 4.7 times compared to WT as shown in Table 5.1 (Figure 5.5), and at 36kb, *rev3Δ* reduced the rate of DSB induced Ura^+ base substitutions by 5.5 times compared to WT.

Based on these results we conclude that Pol ζ (Rev3) is responsible for the majority of base substitutions in BIR. Elimination of *REV3* made base substitutions less frequent in BIR not only at 16kb but even as far as 36kb where no effect was previously observed for BIR-induced frameshift mutations (Deem et al., 2011).

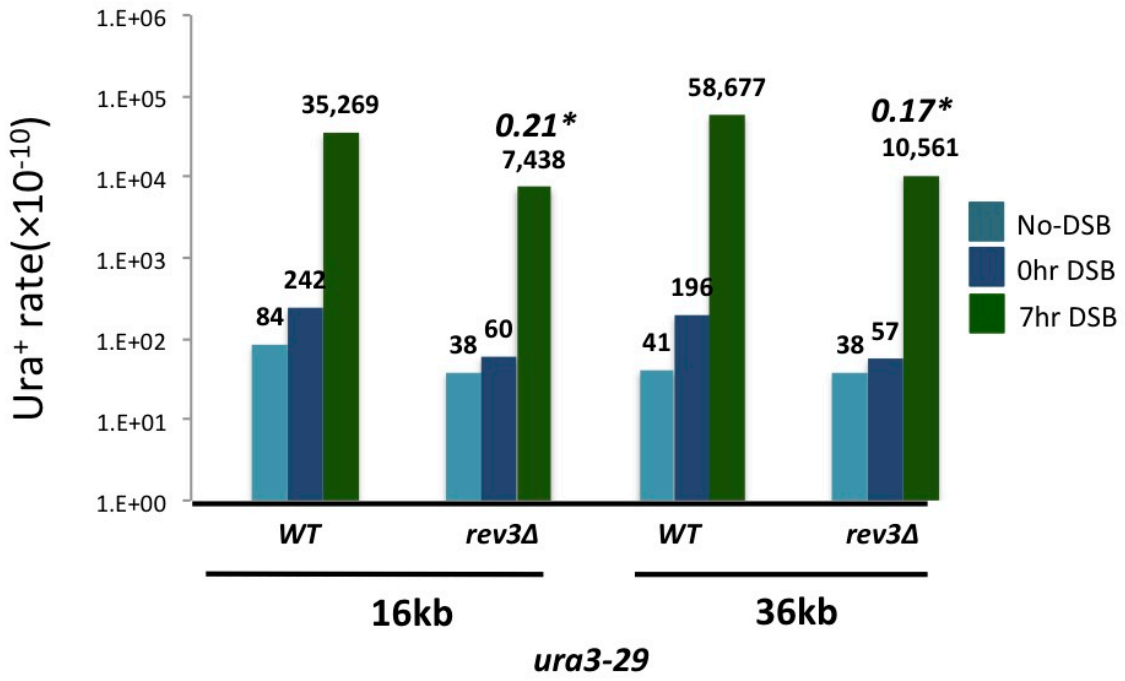

Figure 5.5 The Role of Pol ζ (Rev3) in BIR associated base substitutions.
The rate of Ura+ mutations was determined before (0hr) and (7hr) after addition of galactose to media for WT and *rev3Δ* strains carrying *ura3-29* reporters at positions 16kb and 36kb centromere-distal to *MAT.* The fold difference in BIR mutagenesis rates in mutants as compared to WT (in case of statistically significant difference) is indicated in italics. Statistically significant differences from WT are indicated by an asterisk. Other abbreviations and statistical details are similar to those described in the legend for Figure 5.2.

5.3.4 Orientation bias for base substitutions in BIR

In S-phase replication it was previously demonstrated that changing the orientation of the gene affects the fidelity of DNA synthesis. Pavlov et al. (2002) showed that in S-phase replication DNA synthesis was more mutagenic in the leading strand as compared to the lagging strand by changing the orientation of the *ura3-29* reporter. Further evidence demonstrated such a bias in mutagenesis was due to that mismatch repair preferentially correcting the lagging strand more than the leading strand (Pavlov et al., 2003; McElhinny et al., 2007). Though the identity of leading and lagging strands is unclear in BIR, we were interested to know if changing the orientation of the *ura3-29* reporter gene would affect the already high rate of mutagenesis i.e. to find out whether BIR is more mutagenic in one strand as compared to the other.

We decided to investigate this by inserting the *ura3-29* reporter gene in an opposite orientation in our experimental strains at the 16kb position. First we determined if the rate of BIR induced base substitution mutagenesis was higher that spontaneous mutagenesis for the opposite orientation of the *ura3-29* reporter. We observed that the rate of DSB induced Ura^+ base substitutions exceeded the rate of spontaneous base substitutions by 95 times confirming that BIR was mutagenic in the opposite orientation of *ura3-29* as well (Table 5.1a, b).

To determine if the orientation of reporter gene affected the rate of mutagenesis in BIR, the rate of DSB induced Ura^+ mutagenesis of the *ura3-29* reporter in orientation 1 was compared to the rate of DSB induced Ura^+ mutagenesis of the reporter in orientation 2. As shown in Table 5.1a we found that the rate of DSB induced Ura^+ mutagenesis in orientation 2 of the reporter was 5.65 times higher than the rate in orientation 1 (Figure 5.6). Spontaneously induced Ura^+ mutagenesis was also higher in orientation 2 compared to orientation 1 by 24 times (Table 5.1b).

Based on these results we concluded that changing the orientation of the *ura3-29* reporter gene does affect the rate of mutagenesis in BIR i.e. DNA synthesis in BIR is more mutagenic in one strand as compared to the other.

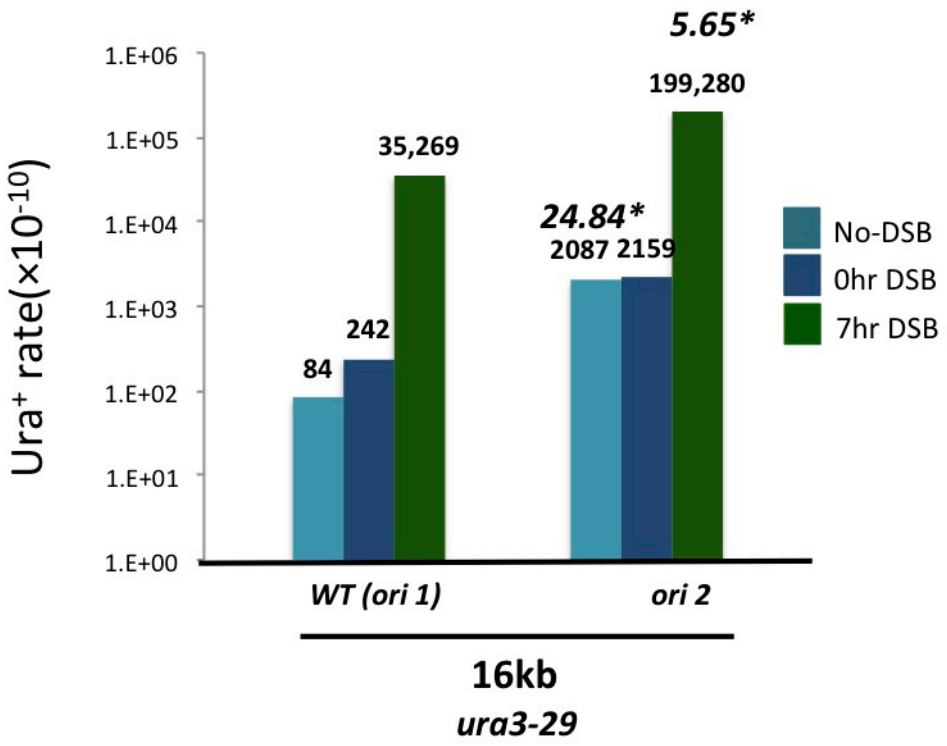

Figure 5.6 The Effect of gene orientation on base substitutions in BIR.
The rate of Ura$^+$ frameshift mutations was determined before (0hr) and (7hr) after addition of galactose to media for WT strains carrying *ura3-29* base substitution reporters in two different orientations (ori1 and ori2) at positions 16kb centromere-distal to *MAT.* The fold difference in BIR mutagenesis rate in ori2 as compared to ori1 (in case of statistically significant difference) is indicated in italics. Statistically significant differences from WT ori1 are indicated by an asterisk. Other abbreviations and statistical details are similar to those described in the legend for Figure 5.2.

5.4 Discussion

In this chapter, we were able to demonstrate that BIR is mutagenic in inducing base substitutions in its entire path of DNA synthesis, with a frequency of 400-1400 times higher than S-phase DNA replication. Base substitutions in BIR were mainly due to errors of DNA Pol δ and Translesion Polymerase ζ. Taken together with our previously demonstrated results (Deem et al., 2011), it can now be conclusively said that BIR is a highly error prone DNA repair process due to a low fidelity of DNA synthesis that leads to a high frequency of both frameshift and base substitution mutations.

5.4.1 The Role of Polymerases in BIR base substitutions

Based on our results showing the effect of *pol3-5DV* on BIR induced base substitutions we are able to say that base substitution errors in BIR are made by Pol δ. This effect was observed for reporters located at 16kb and was found to be consistent to the effect of *pol3-5DV* on BIR-induced frameshift mutations. Future studies will test whether the same is true for other positions as well. Errors made by Pol δ, can be corrected by mismatch repair machinery in addition to proofreading. Thus an accurate estimation of the efficiency of proofreading in BIR can be made only in the absence of mismatch repair. This can be estimated in a *pol35DVmsh2Δ* or *pol35DVmsh3Δ* background. Nevertheless, our data showing a significant increase in BIR base substitutions in a mutant lacking proofreading activity of Pol δ compared to WT and spontaneously induced base substitutions strongly support the idea that base substitutions in BIR must be produced by Pol δ although contribution of other polymerase errors cannot be excluded here (Nick McElhinny et al., 2006; Pavlov et al., 2006).

Our results also demonstrate that *pol2-4* has no effect on base substitutions in BIR. This could suggest several possibilities including Pol ε being non- functional in our strain at the corresponding position, or Pol ε not participating in BIR. These findings are consistent with previous observations which demonstrate that Pol ε is not essential in

BIR and is required only at the later stages (Lydeard et al., 2010). Further studies testing the effect of *pol2-4* at other positions could be useful. Absence of any effect of *pol2-4* also implies other possibilities such as proofreading of Pol ε being non-functional in BIR or Pol ε not contributing to errors in BIR. An accurate estimation of the efficiency of proofreading of *pol2-4* on BIR can be made in the absence of mismatch repair (using a *pol2-4msh2Δ* double mutant) as Pol ε errors are also corrected by mismatch repair. Other mutants of Pol ε such as *pol2-M644G* which has high replication activity, retains proofreading activity but has a reduced fidelity particularly for T-dTMP mismatches leading to a high frequency of T-A mismatches (Pursell et al., 2007) can also be used to determine the role of Pol ε on BIR.

5.4.2 The Role of Pif1 in BIR base substitutions

Our data demonstrating the effect of *pif1Δ* on base substitutions suggest that the Pif1 mutagenesis pathway in BIR is responsible for base substitutions as well. Deletion of *PIF1* reduced the rate of base substitutions at 16kb by 3 times compared to WT. The 3-fold decrease in mutagenesis is similar to the effect of *pif1Δ* on BIR efficiency (shown in Section 4.3.1.1). Therefore, it might mean that the decrease in BIR-induced base substitutions at 16kb observed in *pif1Δ* is due to reduction in the efficiency of BIR *per se*. Deletion of *PIF1* reduced the rate of base substitutions by 98% at 36kb. Thus the decrease in mutagenesis is not due to reduction in BIR itself but BIR being less mutagenic in the absence of *PIF1*. While base substitution mutations were reduced at 16kb and 36kb in *pif1Δ*, we observed that they were increased at *MAT* position. A probable explanation for this effect maybe that in the absence of the helicase activity of Pif1, and subsequent difficulty in the progression of the BIR fork, the large amount of ssDNA persisting during BIR initiation becomes more susceptible to damage through sources such as UV, where Pol ζ maybe responsible for damage induced mutagenesis (Abdulovic and Jinks Roberston, 2006).

Overall we observed that the Pif1 dependent pathway had a different effect of base substitutions in BIR compared to its effect on frameshifts. The effect of *pif1Δ* on frameshift mutations and base substitutions in BIR was only comparable at 36kb, where mutations were rare in *pif1Δ,* and not at other positions.

5.4.3 The Role of Pol ζ (Rev3) in BIR base substitutions

We observed that Pol ζ was responsible for a majority of base substitutions in BIR. Deletion of *REV3* eliminated almost 84% of base substitutions at 16kb and 82% of base substitutions at 36kb. Since the majority of base substitution mutations (98%) at 36kb were already shown to be depended on Pif1, we propose that Pif1 and Rev3 may work in the same pathway to make base substitution mutations at 36kb. Also at 16kb, we know that a Pif1 dependent pathway of mutagenesis exists. Thus the effect of *pif1Δ* on base substitutions at 16kb could be checked in the *rev3Δ* background by using a *pif1Δrev3Δ* double mutant. We were unable to check this double mutant so far due to limitations of available genetic markers.

Also Pol ζ was shown to have modest effects on frameshift mutations in BIR at 16kb and no effect at 36kb. Based on these observations we are able to say that Pol ζ has a lower fidelity for base substitutions as compared to frameshift mutations in BIR, consistent with findings implicating the role of Pol ζ for DSB induced mutagenesis (Holleback and Strathern, 1997).

In addition to Pol ζ (Rev3), yeast *S. Cerevisiae* has 2 other translesion polymerases Rev1 and Pol η. While the function of Rev3 is speculated to be extension past the nucleotide inserted across a lesion or from a mismatched terminus, the actual insertion of the mismatch nucleotide is mediated by either Rev1 (which has a deoxycitydyl transferase activity for inserting dCMP across abasic sites/damaged lesions) (Nelson JR et al., 1996; Haracska et al., 2001) or by Pol η (which can bypass UV-damaged lesions in an error-free

manner). We can achieve a better understanding of the Rev3-dependent mutagenesis pathway by analysis of *rev1Δ, rad30Δ* (*rad30* encodes Pol η) and a double mutant of either *rev1Δrev3Δ* or *rad30Δrev3Δ* for BIR base substitutions.

5.4.4 Orientation bias for base substitutions in BIR

We observed that BIR makes more mutations for one orientation of the *ura3-29* reporter gene as compared to the other. Such information can be usefully applied towards understanding the replication fork associated with BIR. What we observe in BIR could be similar to S-phase replication where more mutagenesis is associated with lagging strand replication as compared to leading strand as demonstrated by Pavlov et al. (2003) and McElhinny et al. (2010). In S-phase replication, while the synthesis of leading strand is continuous, that of the lagging strand is discontinuous, in the form of short Okazaki fragments resulting in stand discontinuity or a free 5' end. Also, the lagging strand is usually associated with more amount of PCNA to synthesize and process the 5' end of these Okazaki fragments. These two factors have been shown to provide a strand discrimination signals for mismatch repair machinery, which ensures that errors in the lagging strand are preferentially corrected compared to those of the leading strand. Since mismatch repair is known to participate and correct errors in BIR, it would be interesting to know if MMR shows a bias in BIR mutagenesis as well.

5.4.5 Proposed System to Study forward mutations in BIR

This current disomic system of identifying BIR induced mutagenesis employs a reversion assay to select for dominant mutations, (Lys^+ (from *lys2*) or Ura^+ (from *ura3-29*)) where the original wild type template allele remains after BIR repair. Recessive mutations (Lys^- or Ura^-) cannot be genetically selected in this system. Also the current reporter system excludes the possibility of analyzing all types of BIR mutations (including frameshifts and base substitutions) simultaneously. Hence an alternative system that employs a forward

mutation assay that can detect the overall BIR mutagenesis spectrum is needed. We are currently developing such a system using the cannavanine (*CAN1*) gene reporter that can identify forward mutations in BIR. The mutants described earlier can all be used in such a system where the entire spectrum of BIR induced mutations can be determined. This proposed system (Figure 5.7) in haploid cells contains the *GAL::HO* site of DSB induction at *LEU2* gene on CHRIII. Following DSB, the broken *U2* piece from *LEU2* can find homology from another *U2* (truncated copy of *LEU2*) inserted 50kb away on the same chromosome on the centromere distal side. In this way BIR is initiated to repair DSB at *LEU2* and results in copying *CAN1* located downstream of *U2*. BIR promoted mutagenesis will result in a *CAN1* resistant mutation (from its WT cannavanine sensitive phenotype) and can be selected because of degradation of CHRIII fragment serving as template for BIR repair thus losing the wild type *CAN1* sensitive phenotype.

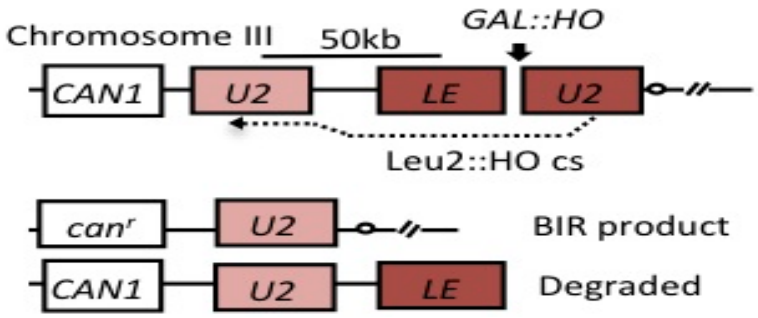

Figure 5.7. Experimental System to study forward mutations associated with BIR. DSB introduced at *LEU2::HO* cut site can be repaired by BIR from *U2* (truncated *LEU2*) located 50kb away from the *LEU2::HO* cs. Subsequent copying of *U2* through strand invasion will result in synthesis through *CAN1*. BIR induced *CAN*^{r} forward mutations can be detected because of degradation of fragment serving as template for BIR synthesis.

CHAPTER 6. THE MODE OF SYNTHESIS ASSOCIATED WITH BREAK-INDUCED REPLICATION

6.1 Background

The high tendency of BIR to produce mutations and chromosomal rearrangements led us to investigate the mode of synthesis associated with BIR. BIR repair of DSBs occurs by synthesis of DNA in sizes comparable to replicons, similar to S-phase DNA replication, making BIR a processive type of DNA replication (Malkova et al., 2005). Even though it is believed that BIR proceeds in the context of a real replication fork with several BIR initiating factors/proteins common to S-phase replication (Lydeard et al., 2010), there are several important differences, which suggest that the BIR fork maybe different from S-phase replication fork. Contrary to S-phase replication that can initiate at specific origins of replication, BIR can only initiate at DSB sites. The roles of the main replicative polymerases differ in BIR, with only Pol δ and Pol α required for BIR initiation and Pol ε remaining non-essential until the later stages of BIR (Lydeard et al., 2010). Also, BIR requires Pol32, the third subunit of DNA Polymerase δ (Deem et al., 2008; Lydeard et al., 2007), and accessory DNA helicase Pif1, both non-essentials to S-phase DNA replication.

Furthermore, even though BIR matches S-phase replication in its rate and processivety at later stages, its initiation is extremely slow (Jain et al., 2007; Malkova et al., 2005). This slow initiation of BIR makes it extremely unstable during early synthesis and leads to frequent template switching to other non-homologous chromosomes (Smith et al., 2007). Our recent data demonstrate that BIR is highly mutagenic and leads to gross

chromosomal rearrangements . Hence unlike the high fidelity and safe DNA replication in S-phase, DNA replication following DSB i.e. BIR is highly error-prone and unstable.

Overall, these observations suggest that BIR may be mechanistically different from S-phase replication in the mode of DNA synthesis, initiated after assembly of a possible, unstable replication fork. While planning this work, we considered two models of DNA synthesis that could explain BIR.

Model No 1 Semiconservative Synthesis: At the DSB site, BIR initiates after 5'-3' resection of the broken chromosome forms a 3' end free to invade and prime DNA synthesis from a homologous chromosome. This invasion and initial synthesis proceeds with the formation of a displacement loop, which represents a single Holliday Junction. Early resolution of this Holliday Junction structure during BIR repair synthesis results in a replication fork similar to that observed in normal S-phase DNA replication. Such a process would result in a semiconservative mode of synthesis similar to S-phase DNA replication (Figure 6.1 B).

Model No 2 Conservative Synthesis: According to this model, Holliday Junction may never be resolved and the D-loop will persist and progressively move forward in the form of a bubble. Such conditions would lead to dissociation (pulling) of newly synthesized strands from their template and their concomitant association together resulting in a conservative inheritance of strands by the broken chromosome (Figure 6.1 A).

The goal of research presented in this chapter was to discriminate between these two models.

6.2 Experimental Approach to determine Mode of Synthesis in BIR

To investigate the mode of DNA synthesis in BIR, the disomic experimental system for assaying BIR frameshift mutagenesis (described earlier in Section 4.2) was used to select Lys^+ mutations occurring with high frequency. These BIR induced Lys^+ mutations represent errors made during DNA repair synthesis of newly formed strands. We set to determine the location of Lys^+ sequence to see whether BIR induced errors or newly synthesized strands were acquired by a semi-conservative or conservative mode of replication.

A semi-conservative mode of replication by BIR predicts that the Lys^+ sequence can be located in either the donor (template) or the recipient (repaired) copy with equal probability (Figure 6.1 B). Conversely, a conservative mode of BIR predicts that Lys^+ sequence will always be located in the recipient/repaired copy (Figure 6.1 A).

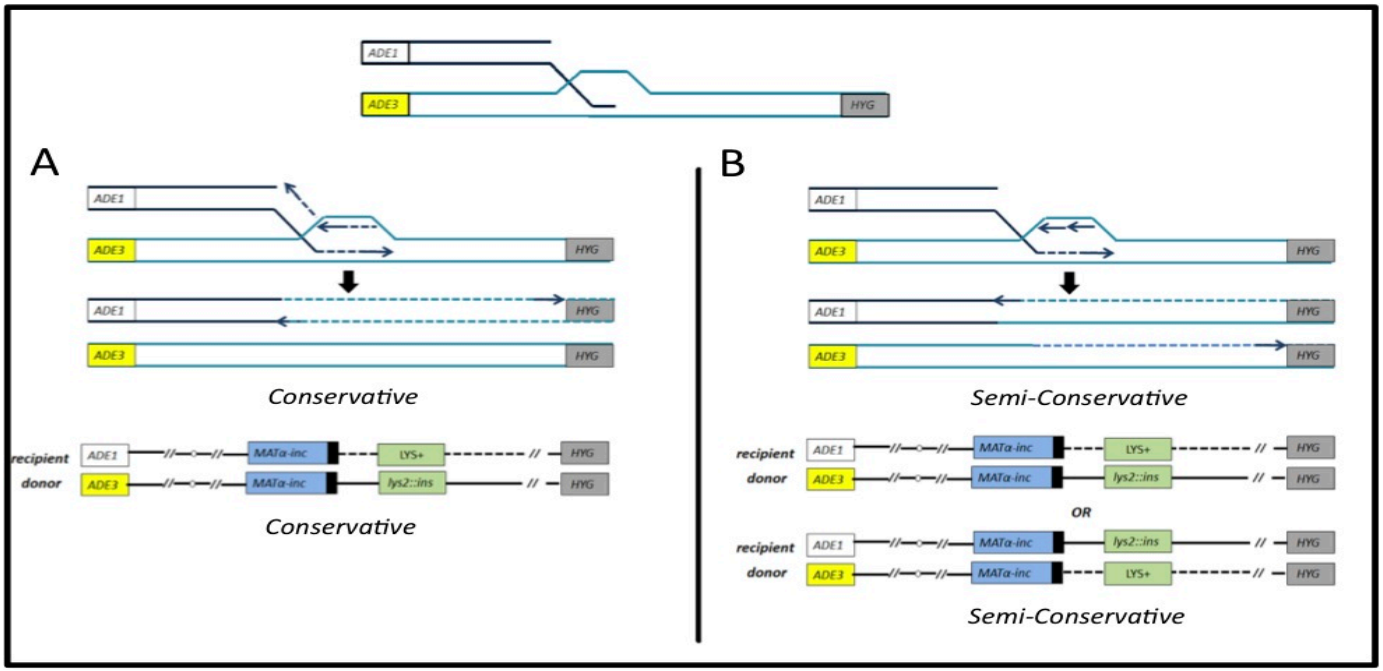

Figure 6.1 Experimental model describing two possible modes of BIR DNA synthesis. After 5' to 3' resection following DSB, strand invasion of the broken (recipient chromosome) into the homologous donor (template) chromosome initiates BIR DNA synthesis. (A) Represents conservative synthesis where the D-loop formed, following strand invasion, migrates progressively in the form of a bubble, without resolution. In this way BIR repairs broken molecule by synthesizing new strands that are together associated with the recipient (repaired) molecule. BIR DNA synthesis of new strands from the template (*lys2::ins*) is mutagenic and hence induces Lys^+ mutations. Hence in a conservative model Lys^+ sequence is associated with the recipient. (B) Represents a semi-conservative model where the D-loop, formed after strand invasion is resolved, to form a unidirectional replication fork. Here, new strands synthesized by BIR to repair the broken chromosome are not displaced and remain attached to a template. Hence, in a semi-conservative model BIR-induced Lys^+ sequences maybe associated either with the donor (template) or recipient (repaired) chromosome with equal probability.

6.3 Location of Lys$^+$ Sequence

To determine which of the above possibilities was more likely, BIR induced Lys$^+$ outcomes were analyzed by Pulse Field Gel Electrophoresis. Using PFGE, these Lys$^+$ outcomes (from CHRIII) were resolved separately into donor (template) and recipient (repaired) chromosomes (Figure 6.2) and DNA from individual chromosomes was purified separately. 400bp of *lys2::ins* reporter from each chromosome was sequenced to determine the location of the Lys+ mutation. This analysis was carried out for *lys2::ins* reporters at loci 16kb and 36kb.

As shown in Table 6.1 for the *lys2::ins* reporter at 16kb, 26 Lys$^+$ outcomes were analyzed. Out of these 26 outcomes, all Lys$^+$ mutations were located in the recipient (repaired) chromosome. Also, for the *lys2::ins* reporter at the 36kb position, all of the 18 Lys$^+$ outcomes analyzed were located in the recipient chromosome (Table 6.1). In each case the donor chromosome remained unchanged.

Thus these results confirm that BIR induced Lys$^+$ mutations are always associated with the recipient (repaired) chromosome; and support the hypothesis of conservative mode of DNA synthesis followed by BIR.

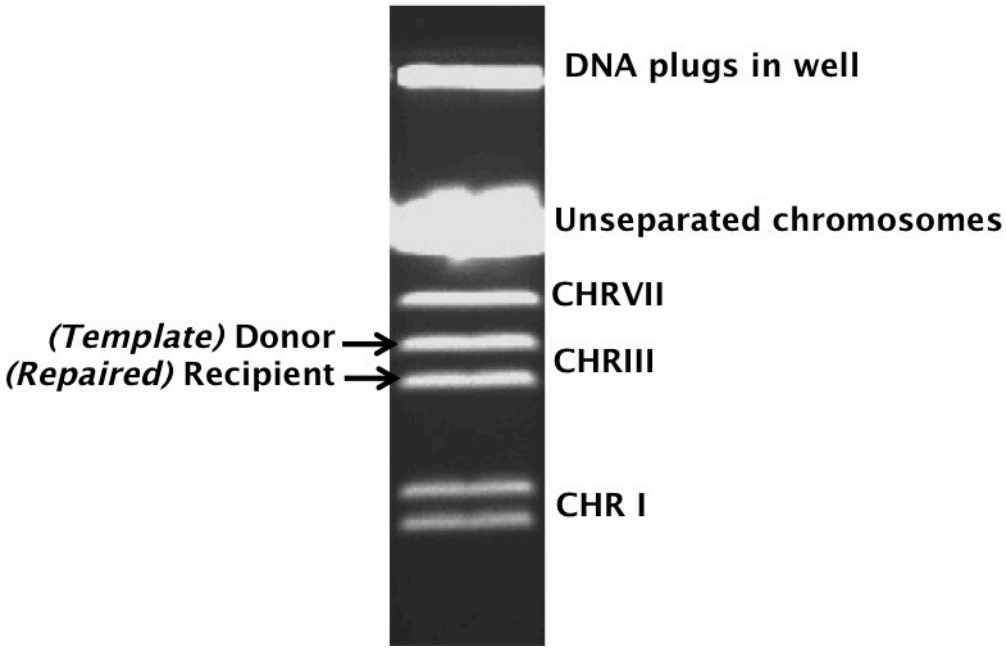

Figure 6.2 Pulse Field Gel Electrophoresis (PFGE) separation of CHRIII.
BIR repaired Lys^+ outcomes purified by high molecular weight DNA extractions are run on PFGE to achieve separation into donor and recipient chromosomes. Individual bands from CHRIII are cut out and purified separately.

Table 6.1 Location of BIR induced Lys^+ mutations in Chromosome III.
BIR induced Lys^+ outcomes in WT strains carrying *lys2::ins* frameshift reporters at 16kb and 36kb centromere distal to *MATα-inc* analyzed by PFGE and DNA sequencing are assigned to donor or recipient chromosomes. Statistically significant values determined by Fischer's exact test are based on p-value ≤ 0.05 and are indicated by an asterisk.

Position	Lys^+ outcomes in Donor chromosome	Lys^+ outcomes in Recipient chromosome
16kb	0/26	26/26*($p < 0.001$)
36kb	0/18	18/18*($p=0.01$)

6.4 Discussion

6.4.1 Conservative Synthesis Responsible for Low Fidelity in BIR

Our results showing that Lys^+ sequences are consistently associated with the recipient chromosome during BIR suggest that BIR follows a conservative mode of DNA synthesis. Such a conservative mode of DNA synthesis has been demonstrated for another DNA repair pathway GC that is also associated with mutagenesis (Hicks et al., 2010). DNA synthesis in BIR is extensive, up to several hundred kilobases (Malkova et al., 2005) unlike GC where it is a short-patch. Our results showing conservative inheritance of Lys^+ up to 36kb suggest that BIR is involved with extensive conservative synthesis of DNA.

Results from our lab have demonstrated that BIR is highly mutagenic and generates a high frequency of Lys^+ mutations, which were subsequently analyzed in this chapter to determine conservative synthesis. These findings imply that the high frequency of mutagenesis observed in BIR results from conservative synthesis of DNA.

In Chapter 4 and 5 it was shown that mutagenesis in BIR is dependent on Pif1 helicase. Pif1 was shown to be responsible for the high efficiency and low fidelity of BIR. Based on the data presented in Chapters 4, 5 and 6 taken together, we suggest that the helicase activity of Pif1 is responsible for the conservative synthesis during BIR that leads to high mutagenesis.

6.4.2 BIR leading to Genomic Instability

We propose a model describing the conservative mode of DNA synthesis during BIR that explains how BIR maybe promoting massive genomic destabilization. Following a DSB that results in 5’ to 3’ resection (Figure 6.3 A), a 3’ overhang of the broken chromosome is created which is free to initiate BIR by invading into a homologous chromosome

(Figure 6.3 B). At this point of strand invasion and displacement loop formation, BIR may be channeled into either one of the two pathways, a safe pathway of semiconservative DNA synthesis (Figure 6.3 E) or an error-prone pathway of conservative DNA synthesis (Figure 6.3 B-D). In the safe BIR pathway, the displacement loop or the 2-way Holliday Junction is efficiently resolved, giving rise to a unidirectional replication fork. This replication fork carries out semiconservative DNA synthesis with high fidelity, similar to DNA replication in S-phase (Figure 6.3 F). However in case of the error-prone BIR pathway, the Holliday Junction may never be resolved and may move in form of a bubble (Figure 6.3 B) This migrating bubble maybe driven by helicases such as Pif1, where the newly synthesized nascent (leading) strand is consistently displaced from its donor template and is conservatively inherited (Figure 6.3 C). This nascent strand, devoid of an accurate template, may contain potential uncorrected errors and serve as the new template for further lagging strand synthesis. Such an arrangement interferes with the ability of mismatch repair, since it uses an inaccurate template as a reference to correct errors. Hence uncorrected errors are left behind leading to high mutagenesis (Figure 6.3 D).

As described in Section 4.4.2, the error-prone pathway initiated as BIR may also end up promoting chromosomal rearrangements by two additional mechanisms. A reverse branch migration of the Holliday Junction may occur which leads to dissociation of the invading strands from the homologous template (Figure 6.3 G). The dissociated strands may invade alternative non-homologous chromosomes and give rise to repeated cycles of dissociation and reinvasion. Such a process can give rise to chromosomal translocations by an ectopic (non-allelic) BIR mechanism. Alternatively, the Holliday Junction may be resolved in an aberrant fashion leading to half-crossovers or non-reciprocal translocations (Figure 6.3 H). Interestingly, both of these types of chromosomal rearrangements maybe associated with mutations.

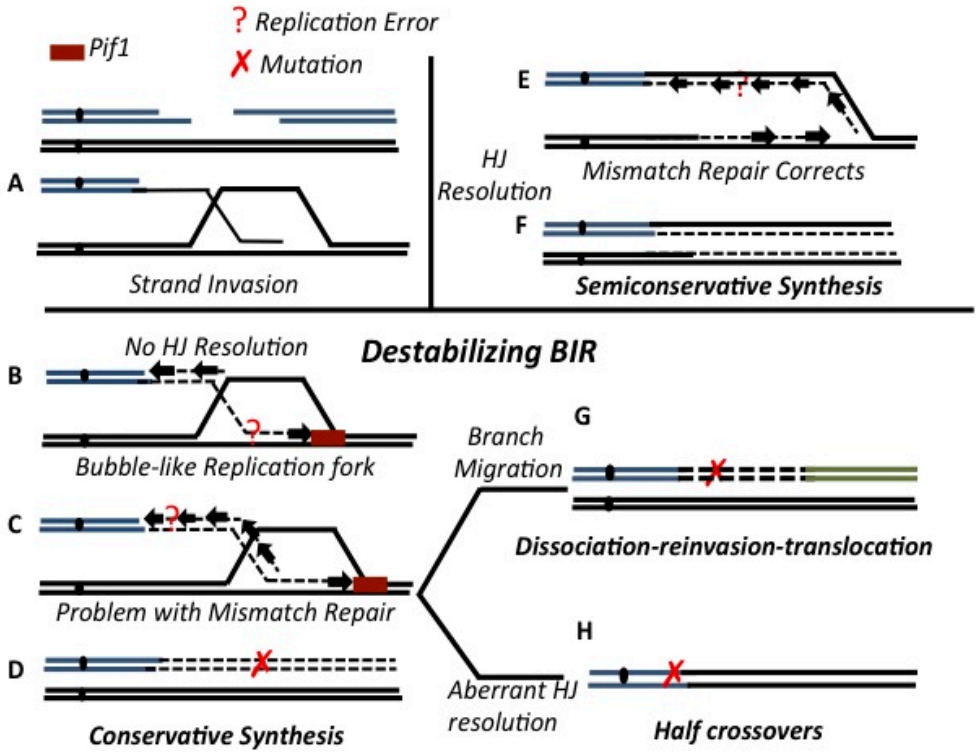

Figure 6.3 Model of Destabilizing BIR.
Schematic representation of BIR associated conservative synthesis and consequent genomic instability.

6.4.3 Future Directions

The results demonstrated in this chapter are consistent with a conservative synthesis operating during BIR. Nevertheless it is possible that this analysis is biased since only Lys^+ mutations were analyzed. Therefore, while a conservative mode of synthesis is likely to explain the high mutagenesis in BIR, it is possible that a mixture of both conservative and semi-conservative synthesis may exist in BIR. Our lab, in association with Dr. Kirril Lobachev at Georgia Institute of Technology, has recently carried out additional physical analysis of BIR synthesis and its intermediates. Dynamic molecular combing (Michal et al., 1997) experiments carried out in collaboration between our labs have revealed that BIR is indeed involved with extensive DNA synthesis and follows a

conservative mode of DNA replication. 2-D gel electrophoresis experiments, which can detect the molecular intermediates in BIR, have indicated the presence of a bubble like replication fork. Hence the results described in this chapter are in agreement with these findings and coherent to the idea that BIR is associated with a novel type of DNA synthesis that proceeds in the form of an unusual bubble-like replication fork where a conservative inheritance of newly synthesized strands occurs.

LIST OF REFERENCES

LIST OF REFERENCES

Aylon, Y., and Kupiec, M. (2003). The checkpoint protein Rad24 of *Saccharomyces Cerevisiae* is involved in processing double-strand break ends and in recombination partner choice. Mol Cell Biol 23, 6585-6596.

Bosco, G., and Haber, J.E. (1998). Chromosome break-induced DNA replication leads to nonreciprocal translocations and telomere capture. Genetics 150, 1037-1047.

Bochman, M.L., Sabouri, N., and Zakian, V.A. (2010). Unwinding the functions of the Pif1 family helicases. DNA Repair (Amst.) 9, 237-249.

Budd, M.E., Reis, C.C., Smith, S., Myung, K., and Campbell, J.L. (2006). Evidence suggesting that Pif1 Helicase Functions in DNA Replication with the Dna2 helicase/nuclease and DNA Polymerase {delta}. Mol Cell Biol 26, 2490-2500.

Bugreev, D.V., Mazina, O.M., and Mazin, A.V. (2006). Rad54 protein promotes branch migration of Holliday junctions. Nature 442, 590-593.

Chabes, A., Georgieva, B., Domkin, V., Zhao, X., Rothstein, R., and Thelander, L. (2003). Survival of DNA damage in yeast directly depends on increased dNTP levels allowed by relaxed feedback inhibition of ribonucleotide reductase. Cell 112, 391-401.

Chung, W.H., Zhu, Z., Papusha, A., Malkova, A., and Ira, G. (2010). Defective resection at DNA double-strand breaks leads to *de novo* telomere formation and enhances gene targeting. PLoS Genet 6, e1000948.

Daley, J.M., Palmbos, P.L., Wu, D., and Wilson, T.E. (2005). Non-homologous end joining in yeast. Annual Review of Genetics 39, 431-451.

Davis, A.P., and Symington, L.S. (2004). RAD51-dependent break-induced replication in yeast. Mol Cell Biol 24, 2344-2351.

Deem, A., Barker, K., Vanhulle, K., Downing, B., Vayl, A., and Malkova, A. (2008). Defective break-induced replication leads to half-crossovers in *Saccharomyces Cerevisiae*. Genetics 179, 1845-1860.

Deem, A., Keszthelyi, A., Blackgrove, T., Vayl, A., Coffey, B., Mathur, R., Chabes, A., and Malkova, A. (2011). Break-Induced Replication Is Highly Inaccurate. PLoS Biol 9, e1000594.

Downing, B., Morgan, R., Van Hulle, K., Deem, A., and Malkova, A. (2008). Large inverted repeats in the vicinity of a single double-strand break strongly affect repair in yeast diploids lacking Rad51. Mutat Res 645, 9-18.

Drake, J.W. (1991). A constant rate of spontaneous mutation in DNA-based microbes. Proceedings of the National Academy of Sciences U.S.A 88, 7160-7164.

Dunn, B., Szauter, P., Pardue, M.L., and Szostak, J.W. (1984). Transfer of yeast telomeres to linear plasmids by recombination. Cell 39, 191-201.

Formosa, T., and Alberts, B.M. (1986). DNA synthesis dependent on genetic recombination: Characterization of a reaction catalyzed by purified bacteriophage T4 proteins. Cell 47, 793-806.

Foury, F., and Kolodynski, J. (1983). Pif1 mutation blocks recombination between mitochondrial rho^{+} and rho^{-} genomes having tandemly arrayed repeat units in *Saccharomyces Cerevisiae*. Proceedings of the National Academy of Sciences U.S.A 80, 5345-5349.

Foury, F., and Van Dyck, E. (1985). A Pif1-dependent recombigenic signal in the mitochondrial DNA of yeast. EMBO 4, 3525-3530.

Gambus, A., Jones, R.C., Sanchez-Diaz, A., Kanemaki, M., Van Deursen, F., Edmondson, R.D., and Labib, K. (2006). GINS maintains association of Cdc45 with MCM in replisome progression complexes at eukaryotic DNA replication forks. Nat Cell Biol 8, 358-366.

George, J.W., and Kreuzer, K.N. (1996). Repair of Double-Strand Breaks in Bacteriophage T4 by a Mechanism that Involves Extensive DNA Replication. Genetics 143, 1507-1520.

Gravel, S., Chapman, J.R., Magill, C., and Jackson, S.P. (2008). DNA helicases Sgs1 and BLM promote DNA double-strand break resection. Genes & Development 22, 2767-2772.

Guthrie, C., and Fink, G.R. (1991). Guide to Yeast Genetics and Molecular Biology. (San Diego: Academic Press).

Hicks, W.M., Kim, M., and Haber, J.E. (2010). Increased Mutagenesis and Unique Mutation Signature Associated with Mitotic Gene Conversion. Science 329, 82-85.

Holbeck, S.L., and Strathern, J.N. (1997). A role for REV3 in mutagenesis during double-strand break repair in *Saccharomyces Cerevisiae*. Genetics 147, 1017-1024.

Huppert, J.L. (2010). Structure, location and interactions of G-quadruplexes. FEBS J. 277, 3452-3458.

Ira, G., Malkova, A., Liberi, G., Foiani, M., and Haber, J.E. (2003). Srs2 and Sgs1-Top3 suppress crossovers during double-strand break repair in yeast. Cell 115, 401-411.

Ira, G., Pellicioli, A., Balijja, A., Wang, X., Fiorani, S., Carotenuto, W., Liberi, G., Bressan, D., Wan, L., Hollingsworth, N.M., et al. (2004). DNA end resection, homologous recombination and DNA damage checkpoint activation require CDK1. Nature 431, 1011 1017.

Ira, G., Satory, D., and Haber, J.E. (2006). Conservative inheritance of newly synthesized DNA in double-strand break-induced gene conversion. Mol Cell Biol 26, 9424-9429.

Ivessa, A.S., Zhou, J.Q. and Zakian, V.A. (2000). The *Saccharomyces Cerevisiae* Pif1p DNA helicase and the highly related Rrm3p have opposite effects on replication fork progression in ribosomal DNA. Cell, 100, 479-489.

Jackson, A.L., and Loeb, L.A. (2001). The contribution of endogenous sources of DNA damage to the multiple mutations in cancer. Mutation Research/Fundamental and Molecular Mechanisms of Mutagenesis 477, 7-21.

Jain, S., Sugawara, N., Lydeard, J., Vaze, M., Tanguy Le Gac, N., and Haber, J.E. (2009). A recombination execution checkpoint regulates the choice of homologous recombination pathway during DNA double-strand break repair. Genes Dev 23, 291-303.

Jin, Y.H., Garg, P., Stith, C.M., Al-Refai, H., Sterling, J.F., Murray, L.J., Kunkel, T.A., Resnick, M.A., Burgers, P.M., and Gordenin, D.A. (2005). The multiple biological roles of the 3'->5' exonuclease of *Saccharomyces Cerevisiae* DNA polymerase delta require switching between the polymerase and exonuclease domains. Mol Cell Biol 25, 461-471.

Kolodner, R.D. (1995). Mismatch repair: Mechanisms and relationship to cancer susceptibility. Trends Biochem Sci 20, 397-401.

Kolodner, R.D., Putnam, C.D., and Myung, K. (2002). Maintenance of Genome Stability in *Saccharomyces Cerevisiae*. Science 297, 552-557.

Kreuzer, K., Saunders, M., Weislo, L., and Kreuzer, H. (1995). Recombination dependent DNA replication stimulated by double-strand breaks in bacteriophage T4. J Bacteriol 177, 6844-6853.

Kreuzer, K.N. (2000). Recombination-dependent DNA replication in phage T4. Trends Biochem Sci 25, 165-173.

Kunkel, T.A., and Bebenek, K. (2000). DNA Replication fidelity. Annual Review of Biochemistry 69, 497.

Kuzminov, A. (1995). Collapse and repair of replication forks in *Escherichia Coli*. Mol Microbiol 16, 373-384.

Kuzminov, A. (1999). Recombinational repair of DNA damage in *Escherichia Coli.* and bacteriophage lambda. Microbiol Mol Biol Rev 63, 751-813.

Lahaye, A., Thines-Sempoux, D., and Foury, F. (1991). Pif1: a DNA helicase in yeast mitochondria. EMBO J 10, 11.

Lang, G.I., and Murray, A.W. (2008). Estimating the per-base-pair mutation rate in the yeast *Saccharomyces Cerevisiae*. Genetics 178, 67-82.

Le, S., Moore, J.K., Haber, J.E., and Greider, C.W. (1999). RAD50 and RAD51 define two pathways that collaborate to maintain telomeres in the absence of telomerase. Genetics 152, 143-152.

Lee, K., and Lee, S.E. (2007). *Saccharomyces Cerevisiae* Sae2- and Tel1-Dependent Single-Strand DNA Formation at DNA Break Promotes Microhomology-Mediated End Joining. Genetics 176, 2003-2014.

Lisby, M., Barlow, J.H., Burgess, R.C., and Rothstein, R. (2004). Choreography of the DNA Damage Response: Spatiotemporal Relationships among Checkpoint and Repair Proteins. Cell 118, 699-713.

Lisby, M., Rothstein, R., and Mortensen, U.H. (2001). Rad52 forms DNA repair and recombination centers during S phase. Proceedings of the National Academy of Sciences of U.S.A. 98, 8276-8282.

Lipps, H.J., and Rhodes, D. (2009). G-quadruplex structures: *in vivo* evidence and function. Trends Cell Biol. 19, 414-422.

Luder, A., and Mosig, G. (1982). Two alternative mechanisms for initiation of DNA replication forks in bacteriophage T4: priming by RNA polymerase and by recombination. Proceedings of the National Academy of Sciences of U.S.A. 79, 1101-1105.

Lundblad, V., and Blackburn, E.H. (1993). An alternative pathway for yeast telomere maintenance rescues est1- senescence. Cell 73, 347-360.

Lydeard, J.R., Jain, S., Yamaguchi, M., and Haber, J.E. (2007). Break-induced replication and telomerase-independent telomere maintenance require Pol32. Nature 448, 820-823.

Lydeard, J.R., L, M.Z., Sheu, Y.J., Stillman. B., Burgers, P.M., and Haber J.E. (2010). Break-induced replication requires all essential DNA replication factors except those specific for pre-RC assembly. Genes Dev 24, 1133-1144.

Ma, J.L., Kim, E.M., Haber, J.E., and Lee, S.E. (2003). Yeast Mre11 and Rad1 proteins define a Ku-independent mechanism to repair double-strand breaks lacking overlapping end sequences. Mol Cell Biol 23, 8820-8828.

Malkova, A., Ivanov, E.L., and Haber, J.E. (1996). Double-strand break repair in the absence of RAD51 in yeast: A possible role for break-induced DNA replication. Proceedings of the National Academy of Sciences of U.S.A. 93, 7131-7136.

Malkova, A., Naylor, M.L., Yamaguchi, M., Ira, G., and Haber, J.E. (2005). RAD51 dependent break-induced replication differs in kinetics and checkpoint responses from RAD51-mediated gene conversion. Mol Cell Biol 25, 933-944.

Malkova, A., Ross, L., Dawson, D., Hoekstra, M.F., and Haber, J.E. (1996). Meiotic recombination initiated by a double-strand break in rad50 delta yeast cells otherwise unable to initiate meiotic recombination. Genetics 143, 741-754.

Malkova, A., Signon, L., Schaefer, C.B., Naylor, M.L., Theis, J.F., Newlon, C.S., and Haber, J.E. (2001). RAD51-independent break-induced replication to repair a broken chromosome depends on a distant enhancer site. Genes Dev 15, 1055-1060.

Mangahas, J.L., Alexander, M.K., Sandell, L.L., and Zakian, V.A. (2001). Repair of Chromosome Ends after Telomere Loss in *Saccharomyces*. Mol Biol Cell 12, 4078-4089.

Mann, H.B., and Whitney, D.R. (1947). On a test of whether one of 2 random variables is stochastically larger than the other. Annals of Mathematical Statistics 18, 50-60.

McCulloch, S.D., and Kunkel, T.A. (2008). The fidelity of DNA synthesis by eukaryotic replicative and translesion synthesis polymerases. Cell Res 18, 148-161.

McEachern, M.J., and Haber, J.E. (2006). Break-induced replication and recombinational telomere elongation in yeast. Annu Rev Biochem 75, 111-135.

Mimitou, E.P., and Symington, L.S. (2008). Sae2, Exo1 and Sgs1 collaborate in DNA double-strand break processing. Nature 455, 770-774.

Mimitou, E.P., and Symington, L.S. (2009). DNA end resection: Many nucleases make light work. DNA Repair 8, 983-995.

Morrison, A.J., Highland, J., Krogan, N.J., Arbel-Eden, A., Greenblatt, J.F., Haber, J.E., and Shen, X. (2004). INO80 and [gamma]-H2AX Interaction Links ATP-Dependent Chromatin Remodeling to DNA Damage Repair. Cell 119, 767-775.

Morrow, D.M., Connelly, C., and Hieter, P. (1997). "Break copy" duplication: a model for chromosome fragment formation in *Saccharomyces Cerevisiae*. Genetics 147, 371-382.

Mosig, G. (1998). Recombination and recombination-dependent DNA replication in bacteriophage T4. Annual Review of Genetics 32, 379-413.

Myung, K., Chen, C., and Kolodner, R.D. (2001). Multiple pathways cooperate in the suppression of genome instability in *Saccharomyces Cerevisiae*. Nature 411, 1073-1076.

Myung, K., Datta, A., and Kolodner, R.D. (2001). Suppression of spontaneous chromosomal rearrangements by S phase checkpoint functions in *Saccharomyces Cerevisiae*. Cell 104, 397-408.

Natarajan, A.T., Obe, G., Van Zeeland, A.A., Palitti, F., Meijers, M., and Verdegaal-Immerzeel, E.A.M. (1980). Molecular mechanisms involved in the production of chromosomal aberrations. Utilization of neurospora endonuclease for the study of aberration production by X-rays in G1 and G2 stages of the cell cycle. Mutation Research/Fundamental and Molecular Mechanisms of Mutagenesis 69, 293-305.

New, J.H., Sugiyama, T., Zaitseva, E., and Kowalczykowski, S.C. (1998). Rad52 protein stimulates DNA strand exchange by Rad51 and replication protein A. Nature 391, 407-410.

Nick McElhinny, S.A., Gordenin, D.A., Stith, C.M., Burgers, P.M., and Kunkel, T.A. (2008). Division of labor at the eukaryotic replication fork. Mol Cell 30, 137-144.

Nick McElhinny, S.A., Pavlov, Y.I., and Kunkel, T.A. (2006). Evidence for extrinsic exonucleolytic proofreading. Cell Cycle 5, 958-962.

Northam, M.R., Robinson, H.A., Kochenova, O.V., and Shcherbakova, P.V. (2010). Participation of DNA polymerase zeta in replication of undamaged DNA in *Saccharomyces Cerevisiae*. Genetics 184, 27-42.

Orr-Weaver, T.L., and Szostak, J.W. (1983). Yeast recombination: The association between double-strand gap repair and crossing-over. Proceedings of the National Academy of Sciences of U.S.A. 80, 4417- 4421.

Orr-Weaver, T.L., Szostak, J.W., and Rothstein, R.J. (1981). Yeast transformation: A model system for the study of recombination. Proceedings of the National Academy of Sciences of U.S.A. 78, 6354- 6358.

Paeschke, K., Capre, J.A., and Zakian, V.A. (2011). DNA Replication through G-Quadruplex Motifs is promoted by *Saccharomyces Cerevisiae* Pif1 DNA helicase. Cell 10, 1016

Paques, F., and Haber, J.E. (1999). Multiple pathways of recombination induced by double-strand breaks in *Saccharomyces Cerevisiae*. Microbiol Mol Biol Rev 63, 349-404.

Paques, F., Leung, W.Y., and Haber, J.E. (1998). Expansions and contractions in a tandem repeat induced by double-strand break repair. Mol Cell Biol 18, 2045-2054.

Paques, F., Richard, G.F., and Haber, J.E. (2001). Expansions and contractions in 36-bp minisatellites by gene conversion in yeast. Genetics 158, 155-166.

Pavlov, Y.I., Frahm, C., Nick McElhinny, S.A., Niimi, A., Suzuki, M., and Kunkel, T.A. (2006). Evidence that errors made by DNA polymerase alpha are corrected by DNA polymerase delta. Curr Biol 16, 202-207.

Pavlov, Y.I., Shcherbakova, P.V., and Rogozin, I.B. (2006). Roles of DNA polymerases in replication, repair, and recombination in eukaryotes. Int Rev Cytol 255, 41-132.

Ribeyre, C., Lopes, J., Boule, J., Piazza, P., Gue din, A., Zakian, V., Mergny, J.L., and Nicolas, A. (2009). The yeast Pif1 helicase prevents genomic instability caused by G quadruplex-forming CEB1 sequences *in vivo*. PLoS Genet. 5, e1000475.

Rattray, A.J., Shafer, B.K., McGill, C.B., and Strathern, J.N. (2002). The roles of REV3 and RAD57 in double-strand-break-repair-induced mutagenesis of *Saccharomyces Cerevisiae*. Genetics 162, 1063-1077.

Sanders, C.M. (2010). Human Pif1 helicase is a G-quadruplex DNA binding protein with G-quadruplex DNA unwinding activity. Biochem J. 430, 119-128.

Schulz, V.P., and Zakian, V.A. (1994). The *Saccharomyces* Pif1 DNA helicase inhibits telomere elongation and *de novo* telomere formation. Cell 76, 145-155.

Shinohara, A., and Ogawa, T. (1998). Stimulation by Rad52 of yeast Rad51- mediated recombination. Nature 391, 404-407.

Shinohara, M., Shita-Yamaguchi, E., Buerstedde, J.M., Shinagawa, H., Ogawa, H., and Shinohara, A. (1997). Characterization of the Roles of the *Saccharomyces Cerevisiae* RAD54 Gene and a Homologue of RAD54, RDH54/TID1, in Mitosis and Meiosis. Genetics 147, 1545-1556.

Smith, C.E., Lam, A.F., and Symington, L.S. (2009). Aberrant double-strand break repair resulting in half crossovers in mutants defective for Rad51 or the DNA polymerase delta complex. Mol Cell Biol 29, 1432-1441.

Smith, C.E., Llorente, B., and Symington, L.S. (2007). Template switching during break-induced replication. Nature 447, 102-105.

Solinger, J.A., and Heyer, W.D. (2001). Rad54 protein stimulates the postsynaptic phase of Rad51 protein-mediated DNA strand exchange. Proceedings of the National Academy of Sciences of U.S.A 98, 8447-8453.

Storici, F., Lewis, L.K., and Resnick, M.A. (2001). *In vivo* site-directed mutagenesis using oligonucleotides. Nat Biotechnology 19, 773-776.

Storici, F., and Resnick, M.A. (2006). The *delitto perfetto* approach to *in vivo* site-directed mutagenesis and chromosome rearrangements with synthetic oligonucleotides in yeast. Methods Enzymol 409, 329-345.

Strathern, J.N., Klar, A.J.S., Hicks, J.B., Abraham, J.A., Ivy, J.M., Nasmyth, K.A., and McGill, C. (1982). Homothallic switching of yeast mating type cassettes is initiated by a double-stranded cut in the *MAT* locus. Cell 31, 183-192.

Strathern, J.N., Shafer, B.K., and McGill, C.B. (1995). DNA synthesis errors associated with double-strand-break repair. Genetics 140, 965-972.

Sugawara, N., Paques, F., Colaiacovo, M., and Haber, J.E. (1997). Role of *Saccharomyces Cerevisiae* Msh2 and Msh3 repair proteins in double-strand break-induced recombination. Proceedings of the National Academy of Sciences of U.S.A 94, 9214-9219.

Sugiyama, T., New, J.H., and Kowalczykowski, S.C. (1998). DNA annealing by Rad52 Protein is stimulated by specific interaction with the complex of replication protein A and single-stranded DNA. Proceedings of the National Academy of Sciences of U.S.A 95, 6049-6054.

Sung, P. (1994). Catalysis of ATP-dependent homologous DNA pairing and strand exchange by yeast RAD51 protein. Science 265, 1241-1243.

Sung, P. (1997). Yeast Rad55 and Rad57 proteins form a heterodimer that functions with replication protein A to promote DNA strand exchange by Rad51 recombinase. Genes & Development 11, 1111-1121.

Szostak, J.W., Orr-Weaver, T.L., Rothstein, R.J., and Stahl, F.W. (1983). The double strand-break repair model for recombination. Cell 33, 25-35.

Tran, H.T., Degtyareva, N.P., Koloteva, N.N., Sugino, A., Masumoto, H., Gordenin, D.A., and Resnick, M.A. (1995). Replication slippage between distant short repeats in *Saccharomyces Cerevisiae* depends on the direction of replication and the RAD50 and RAD52 genes. Mol Cell Biol 15, 5607-5617.

Tran, H.T., Gordenin, D.A., and Resnick, M.A. (1999). The 3'->5' exonucleases of DNA polymerases delta and epsilon and the 5'->3' exonuclease Exo1 have major roles in postreplication mutation avoidance in *Saccharomyces Cerevisiae*. Mol Cell Biol 19, 2000-2007.

Tran, H.T., Keen, J.D., Kricker, M., Resnick, M.A., and Gordenin, D.A. (1997). Hypermutability of homonucleotide runs in mismatch repair and DNA polymerase proofreading yeast mutants. Mol Cell Biol 17, 2859-2865.

VanHulle, K., Lemoine, F.J., Narayanan, V., Downing, B., Hull, K., McCullough, C., Bellinger, M., Lobachev, K., Petes, T.D., and Malkova, A. (2007). Inverted DNA repeats channel repair of distant double-strand breaks into chromatid fusions and chromosomal rearrangements. Mol Cell Biol 7,2601-14.

Van Gent D.C., Hoeijmakers J.H., and Kanaar R. (2001). Chromosomal stability and the DNA double-stranded break connection. Nature Rev Genetics 2, 196-206.

Wach, A., Brachat, A., Pohlmann, R., and Philippsen, P. (1994). New heterologous modules for classical or PCR-based gene disruptions in *Saccharomyces Cerevisiae*. Yeast 10, 1793-1808.

Wang, J., Gonzalez, K.D., Scaringe, W.A., Tsai, K., Liu, N., Gu, D., Li, W., Hill, K.A., and Sommer, S.S. (2007). Evidence for mutation showers. Proceedings of the National Academy of Sciences of U.S.A 104, 8403-8408.

Wang, X., Ira, G., Tercero, J.A., Holmes, A.M., Diffley, J.F., and Haber, J.E. (2004). Role of DNA replication proteins in double-strand break-induced recombination in *Saccharomyces Cerevisiae*. Mol Cell Biol 24, 6891-6899.

Yang, Y., Sterling, J., Storici, F., Resnick, M.A., and Gordenin, D.A. (2008). Hypermutability of damaged single-strand DNA formed at double-strand breaks and uncapped telomeres in yeast *Saccharomyces Cerevisiae*. PLoS Genet 4, e1000264.

Zhou, J., Monson, E.K., Teng, S.C., Schulz, V.P., and Zakian, V.A. (2000). Pif1p helicase, a catalytic inhibitor of telomerase in yeast. Science 289, 771-774.

Zhou, J.Q., Schulz, V.P., Mateyak, M.K., Monson, E.K., and Zakian, V.A. (2002). *Schizosaccharomyces Pombe* pfh1+ encodes an essential 5' to 3' DNA helicase that is a member of the Pif1 subfamily of DNA helicases. Mol Biol Cell 13, 12.

Zhu, Z., Chung, W.H., Shim, E.Y., Lee, S.E., and Ira, G. (2008). Sgs1 helicase and two nucleases Dna2 and Exo1 resect DNA double-strand break ends. Cell 134, 981-994.